



Norwegian University of
Science and Technology

Moisture production in buildings

Anders Saasen Pedersen

Master of Energy and Environmental Engineering

Submission date: August 2018

Supervisor: Hans Martin Mathisen, EPT

Co-supervisor: Maria Justo-Alonso, EPT

Norwegian University of Science and Technology
Department of Energy and Process Engineering

EPT-M-2018-65

MASTER THESIS

for

student Anders Saasen Pedersen

Spring 2018

Moisture production in buildings

*Fuktproduksjon i boliger***Background and objective**

In order to reduce energy consumption, tightening of building envelopes has become a required action together with increased insulation. In order to control indoor air quality in modern airtight buildings, balanced mechanical ventilation has a major role.

The amount of moisture within a building depend on the production of moisture from occupants and their activities. The ventilation system and recovery of moisture are also important for the moisture level. Moisture content in the extract air is important for the performance of heat recovery exchangers.

High levels of moisture may be related to respiratory diseases and asthma. In addition, high levels of moisture are related to growth of mould.

The objective of this master work is to further develop and verify a moisture production model based on measurements and data collected from other studies. Most of the measurements should be from high-insulated buildings. If reliable data is not available, supplementary measurements should be done.

The work is a continuation of the candidate's specialization project

The project is connected to the research project EnergiBolig owned by Flexit AS. NTNU and SINTEF are partners in this project.

The following tasks could be considered:

1. Further develop the literature study and theory on moisture and moisture production in residential buildings from the specialization project
2. Evaluate if adsorption of moisture in building materials influence domestic moisture level
3. Measurements and evaluation of the moisture production model.
4. Discussion and conclusions

Within 14 days of receiving the written text on the master thesis, the candidate shall submit a research plan for his project to the department.

When the thesis is evaluated, emphasis is put on processing of the results, and that they are presented in tabular and/or graphic form in a clear manner, and that they are analyzed carefully.

The thesis should be formulated as a research report with summary both in English and Norwegian, conclusion, literature references, table of contents etc. During the preparation of the text, the candidate should make an effort to produce a well-structured and easily readable report. In order to ease the evaluation of the thesis, it is important that the cross-references are correct. In the making of the report, strong emphasis should be placed on both a thorough discussion of the results and an orderly presentation.

The candidate is requested to initiate and keep close contact with his/her academic supervisor(s) throughout the working period. The candidate must follow the rules and regulations of NTNU as well as passive directions given by the Department of Energy and Process Engineering.


Risk assessment of the candidate's work shall be carried out according to the department's procedures. The risk assessment must be documented and included as part of the final report. Events related to the candidate's work adversely affecting the health, safety or security, must be documented and included as part of the final report. If the documentation on risk assessment represents a large number of pages, the full version is to be submitted electronically to the supervisor and an excerpt is included in the report.

Pursuant to "Regulations concerning the supplementary provisions to the technology study program/Master of Science" at NTNU §20, the Department reserves the permission to utilize all the results and data for teaching and research purposes as well as in future publications.

The final report is to be submitted digitally in DAIM. An executive summary of the thesis including title, student's name, supervisor's name, year, department name, and NTNU's logo and name, shall be submitted to the department as a separate pdf file. Based on an agreement with the supervisor, the final report and other material and documents may be given to the supervisor in digital format.

- Work to be done in lab (Water power lab, Fluids engineering lab, Thermal engineering lab)
- Field work

Department of Energy and Process Engineering, 15. February 2018



Hans Martin Mathisen
Academic Supervisor

Research Advisor:
Maria Justo Alonso

Preface

This master's thesis, regarding moisture production in residential buildings was carried out at the Department of Energy and Process Engineering (EPT) at the Norwegian University of Science and Technology (NTNU) in Trondheim, Norway, during the spring semester of 2018.

The thesis comprises 30 ECTS during the 10th and last semester of a master's degree in Energy and Environmental Engineering. The work is an expansion of the project work written by the author during the autumn semester of 2017.

A special gesture goes to my supervisor and colleague Prof. Hans Martin Mathisen at ETP and my co-supervisor, Ph.D. candidate Maria Justo-Alonso. Their support and guidance has made my work the product it is, and helped me through the struggles encountered. Good luck with your future, I am sure you will continue to succeed on all arenas in life.

After five years studying here at NTNU, many people deserves a gesture. However, the greatest one goes to my family for their caring support on my journey to become an engineer. I am proud of everything you have thought me.

Trondheim, August 30, 2018



Anders Saasen Pedersen

Department of Energy- and Process Engineering, NTNU

Abstract

This master thesis is investigating the moisture production from indoor activities, and how it influences the indoor relative humidity. The main goal is to verify a moisture production model for residential buildings, currently under development at NTNU. The first three chapters of the thesis presents the mathematical background to indoor moisture production, and the state of the art research on the area. A suggested calculation method on how the release of moisture from an indoor activity can be quantified by measurements is presented. The second part of the thesis present the moisture production model and the planned method on how the model can be verified. By conducting a series of showering experiments, and using the suggested calculation method to quantify the moisture produced, the verification was attempted. The third part presents the results from a series of conducted experiments performed in Living Lab at NTNU. The data from the experiments is processed and compared to the existing model, and discussed.

Moisture in general is the number one cause of building related damages, whereas about 6 % - 8 % is directly related to indoor moisture. With increased demand for building tightness, it is crucial to have a properly sized mechanical ventilation system to ventilate the excess moisture out of the building, preventing it to accumulate. An indoor relative humidity of above 70 % gives favorable conditions for mold and bacterial growth on indoor surfaces, and can worsen asthmatic symptoms. Monitoring and studying the indoor levels of humidity is essential in order to understand and prevent these situations.

A number of processes and activities in an indoor environment generates moisture. Breathing, showering, bathing, cooking, cleaning, and drying of clothes are all generating moisture to the surrounding air. However, the indoor moisture production rates varies greatly between the different sources, as seen from research. For showering, the moisture production varies with a number of parameters. Water temperature, flow rate of water and the length of the shower is just some of the variables determining the total moisture production. These three parameters are used as variables during the experiments in Living Lab.

The ultimate goal of the moisture production model is to prevent frosting and condensation in the rotary heat exchanger of the air-handling unit. By creating a model that can predict indoor relative humidity fluctuations in a building and how the humidity is recycled through the heat exchanger, these unwanted effects could ultimately be avoided. The model uses data on moisture production from a number of sources, and by the help of input data on occupant behavior from the user, the indoor relative humidity levels is mapped.

This thesis focuses on verifying the moisture production from showering. Showering is the most intensive indoor moisture producing source, as it has the ability to saturate the surrounding air. By conducting a series of showering experiments, while changing different parameters, the moisture production, along with the transient development in relative humidity has been mapped. From the results, it can be seen that the moisture production calculated from experimental data is higher than suggested data from the literature. The experiments showed a total release of moisture ranging from 200 g/shower – 750 g/shower. The literature suggest values from 200 g/shower to 400 g/shower.

The transient development in relative humidity from the experiments is compared to the simulated results from the moisture production model. These relation is very similar until two minutes after the shower has been turned off. At this point the decrease rate slows down in real life, while the model continues to descend at the same rate. This difference makes the total time for the relative humidity to reach a stationary condition merely 40 minutes for the model, while in reality it takes from 2 hours – 2.5 hours. This is assumed to have to do with the transition

from water vapor present in the air, which is rapidly ventilated out, to the evaporation of liquid water left in the bathroom, which takes a longer time. The model does not take this into consideration, and it is suggested that it should.

The secondary goal of the thesis is to conduct a literature review on whether moisture buffering can be utilized to reduce the peaks in indoor relative humidity or not. Based on the research it is suggested that the effect should be implemented into the model at a later stage. The accuracy of the model is at this stage not high enough that this effect is essential. From the literature it is shown that the capability of a material to reduce the peaks in relative humidity is up to 30 % if used correctly. The author does however doubt that this can happen within a shower, as the moisture is released at such high rate, and ventilated out at almost equal rate. The moisture buffering is thus assumed ineffective on damping the effect from showering.

Sammendrag

I denne masteroppgaven har det blitt undersøkt hvor mye fuktighet som blir produsert ved dusjing, og hvordan dette påvirker innendørs relativ luftfuktighet. Hovedmålet har vært å verifisere en fuktproduksjonsmodell under utvikling ved NTNU. De første tre kapitlene i oppgaven fokuserer på det fundamentale matematikken bak fuktproduksjon, og presenterer siste nytt på området fra forskningen. Det foreslås å bruke en beregningsmetode på hvordan totalt produsert fuktmengde kan kvantifiseres ved å gjennomføre målinger. I tillegg følger en forklaring av- og et litteraturstudie på hvordan fuktbufring kan brukes til å redusere toppen i innendørs fuktnivåer. Den andre delen av oppgaven går kort gjennom fuktproduksjonsmodellen samt metode for hvordan modellen kan verifiseres. Ved å gjennomføre en serie dusjeksperimenter, samt å anvende den foreslåtte beregningsmetoden til å kvantifisere mengden fuktighet produsert, kan modellen verifiseres. Den tredje delen presenterer resultatene fra en serie gjennomførte eksperimenter i Living Lab ved NTNU. Dataen fra eksperimentene blir prosessert og sammenlignet med den eksisterende modellen, samt videre diskutert.

Fukt er den største årsaken til byggskader, hvor innendørs fuktbelastning står for omtrent 6 % - 8 %. Med stadig økte krav til tetthet i bygg, er det viktig å ha riktig dimensjonerte ventilasjonsanlegg. Den overflødig fuktigheten produsert må ventileres ut av bygget, for å unngå at den akkumuleres. En relativ fukt over 70 % gir grunnlag for mugg- og bakterievekst på innendørs overflater, samt forverre symptomer på astma. Overvåkning og forskning på innendørs fuktnivåer er essensielt for å kunne forstå og unngå slike situasjoner.

Mange innendørs prosesser og aktiviteter genererer fukt. Utånding, dusjing, bading, matlaging, rengjøring og tørking av klær er alle kilder til fukt i inneluften. Fuktproduksjon innendørs varierer stort fra kilde til kilde, som gjentatte ganger er bevist ved forskning. For dusjing varierer fuktproduksjonen med en rekke parametere. Vanntemperatur, massestrøm, dusjlengthe er bare noen av variablene som er med på å bestemme total fuktproduksjon. Disse tre parameterne er brukt som variabler under forsøkene gjennomført i Living Lab.

Målet for fuktproduksjonsmodellen er å unngå gjenfrysing og kondensering i roterende varmegjenvinnere. Ved å utvikle en modell som kan forutse utviklingen i innendørs relativ fuktighet, og hvordan denne blir gjenvunnet i varmegjenvinnere, de uønskede konsekvensene kan unngås i større grad. Modellen benytter data på fuktproduksjon fra en rekke kilder, og ved at brukeren fører inn data på brukeratferd, kan utviklingen i relativ fuktighet kartlegges.

Denne oppgaven fokuserer på å verifisere data på fuktproduksjon fra dusjing. Dusjing er en av de mest intensive fuktildene innendørs, da den har evnen til å mette luften med vann. Ved å gjennomføre en rekke eksperimenter med forskjellige parametere varieres, har fuktproduksjonen, samt det transiente forløpet til relativ fuktighet blitt kartlagt. Fra resultatene kan det sees at fuktproduksjonen fra eksperimentene er høyere enn hva som er foreslått i litteraturen. Eksperimentene viser en total produksjon på mellom 200 g/ dusj– 750 g/ dusj, avhengig av kombinasjonen av parametere. I litteraturen fins data på verdier mellom 200 g/dusj og 400 g/dusj.

Det transiente forløpet til den relative fuktigheten fra eksperimenter er sammenlignet med simulerte resultater fra modellen. Fra dette kan det sees at forløpet mellom de to er så å si like fram til to minutter etter vannet er slått av. Ved dette punktet bremses avtagelsesraten for den reelle situasjonen, mens modellens rate fortsetter i samme tempo. Denne forskjellen gjør at det tar ca. 40 minutter før modellens relative fuktighet når stasjonær tilstand, mens det tar mellom 2 timer og 2.5 timer før den faktisk når denne. Dette er antatt å skyldes overgangen mellom damp i luften, som ventileres raskt ut, og fordampningen av vann som ligger igjen på badet som

det tar lenger tid å ventilere ut. Modellen tar ikke hensyn til dette, og det er foreslått at den burde.

Det andre målet med moppgaven er å gjennomføre en litteraturstudie på om fuktbufring i materialer kan bli utnyttet til å kutte toppene i innendørs relativ fuktighet. Basert på forskningen er det foreslått at effekten bør implementeres i modellen på et senere tidspunkt. Nøyaktigheten på modellen er på nåværende tidspunkt ikke høy nok til at denne er avgjørende. Fra litteraturstudiet er det vist at materialer kan bufre i den grad at toppene i relativ fuktighet kan reduseres med 30 % dersom den er brukt korrekt. Forfatteren tviler derimot at dette er tilfelle ved en dusjsekvens, da fuktigheten produseres med såpass høy rate, og ventileres raskt ut. Fuktbufring er derfor antatt å være ineffektiv til å dempe påvirkningen fra dusjing.

Table of contents

Preface.....	i
Abstract.....	iii
Sammendrag.....	iv
1. Introduction.....	1
1.1 Motivation	1
1.2 Scope	1
1.3 Structure of the report.....	2
2. Theoretical background	5
2.1 Humid Air.....	5
2.1.1 <i>Ideal Gas</i>	5
2.1.2 <i>Relative humidity</i>	6
2.1.3 <i>Specific Humidity</i>	7
2.1.4 <i>Total air pressure</i>	8
2.1.5 <i>Air density</i>	10
2.2 Mollier diagram	12
2.3 Relative humidity	14
2.3.1 <i>Outdoor</i>	14
2.3.2 <i>Indoor</i>	16
2.4 Moisture production	17
2.4.1 <i>Calculating the moisture production from a transient process</i>	18
3. Literature Review	23
3.1 Moisture affections on materials and living life.....	23
3.1.1 <i>Thermal environment</i>	23
3.1.2 <i>Relative humidity</i>	23
3.2 Moisture production	24
3.2.1 <i>Moisture production rates</i>	25
3.3 Moisture buffering.....	28
3.3.1 <i>Moisture buffer value</i>	30
3.3.2 <i>Material thickness</i>	33
4. Method	35
4.1 Introduction	35
4.2 Test facility	36
4.3 Experimental set- up.....	37
4.4 Preparations for measurements	40
4.4.1 <i>Ventilation system</i>	40
4.4.2 <i>Calibration of sensors</i>	41
4.5 From experiment to data.....	45
4.6 Plan for measurements	46
5. Moisture production model	49
5.1 The model.....	49
5.2 Output from the model	50
6. Results.....	53
6.1 Introduction and results	53
6.2 Transient analysis	55

6.2.1	<i>RH</i>	55
6.2.2	<i>Temperature</i>	57
6.2.3	<i>Specific humidity</i>	58
6.2.4	<i>Humid air density</i>	60
6.3	Moisture production model vs real cases	61
7.	Discussion	65
7.1	Transient development during and after a showering sequence.....	65
7.2	Moisture production	69
7.2.1	<i>Humans</i>	69
7.2.2	<i>Showering</i>	70
7.3	Moisture buffering.....	71
8.	Conclusion	73
9.	Further work	75
10.	Bibliography	77
A	Living lab	83
B	Balancing chart	85
C	Calibration of sensors	87
C.1	Velocity	87
C.2	Relative humidity	91
D	Moisture production model	93
E	Matlab scripts	95
E.1	Surface plot: Specific humidity	95
E.2	Surface plot: Humid air density	96
F.	Calibration via curve fitting	97
F.1	<i>RH</i>	97
F.2	<i>Temperature</i>	98
G.	Human activity pattern	99

List of tables

Table 2-1: Description of some the properties a Mollier diagram can provide, and how to locate them (Ingebrigtsen, 2016a).	13
Table 2-2: The two states used in the Mollier diagram in Figure 2.7.	15
Table 3-1: Sources of moisture production at different room types of a dwelling (Johansson et al., 2010).	25
Table 3-2: Moisture production from different indoor sources.	27
Table 4-1: Nominal airflow rates in ZeB Living lab during normal occupancy.	40
Table 4-2: The numbers of the exponentiation function used to calibrate the sensor type Vaisala HMT333	43
Table 4-3: Research plan for the verification of the moisture produced from showering. “X” implies that the set of parameters was tested, while “-“ was not tested. A total of eight tests were conducted.	47
Table 5-1: Processed moisture production rates used in the moisture production model, originally found in Yik et al. (2004).	50
Table 6-1: Measured moisture production from showering, G [g/event].	54
Table 6-2: Analysis of the moisture production rate (per minute showered) categorized after parameter.	55
Table D-1: Data moisture production rates utilized in the MPM (Yik et al., 2004)	93
Table E-1: Matlab scrip for producing a surface plot showing the relation between specific humidity, RH and temperature.	95
Table E-2: Matlab scrip for producing a surface plot showing the relation between the density of humid air, RH and temperature.	96

Table of figures

Figure 2.1: The relation between air temperature and partial pressure of water vapor at different relative humidity.....	7
Figure 2.2: The daily average total air pressure and extreme values of outside air in Trondheim, Voll, generated through data from the period 2008-2017. (Meteorologisk Institutt, 2018)	9
Figure 2.3: Surface plot that shows the influence of changes in both temperature and relative humidity on the specific humidity. The coloring illustrates the error in specific humidity when using the extreme values from Figure 2.2 relative to 1 013.25hPa.	10
Figure 2.4: Density of humid air relative to temperature and surrounding air pressure, at extreme values of RH.	11
Figure 2.5: Simplified version of a Mollier diagram, showing the relation between air temperature, moisture content and enthalpy at constant air pressure of 1 bar.	12
Figure 2.6: The average relative humidity and specific humidity of outdoor air in Trondheim, Voll, generated from daily averages over a period of ten years from 2008-2017 (Meteorologisk Institutt, 2018).	14
Figure 2.7: Mollier diagram showing the relation between the state of outdoor air in the typical Nordic winter and summer climate.	15
Figure 2.8: Conceptual illustration of a lower Riemann sum with $n = 6$, used to calculate the moisture production in a transient process.	20
Figure 2.9: Conceptual illustration of composite Simpson's rule with $n = 6$, used to calculate the moisture production in a transient process.	21
Figure 3.1: The buffering capacity of materials are damping the effects of changes the moisture content of indoor air (Pallin et al., 2011)	29
Figure 3.2: The three description levels for the moisture buffering phenomena (Rode et al., 2007).....	30
Figure 3.3: Mass change of a material sample, when exposed to waveform changes in RH (Rode et al., 2007).	31
Figure 3.4: Moisture Buffer Values found by different institutions for the different materials (Rode et al., 2007).	32
Figure 3.5: Mass change of three types of plasters when exposed to waveform changes in RH. (Maskell et al., 2017).....	33
Figure 3.6: Optimal moisture penetration depth for a material, following a period of raised RH. (Maskell et al., 2017)	34
Figure 4.1: Parameters measured to and from a control volume, to calculate the moisture production of a process.	35
Figure 4.2: Four different views of the test facility at Living lab, Where left image is the entrance to the bathroom, while the other three shows three different angles inside it. The extract valve can be seen in the rightmost image, located above the shower.	37
Figure 4.3: The left image shows the placement of the RH/ temperature sensor monitoring the state of the supplied air to the bathroom. At the right image, the equivalent sensor registering the state of the extract air from the bathroom can be seen. This sensor is mounted inside the ventilation duct.	38
Figure 4.4: All the sensors used to monitor the state of the air was connected to a data logger, as seen to the left of the image. At the right, a DC voltage source for the sensors can be seen.....	39
Figure 4.5: In the process of calibrating one of the humidity sensors with Vaisala Humidity Calibrator HMK15.	42

Figure 4.6: The calibration of the sensor type HMT333 was conducted towards the installed sensor HMT120 in the ventilation extract duct in the bathroom of Living Lab.	43
Figure 4.7: The orifice plate fitted between the two sections, where pressure drop is measured and the airflow rate is accurately calculated.	44
Figure 4.8: The rig built for calibration of velocity sensors.....	45
Figure 4.9: Flow process chart on how the excel script calculates the moisture production from a measured data in Living lab. The calculations are based on equation (14), evaluated in the transient regime.....	46
Figure 5.1: Output from the MPM, showing the transient response in RH for four zones of a building, during 24h in the spring of Norway.	51
Figure 6.1: The transient development in RH during a 5 min shower experiment, using 4 sensors.	56
Figure 6.2: The transient development in temperature during a 5 min shower experiment, using 4 sensors.	57
Figure 6.3: The transient difference in specific humidity between extract and supply air during a 5- min shower, with 35 °C water temperature and medium flow rate.	58
Figure 6.4: Comparison of the transient specific humidity difference between the bathroom inlet and extract, for three different showering experiments.	59
Figure 6.5: The humid air density changes at three different positions during a 5- min shower, with 35 °C water temperature and medium flow rate.	60
Figure 6.6: The transient response in RH, of four different shower lengths as they appear in the MPM.....	61
Figure 6.7: Comparison of the transient development in RH, from a four- minute shower with different initial RH.	62
Figure 6.8: A comparison of the transient response in RH during and after a four- minute showering sequence, between a real case experiment conducted in Living Lab, and the MPM.....	63
Figure 7.1: The transient relation in RH during and after a shower experiment.....	66
Figure 7.2: Logarithmic presentation of the decay curve in RH from a showering experiment after the water is turned off.	67
Figure 7.3: Logarithmic presentation of the decay curve in RH from the first two minutes of showering experiment after the water is turned off.....	68
Figure 7.4: Logarithmic presentation of the decay curve in RH after the first two minutes of showering experiment after the water is turned off.....	69
Figure A.1: Zeb Living lab floor plan, with zone names (Francesco et al., 2014)	83
Figure A.2: Projected ventilation rates in Living Lab. A “+” sign implies supply of air, and a “-“ sign implies an extract (PROSJEKTUTVIKLING MIDT-NORGE AS, 2014)	84
Figure B.1: Balancing chart for supply ducts, before adjusting the fan speed to match projected airflow rate.	85
Figure C.1: Location of sensors in the ductwork of ZeB Living Lab. Those calibrated are marked in yellow.	87
Figure C.2: Results from three runs of calibration of the AST2 velocity sensor.	88
Figure C.3: Calibration data for velocity sensor AST2, based on three separate runs of calibration. A second-degree formula is generated to fit between the three runs.	89
Figure C.4: Results from three runs of calibration of the AST5 velocity sensor.	90
Figure C.5: Calibration data for velocity sensor AST5, based on three separate runs of calibration. A second-degree formula is generated to fit between the three runs.	91
Figure C.6: Correlation between temperature and RH when a pure salt/distilled water solution is enclosed in a container (Vaisala, 2018).....	92

Figure C.7: Calibration data for three hygrometers, based on average of three separate runs of calibration.....	92
Figure F.1: Calibration of sensor type Vaisala HMT333 vs pre- calibrated sensor type Vaisala HMT120. The graph shows the response in RH, when applying a moisture production, <i>before</i> the curve fitting towards the pre- calibrated sensor.	97
Figure F.2: Calibration of sensor type Vaisala HMT333 vs pre- calibrated sensor type Vaisala HMT120. The graph shows the response in RH, when applying a moisture production, <i>after</i> the curve fitting towards the pre- calibrated sensor.....	97
Figure F.3: Calibration of sensor type Vaisala HMT333 vs pre- calibrated sensor type Vaisala HMT120. The graph shows the response in temperature, when applying a moisture production, <i>before</i> the curve fitting towards the pre- calibrated sensor.....	98
Figure F.4: Calibration of sensor type Vaisala HMT333 vs pre- calibrated sensor type Vaisala HMT120. The graph shows the response in temperature, when applying a moisture production, <i>after</i> the curve fitting towards the pre- calibrated sensor.	98
Figure G.1: Activity pattern for two types of household families, including moisture production rate. In addition the total time each activity is performed during a day is given, and the percentages represents the probability for the occurrence during a day.(Johansson et al., 2010)	99

Nomenclature

G	Moisture production rate	g/h
h	Enthalpy	kJ/kg
n	Air change-rate	h^{-1}
m	Mass	kg
m_a	Mass of dry air	kg- dry air
m_v	Mass of water vapor	kg- water vapor
M_g	Molecular mass of a gas	kg/kmol
p	Pressure	Pa
p_c	Critical pressure	Pa
p_i	Partial pressure	Pa
p_{tot}	Total air pressure	Pa
p_{sat}	Saturation pressure	Pa
p_v	Partial pressure of water vapor	Pa
p_a	Partial pressure of dry air	Pa
R	Universal molar gas constant	J/(kmol*K)
RH	Relative humidity	%
ρ	Density	kg/m ³
T	Temperature	K
T_d	Dry bulb temperature	°C
V	Volume	m ³
\dot{V}	Volumetric flow rate	m ³ /h
x	Specific humidity	kg-vapor/kg-dry air
x_i	Specific humidity indoor	kg/kg
x_e	Specific humidity outdoor	kg/kg

Abbreviations

MPM – Moisture production model

RH – Relative humidity

ZeB – Zero emission building

MBV – Moisture buffer value

1. Introduction

This is the first chapter of the thesis. It gives an understanding of the background for the given problem, and the motivation behind it. In addition, the scope of the report is presented, before the research questions is presented

1.1 Motivation

Air humidity is the amount of water vapor present in the air. Knowledge of how indoor air humidity levels varies with different influencing factors and how it affects humans and their surroundings is required for many purposes. 60-80 % of building related damages is estimated to be caused by a form of moisture damage (Edvardsen and Ramstad, 2014). About 10 % of this is a direct consequence of the moisture of the indoor air. Wrong treatment of the air, excessive moisture production or a construction error, can in extreme cases lead to excessive amounts of indoor moisture. It is crucial to investigate how the overall building related damages can be reduced, in order to reach the global climate goals. By looking into indoor relative humidity (RH) and moisture production, potential damage can be avoided.

Both living life and building materials are affected by the fluctuations in the moisture content of indoor air. High levels of moisture in a building can be related to respiratory diseases and asthma in addition to the growth of mould, fungus and bacterial resurgence (Adan and Samson, 2011). Knowledge of which parameters affects the indoor moisture levels is essential in order to predict and prevent a RH outside predetermined boundaries.

In general, several processes and household activities generate moisture. First, there is the respiratory activity from living objects, such as humans, animals and plants. Secondly, the indoor activities the residents conducts influence the moisture content. Here all sorts of moisture related activities contributes, such as showering, washing- and drying clothes, cleaning and cooking. Other effects of moisture production comes from the building and indoor furniture's themselves, with the hygroscopic exchange of moisture with the indoor environment, or the release from materials in newly constructed buildings.

1.2 Scope

The goal of the master thesis work is to verify a household moisture production model (MPM), made by Maria Justo-Alonso, at NTNU. The model simulates the indoor RH under different outdoor conditions, and building specific parameters. Different indoor activities generates different amounts of moisture to the air, which has an influence on the RH. In combination with a rotary heat exchanger, the moisture released can be recycled from the extract air. There is a risk of condensation and frosting, which can decrease the efficiency of the heat exchanger.

In the moisture production model, different moisture producing activities is implemented, and assigned to a unique moisture production rate. The primary goal of the thesis is to verify these moisture production rates. By conducting a literature review on moisture production rates, the latest values can be evaluated against the model. Furthermore a real life test will be conducted to verify the rates used. By conducting a series of moisture producing experiments in the bathroom of a test facility at NTNU, called Living Lab, the moisture production from showering will be tested. Indoor moisture production is generated in very small quantities, and measuring it must be done in a very accurate way. Thus, properly calibrated instruments is of great essence, so calibration of sensors will be prioritized.

The secondary goal of the thesis is to suggest whether moisture buffering should be implemented into the moisture production model, or not. By conducting a literature review on the topic and discussing the findings. Suggestions to the model will be made.

The use of Living Lab as a test facility has not been without issues. Significant downtime of the monitoring systems has postponed the field tests, to the extent that the focus ended on looking into moisture production from showering only, as the original plan was to verify a broader range of sources.

1.3 Structure of the report

The structure of the report has the purpose of being organized in a scientific manner, starting with a literature review, followed by a method, results, discussion and at last a conclusion followed by a list of suggestions for further work.

- Chapter 2 presents the mathematic and theoretical background for understanding the concept of moisture production, and is divided into two parts. The first part gives a thorough background to humid air and RH in addition to the important parameters the reader will encounter later in the thesis. The second part of the chapter presents the mathematical background for the experimental method used to verify the moisture production rates used in the moisture production model.
- Chapter 3 is a literature review. The chapter is divided into three main parts. The first focuses on how indoor moisture production and RH is affecting humans and materials, while the second part presents the state of the art research on moisture production rates from other authors work. The third part of the literature review is an introduction to, and an explanation of the moisture buffering effect that materials can have on the on door RH.
- Chapter 4 is a method chapter that presents the research plan for the test facility Living Lab. The goal of this chapter is to give the reader an understanding of the limitations and methodology behind the conducted experiments.
- Chapter 5 briefly presents the moisture production model. The purpose and limitations of the model is presented while being angled towards the conducted showering experiments in Living Lab.

-
- Chapter 6 presents the calculated data on moisture production from the experiments, and discusses it from a RH, temperature and specific humidity perspective. A comparison between the simulated results and the real case is also presented and discussed.
 - Chapter 7 is a discussion of the findings from the thesis. It sheds light on the aspects examined, and discusses its validity. In this chapter moisture, buffering is discussed towards the moisture production model.
 - Chapter 8 is the conclusion, whose purpose is to present the most important findings and results from the thesis work, and sheds light on the prospects that worked and did not work.
 - Chapter 9 is a list of recommendations to further work that can or should be done to improve the outcome of the findings in this thesis.
 - References and appendices are following Chapter 9.

2. Theoretical background

This chapter holds the theoretical background for moisture production. It starts with the elementary physical understanding of humid air, then continues with more specific content relating relative humidity with moisture production. It ends with the mathematical theory on how moisture production can be measured and calculated.

2.1 Humid Air

The chemical composition of clean, dry atmospheric air consists mainly of the gases nitrogen (78 %), oxygen (21 %) and argon (0.9 %), by volume (Nilsson, 2003). In addition to these and all other gaseous substances found in the atmosphere, air contains varying amounts of water vapor, depending on climate and temperature. Characteristics for air is that the dry part of the air remains constant, while the moisture content varies. The mixture of dry air and water vapor is referred to the terms humid air or moist air (Moran et al., 2012).

2.1.1 Ideal Gas

The relation between the physical parameters of a gaseous compound is determined by the gasses' individual properties and how they interact between each other. By applying assumptions that the gasses has pure translational motion, elastic collisions and non-attractive forces between the molecules the relations can be approximated (Moran et al., 2012). At states of a gas where the pressure p is small relative to the critical pressure p_c and/or the temperature T is large relative to the critical temperature T_c , we can assume with reasonable accuracy that the ideal gas law applies (Moran et al., 2012). Within the pressure- and temperature range of the atmosphere, both the dry air and the water vapor is well below the critical limits, and thus considered ideal gasses (Geving and Thue, 2002). (1) gives the equation of state of an ideal gas

$$pV = \frac{m}{M_g} RT \quad (1)$$

, where p is the pressure of the gas in Pa, V is the volume of the gas in m^3 , m is the mass of the gas in kg, M_g is the molecular mass of the gas in kg/mol R is the universal (molar) gas constant of $8\,314.41 \text{ J/(kmol}\cdot\text{K)}$, and T is the temperature of the gas in K.

As atmospheric air is considered a mixture of two ideal gasses (water vapor and dry air), Daltons' model applies. This model assumes that each component in a gaseous mixture behaves as an ideal gas as if it were alone at temperature T , and volume V (Moran et al., 2012). Each

2. Theoretical background

component at its own would not exert the mixture total air pressure, p_{tot} but rather a partial pressure, p_i . It can be shown that the total air pressure, p_{tot} of the mixture is equal to the sum of the partial pressure p_i of each component, known as Dalton's Model (2).

$$\sum_i p_i = p_{tot} \quad (2)$$

The equation of state (1) can thus be applied component wise, either on the water vapor itself or on the humid air as a whole. By applying Dalton's Model (2) to the equation of state, the resulting equation of state for a component i , is given by (3).

$$p_i V = \frac{m_i}{M_i} RT \quad (3)$$

2.1.2 Relative humidity

Air can only hold a certain amount of water vapor before condensation of the vapor into liquid water occurs. The upper limit for the moisture content is given by the saturation pressure, p_{sat} (Pa) of the water vapor, and is a function of temperature. This relation is determined empirically. An equation (4) to calculate the saturation pressure is given by Oyj (2013). The equation has a maximal error of 0.083 % within the temperature range -20...+50 °C.

$$p_{sat} = A * 10^{\left(\frac{r*T}{T+T_n}\right)} \quad (4)$$

$$A = 611.6441 \text{ Pa}$$

$$R = 7.591386 \text{ [-]}$$

$$T_n = 240.7263 \text{ °C}$$

$$T = \text{dry bulb temperature, [°C]}$$

Equation (4) shows that the saturation pressure is increasing with temperature, and thus the air is able to hold more moisture with higher temperatures and vice versa. A way of describing the grade of saturation in the air is the relative humidity (RH) [%]. The RH is defined as (5)

$$RH = \frac{p_v(T)}{p_{sat}(T)} * 100 \% \quad (5)$$

p_v is the partial pressure of the water vapor at a given temperature T in Pa. This property is calculated from the equation of state of a component, equation (3). The RH ranges from 0 to 100 %, where at 100 % the air cannot hold any more vapor and condensation occurs if more vapor is added. The relation between p_v and T at different moisture saturation grades of the air, is shown in Figure 2.1.

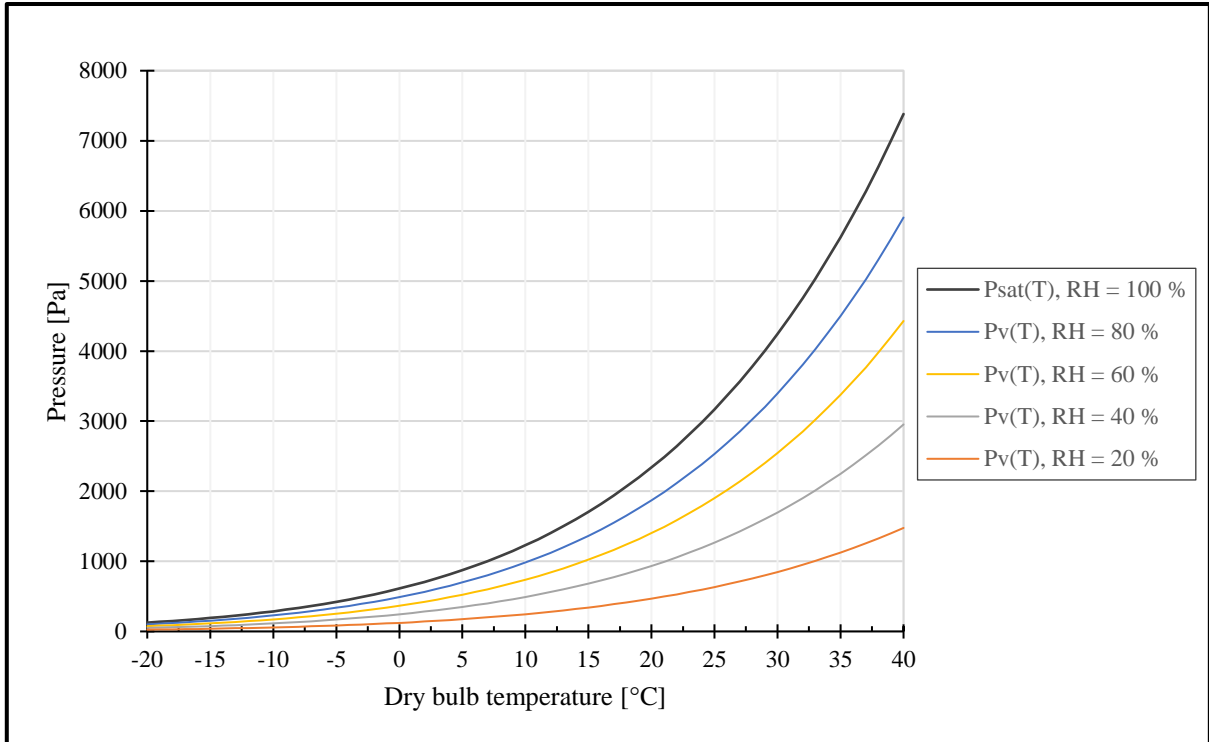


Figure 2.1: The relation between air temperature and partial pressure of water vapor at different relative humidity.

2.1.3 Specific Humidity

While the RH gives the percentage of saturation of the air, it does not directly give the actual amount of vapor in terms of mass or volume.

The specific humidity, x (kg-vapor/kg-dry air) of air relates the mass of water vapor to the mass of dry air, and is represented as the ratio of those masses respectively (6):

$$x = \frac{m_v}{m_a} \quad (6)$$

Equation (6) can be expressed in terms of partial pressures and molecular weights by manipulating equation (3) for both water vapor and dry air, and substituting the resulting expressions into equation (6), to obtain (7).

$$X = \frac{m_v}{m_a} = \frac{\frac{M_v p_v V}{RT}}{\frac{M_a p_a V}{R * T}} = \frac{M_v p_v}{M_a p_a} \quad (7)$$

By applying Daltons model, (2), and inserting the molecular weights, of water (18.015 kg/kmol) and dry air (28.971 kg/kmol), the resulting expression for the specific humidity of air is given by (8).

2. Theoretical background

$$X = 0.621979 * \frac{p_v(T)}{p_{tot} - p_v(T)} \quad (8)$$

The specific humidity is thus a function of the partial pressure of water vapor and the total air pressure of the air.

By combining (4), (5) and (8), the resulting equation (9) is a method for calculating the specific humidity when the RH, dry bulb temperature and the total air pressure of the air is known through measurements.

$$X = 0.621979 * \frac{RH * a * 10^{\left(\frac{r*T}{T_d+T_n}\right)}}{100 * p_{tot} - RH * a * 10^{\left(\frac{r*T}{T_d+T_n}\right)}} \quad (9)$$

a	=	611.6441 Pa
r	=	7.591386
T _n	=	240.7263 °C
T _d	=	dry bulb temperature [°C]
RH	=	relative humidity [%]
p _{tot}	=	total air pressure of the surroundings [Pa]

2.1.4 Total air pressure

When conducting moisture related calculations on an open system, the total air pressure is often approximated to have a constant value of 1 013.25 hPa, or 1atm (Moran et al., 2012). This value is the standard pressure at sea level. An open system is however subjected to the local surroundings, with total air pressure variations in both climate, season and height above sea level. Figure 2.2 is a presentation of the variations in total air pressure throughout a year, collected from the weather station at Voll, Trondheim, Norway, 127 m above sea level. The raw data is acquired from a ten- year period between 2008-2017, separated into three graphs presenting both the extreme values of each day as well as the average of the same days each year. From the graphs it can be seen that the extreme values ranges from about 950 hPa to 1 030 hPa, making the use of the standard pressure (1 013.25 hPa) in moisture calculations possibly inaccurate.

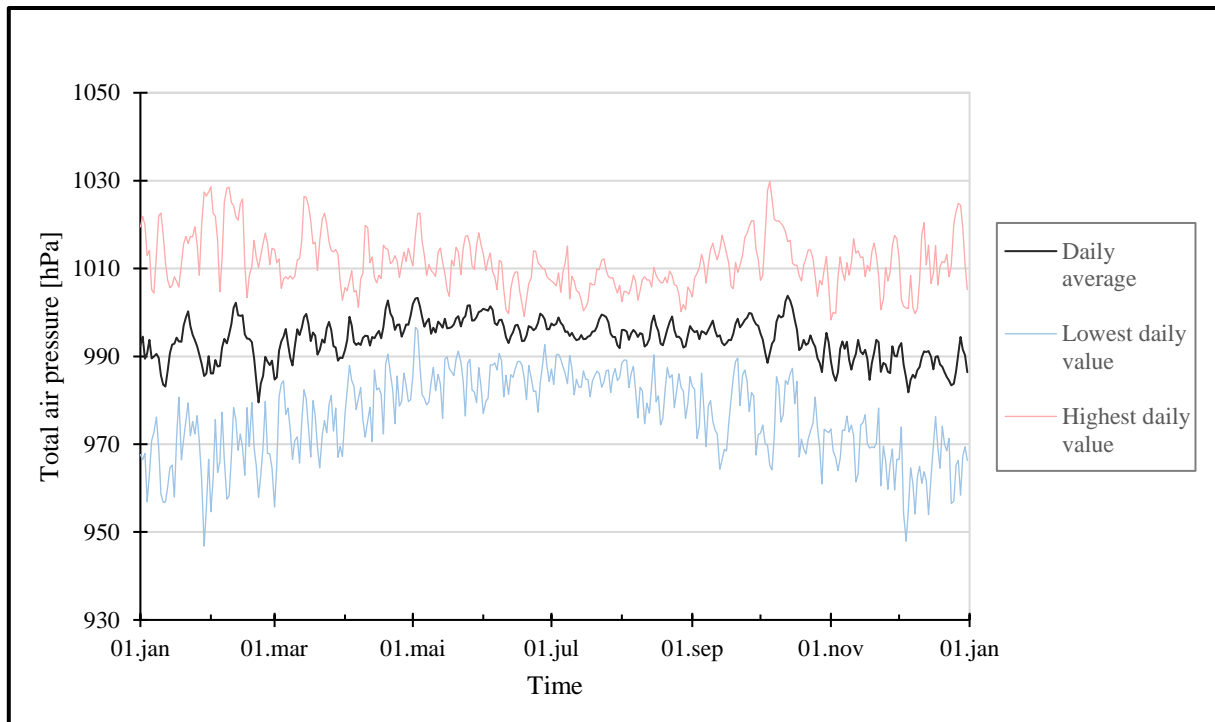


Figure 2.2: The daily average total air pressure and extreme values of outside air in Trondheim, Voll, generated through data from the period 2008-2017. (Meteorologisk Institutt, 2018)

The significance the variations in total air pressure has on the specific humidity is viewed through the 4D- image in Figure 2.3. It is a graphical presentation of the equation for the specific humidity from equation (9). The script for the plot is found in Appendix E. In the equation, there are three variables; RH, temperature and total air pressure. The RH ranges from 0 % to 100 %, while temperature ranges from -20 °C to + 40 °C. The specific humidity is read of in the z- direction (xyz). The effect of changes in total air pressure is viewed through the coloring map within the image. Both the upper and the lower extreme value is compared to the standard pressure in terms of percentwise error. If comparing Volls' lower extreme value of 950 hPa to the standard pressure of 1 013.25 hPa, the error in specific humidity is between 6.66 % - 7.20%, depending on RH and temperature. When comparing the higher extrema of 1 030 hPa to the standard pressure, the error becomes smaller, ranging from 1.63 % – 1.75 %, again depending on RH and temperature.

In both the cases, the error is greatest when the temperature and RH is at its highest at the same time. That is, when the temperature is 40 °C and the RH is 100 %. In Trondheim, this has never been the case, and if a more realistic situation regarding weather and season is used, the errors are reduced.

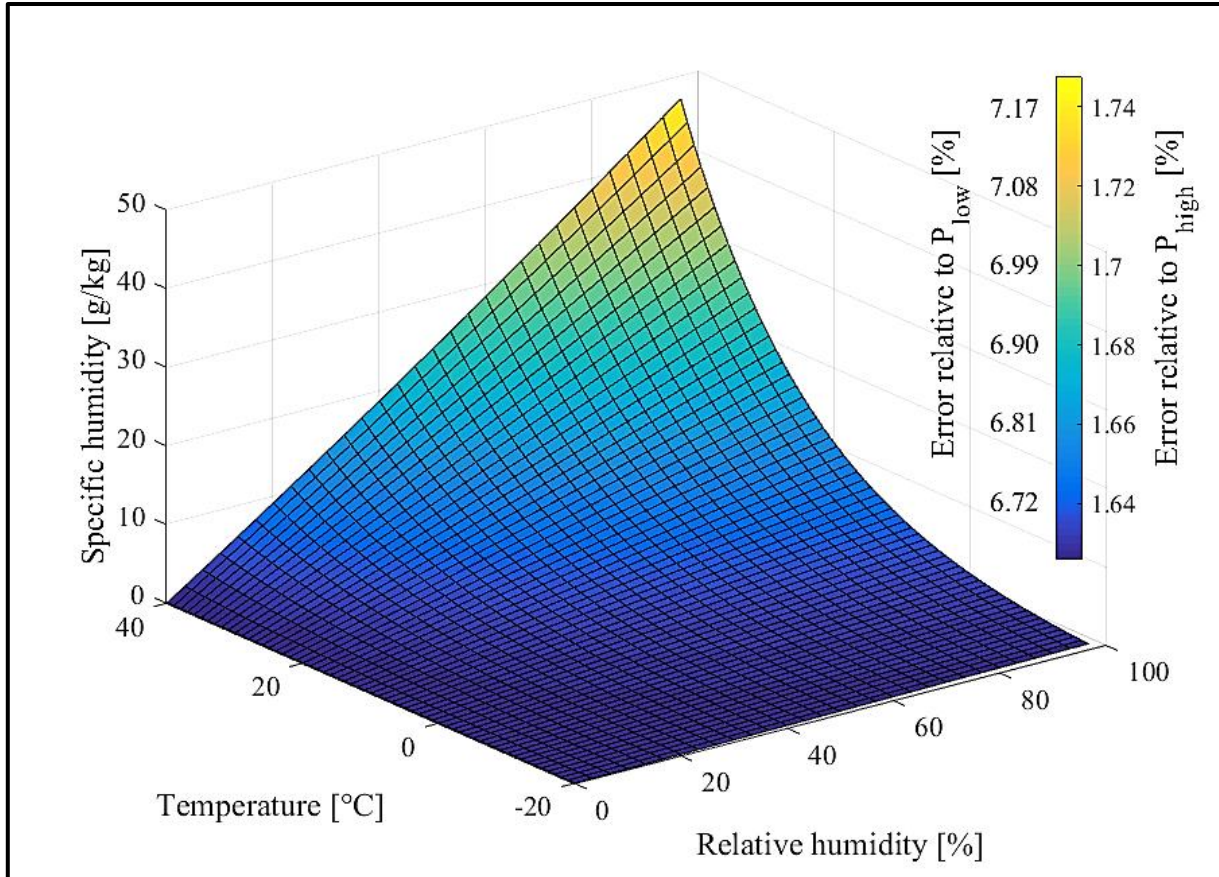


Figure 2.3: Surface plot that shows the influence of changes in both temperature and relative humidity on the specific humidity. The coloring illustrates the error in specific humidity when using the extreme values from Figure 2.2 relative to 1 013.25hPa.

2.1.5 Air density

The density of air is the mass unit divided by its volume, normally denoted ρ (kg/m^3). From the ideal gas law (1) the density of dry air is dependent on both temperature and pressure, decreasing with temperature and increasing with pressure. In most calculations, the air density is considered uniform, with dry air as its only component. However when more accurate and sensitive calculations is considered necessary, the amount of water vapor in the air must be accounted for. The calculations are now dependent on the amount of water vapor present in the given air sample, and the equation is extended to include this. To calculate the air density, the humid air is treated as a mixture of two ideal gases, and by utilizing Daltons Model (2), the resulting expression may be written as (10) (Shelquist, 1998)

$$\rho = \frac{p_{tot} - RH * a * 10^{\left(\frac{r*T}{T_d+T_n}\right)}}{R_{dry} * (T + 273.15)} + \frac{RH * a * 10^{\left(\frac{r*T}{T_d+T_n}\right)}}{R_{vapor} * (T + 273.15)} \quad (10)$$

Where, R_{dry} is equal to 287.05 J/ ($\text{kg} * \text{K}$), and R_{vapor} is equal to 461.498 J/ ($\text{kg} * \text{K}$), which respectively are the specific gas constants for dry- and humid air.

Figure 2.4 is an illustrative coherence between the different parameters included in the air density equation (10) for humid air. The equation is ran twice through the software Matlab resulting in the two surface plots. The script for the plot is found in Appendix E. In the plot lying on top of the other, the air contains no water vapor, as the RH is set to merely 0 %. In the bottom most plot, the RH is set to 100 %, meaning that the air is saturated and thus cannot hold more water. The coherence between these two plots shows that the water content has relatively low impact on the air density within the circumstances of the ranges given. It also shows that the impact of changes in RH is greatest when the temperature is high. If looking at the air state when the humidity has greatest impact, the maximum deviation in air density is about 0.03 kg/m³. Within the limits used, this point is when the air pressure is 1,030 hPa and the temperature is + 40°C.

From the plot, it can be seen that the air density is mostly dependent on temperature, decreasing with increasing temperature. The difference in air density with extreme values of the temperature scale from -20 °C to + 40 °C is at most 0.3 kg/m³.

With increased air pressure, the density of humid air increases. Within the ranges of the plot, from 950 hPa to 1 030 hPa, the difference in air density is about 0.1 kg/m³.

The changes in air density with extreme values within the ranges of Figure 2.4 is about 0.4 kg/m³. This difference is from low air pressure, high temperature and high RH where the density is at its lowest, to low temperature, high air pressure and low RH where the air density is at its highest.

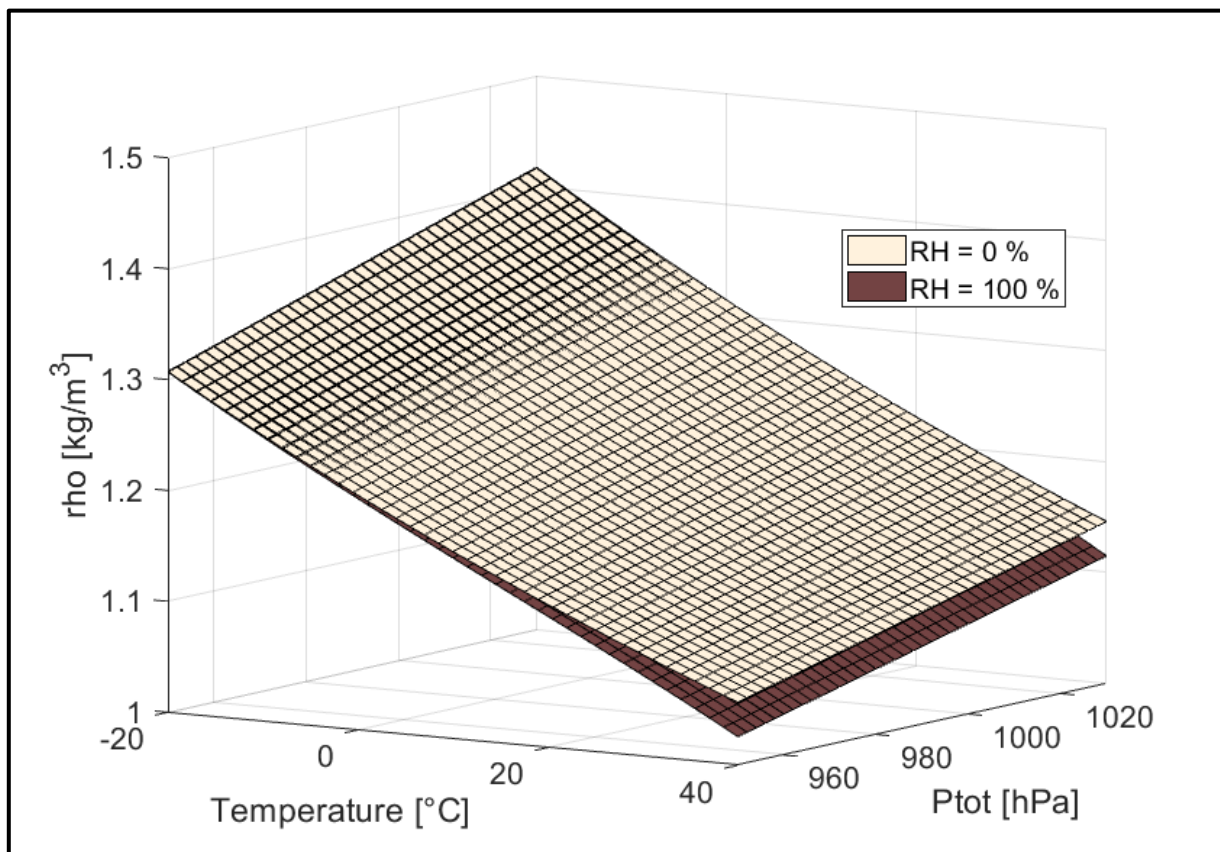


Figure 2.4: Density of humid air relative to temperature and surrounding air pressure, at extreme values of RH.

2.2 Mollier diagram

When studying and estimating changes in the state of humid air, a Mollier diagram is a handy tool. The Mollier diagram is a graphic representation of the relation between temperature, moisture content and enthalpy for systems involving humid air. The total air pressure in the diagram is usually 1 bar (1 000 hPa), considering the humid air as an ideal gas, but can be given at any pressure other than that. (Moran et al., 2012)

Mollier diagrams are either h - x or t - x diagrams, where h is the enthalpy in kJ/kg, x is the specific humidity of the air in kg/kg and t is the temperature in °C. A simplified version of a Mollier diagram, in the form of a t - x diagram is given in Figure 2.5. On the vertical axis of the diagram, a temperature scale serves as the standard variable. The range of the axis is limited by the need, and for HVAC- calculations, the range is usually between -15 °C to 40 °C (Ingebrigtsen, 2016a). The lines extending from the vertical axis are isotherms, lines with constant temperature. The isotherms usually tilts slightly upwards, increasing its tilt with temperature, however in this diagram they are horizontal. The horizontal axis at the bottom is the specific humidity, and vertically running lines from this axis are designated lines of constant specific humidity. The topmost horizontal axis is the partial pressure of the humid air. The diagonal lines that goes from the y- axis and down to the right are isenthalpic lines, or constant enthalpy lines, governing from the specific heats of the humid air. The lines curving from the origin of the diagram and upwards to the right is the RH- lines, increasing in the right direction. The rightmost of those lines is the saturation line, where the air is saturated with water vapor, and thus cannot store any more water.

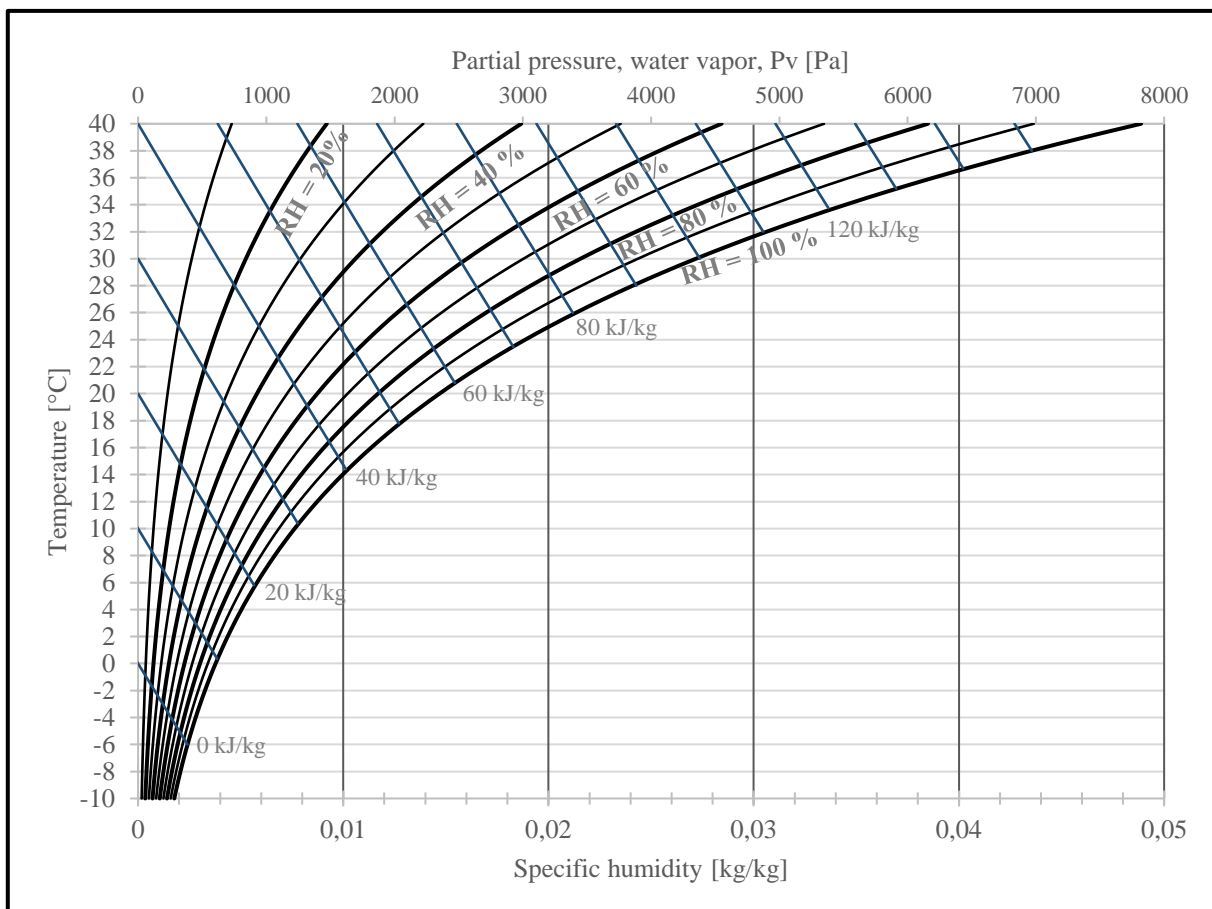


Figure 2.5: Simplified version of a Mollier diagram, showing the relation between air temperature, moisture content and enthalpy at constant air pressure of 1 bar.

When using the Mollier diagram, information about thermodynamic properties of the humid air is approximated, as the diagram is used by reading off data directly. The diagram is built such that if two of the properties are known, all other can be found by inspection. A summary of the most important properties of the Mollier diagram, and how to find them, can be found in Table 2-1. More about the diagram can be read in any basic thermodynamics theory book.

Table 2-1: Description of some the properties a Mollier diagram can provide, and how to locate them (Ingebrigtsen, 2016a).

What	Unit	Designation	Where
Specific humidity	[kg- vapor/ kg- dry air]	x	Read of the x-axis at the bottom of the diagram. A change in water content gives a change in latent heat.
Enthalpy	[kJ/kg]	h	Read of below the saturation line of the humid air. Constant lines inclined downwards to the right. A change of enthalpy means a change in total heat, both sensible and latent.
Dry bulb temperature	[°C]	T	The y- axis of the diagram. Given isotherms is approximately horizontal lines. Measured with a normal temperature gauge. A change in dry bulb temperature implies a change in sensible heat.
Relative humidity	[%]	RH	Multiple curved lines stretching from the origin of the diagram and through it towards the top right. Designated lines for a number of points from 0-100 % RH.
Dew point temperature	[°C]	T _d	Read of by following the constant specific humidity line to the saturation line, and then horizontally to the y- axis on the left.
Partial pressure of the water vapor	[kPa]	P _d	From the given state, follow the diagram horizontally to the topmost x- axis and read off.
Saturation pressure of the water vapor	[kPa]	P _{sat}	From the given state, follow the diagram horizontally until the saturation line is reached. Then follow the diagram vertically to the topmost x- axis and read off.

2.3 Relative humidity

The state of the air in any environment is at constant change, striving to reach equilibrium with the surroundings. By natural or active measures, the air can be affected such that humidity levels changes.

2.3.1 Outdoor

In outdoor air, the nature controls the humidity levels by itself, and cannot be notably affected by humans. Depending on temperature (seasonal variations) and local climate, the state of the air varies throughout the year. Figure 2.6 is showing the annual variations in RH and specific humidity in the Nordic coastal climate of Trondheim. It can be seen that the RH is relatively stable around the year within about 65% -85 %. At the same time, the specific humidity varies between 2 g/kg to 9 g/kg being highest in the summer months. This shows that for the typical summer conditions, air contains more water vapor than in winter conditions. This has to do with temperature variations. If looking back at the Mollier diagram from Figure 2.5, where it can be seen that the ability for the air to store moisture is depending on temperature. The higher the dry bulb temperature, the higher the saturation pressure for the water vapor, ref equation (4). Where the saturation pressure and dry bulb temperature increases, the ability for the specific humidity increases. Thus, the RH does not say anything but the grade of saturation of the air.

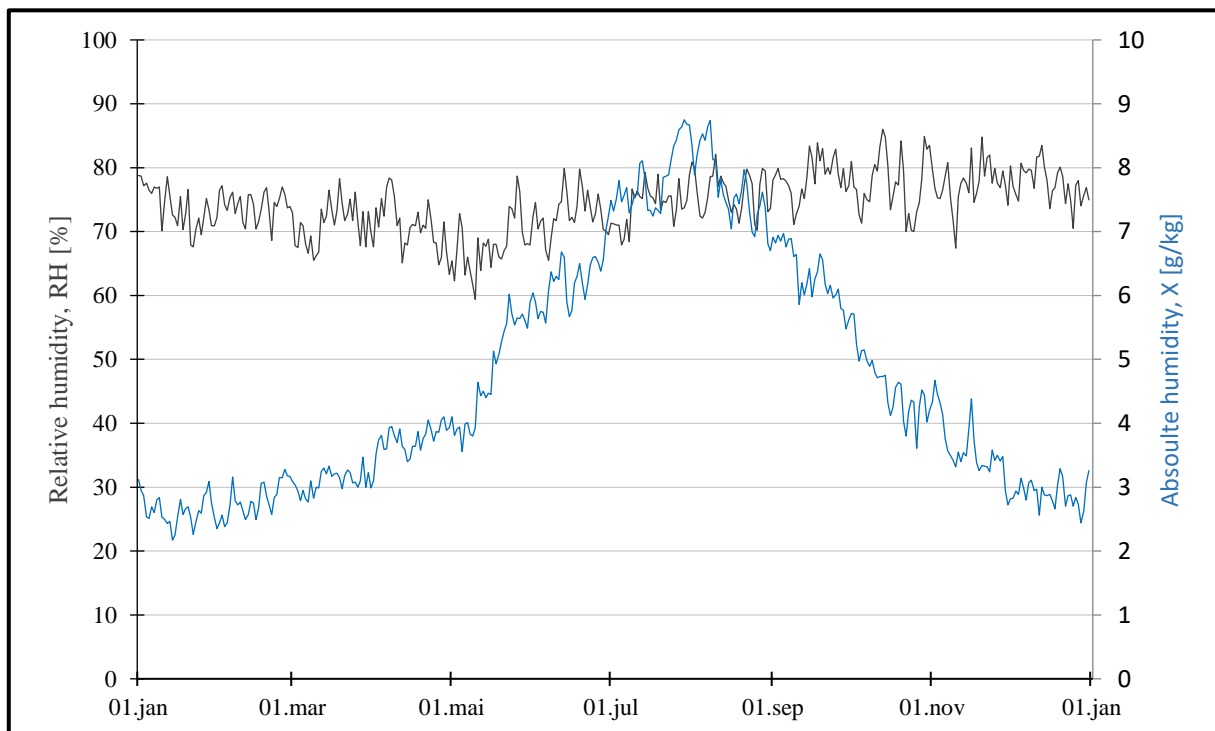


Figure 2.6: The average relative humidity and specific humidity of outdoor air in Trondheim, Voll, generated from daily averages over a period of ten years from 2008-2017 (Meteorologisk Institutt, 2018).

To relate the findings between RH and specific humidity from Figure 2.6 to the Mollier diagram, two typical states, one from winter- and one for summer condition are chosen. Both the winter- and the summer condition has a RH of 70 %, whereas the temperatures differ. The winter case has a temperature of $-5\text{ }^{\circ}\text{C}$ and summer case $+20\text{ }^{\circ}\text{C}$. The two states are plotted in

Figure 2.7. It is evident that one of the notable differences is that the moisture content is, as assumed higher in the summer when the temperature is higher. In terms of specific humidity, based on calculations from (9), the winter case holds 1.84 g/kg while the summer case holds 10.25 g/kg. With increased temperature, the air has the ability to store more humidity, which become evident in this situation. The temperature is higher in the summer than the winter, thus can store more moisture. This situation is reflected into the figure, where the two conditions are equally saturated, but differ in specific humidity. A summary can be found in Table 2-2.

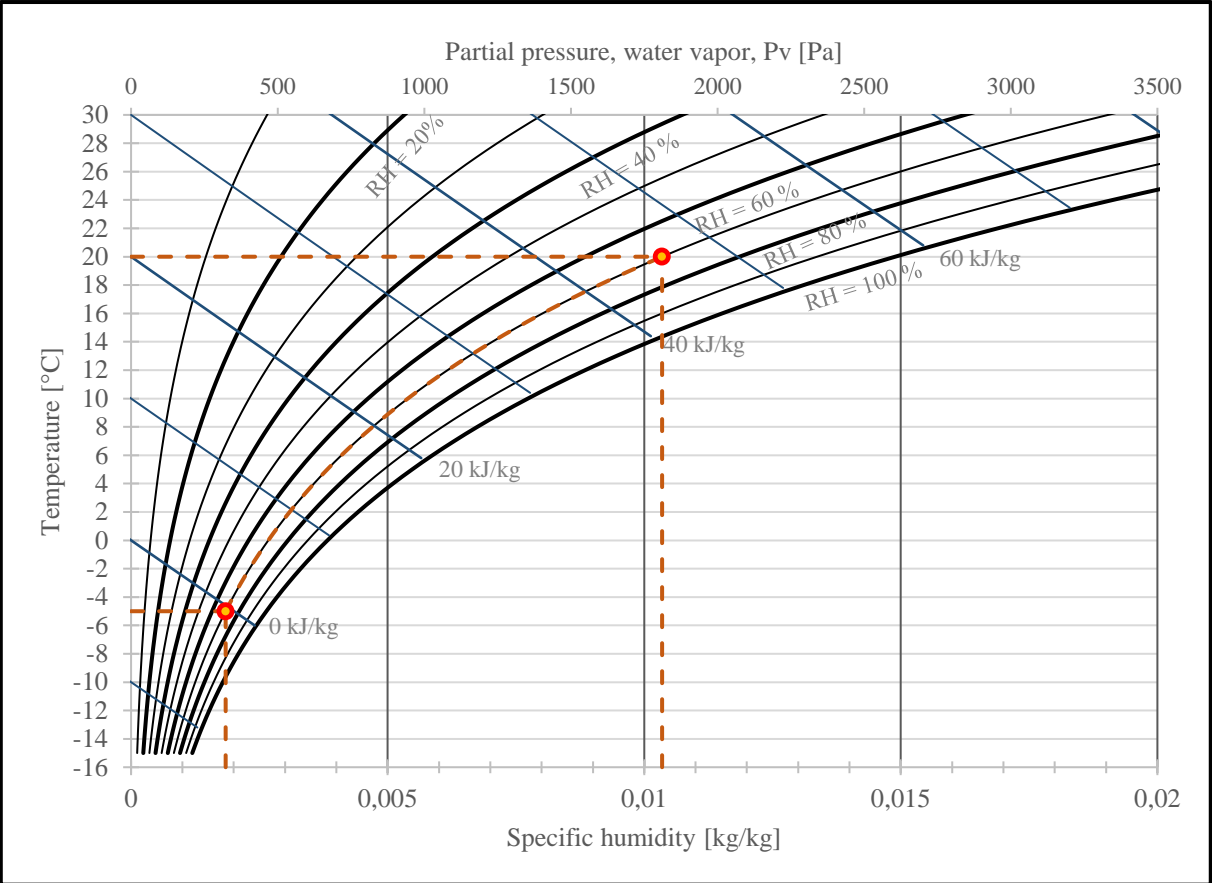


Figure 2.7: Mollier diagram showing the relation between the state of outdoor air in the typical Nordic winter and summer climate.

Table 2-2: The two states used in the Mollier diagram in Figure 2.7.

Case	Temp	RH	Specific humidity
Winter	- 5 °C	70 %	1.84 g/kg
Summer	+ 20 °C	70 %	10.25 g/kg

It must be noted that the outdoor relative humidity is often higher than the presented example. When there is rainy weather outside, the RH is often 100 % regardless of temperature, and while other effects concerning the saturation line can result in condensation on surfaces or creation of fog in the air.

2.3.2 Indoor

The humidity content in an indoor environment is mainly determined by three parameters. The first is the ventilation rate through the building envelope, and this is transferred. Secondly, it is the condition of the air supplied, while the third factor is the addition of moisture from indoor sources, or moisture production. It is the natural balance between moisture gains and losses, which determines the indoor humidity level.

The amount of air exchanged through the building envelope with the outdoor air is determined by the size and use of a ventilation system, openable windows and doors and by infiltration through the building envelope. Increased demand for building tightness makes the use of a mechanical ventilation system necessary in order to ensure a good indoor air quality (Jensen et al., 2011). Infiltration in modern dwellings built today, or totally renovated is required to have a leakage number of 0.6 h^{-1} or less. That is, the amount of outdoor air that enters the building through leakages relative to the total air volume of the building should not exceed 0.6 h^{-1} .

In modern airtight buildings, air is primarily supplied through a mechanical ventilation system. By the use of a heat exchanger, outdoor air is heated through heat transfer with the extract air. In this process, the temperature of the supply air increases towards desired value. Depending on the use of regenerative or recuperative heat exchanges, humidity can also be transferred in the process. In all the supplied air is heated while the RH usually decreases.

RH is one of the key factors in the indoor environment, and one of the parameters the HVAC system has the ability to influence. By the use of active or passive methods, the indoor moisture level can be monitored and controlled, either by preventing it from accumulating in- or diluting it from the indoor air depending on climate, use and requirements. In modern buildings, the use of balanced mechanical ventilation ensures an efficient removal of excess humidity. Though this is usually enough to keep RH within recommended limits it is sometimes necessary with additional measures, either passive or active. Some of these measures are:

- Natural ventilation by opening windows and doors
- Humidifier/ dehumidifier, either in the HVAC plant or other indoor location
- Regeneration of moisture towards an equality through a regenerative heat exchanger
- Actively increasing or reducing the indoor moisture production
- Raising or lowering the indoor temperature, thus decreasing or increasing the RH
- Utilizing materials with high moisture buffering capacities

By the use of active measures, the RH can be held between certain limits. As further elaborated in Section 3.1.2, excessively low or high indoor RH has potential harmful consequences for living life and building structure. By that mean, it is desirable that a certain control is at place. The presented methods differ in their controllability, as some are passively contributing to control, while others can monitor and control the levels directly. Which method to use is depending on the construction type, use or climate. I.e. in tropical climates it is desired to dehumidify the air, while in Nordic winter like climate it is desired (though not common) to rater humidify the air. It is a demand (in Norway) that building built or fully renovated today have to use extract ventilation in wet rooms and kitchen, however it is not a demand that RH should be kept within specific limits (Ingebrigtsen, 2016a). The mechanical extracts in the wet rooms creates an under pressure and ensures that the moisture produced there is not let in to other zones. This prevents the spread of high concentrations of moisture, which could lead to excessive moisture levels and accumulation in unwanted locations.

The indoor RH is also determined by the supplement of moisture through generation from processes and activities indoor. Showering, washing- and drying clothes, cleaning, cooking, evaporation from humans, animals and plants and breathing are examples of indoor processes that generates moisture to the air. Moisture production is thoroughly elaborated in section 3.2.

Indoor RH varies between zones and time of the day due to moisture generation and different use of the space. The room with the largest fluctuations in RH within the shortest time interval is the bathroom. This is due to extensive generation of moisture from showering, use of the sink and similar. When the shower is in use, the RH can reach the saturation point, and condensation occurs on the surfaces. Over time, this moisture will evaporate again and slowly release moisture to the bathroom.

How the state of the air is changing to addition of water depends on *how* the water is added. This can happen in two *main* ways:

- Humidification with steam
- Humidification with water

With the addition of water in the form of steam, the change in the state of the air is approximately horizontal to the right in the Mollier diagram. Depending on the state of the steam, a small temperature rise occurs, however it is usually considered an isotherm change (Ingebrigtsen, 2016a). It must be noted that if the addition of steam results in saturation of the air, with a RH of 100 %, the temperature will increase more rapidly. This is because the isotherms are following parallel to the constant enthalpy lines outside of the saturation line.

If instead water is added, the water will need to evaporate before entering the air. The energy the liquid water needs to evaporate, the evaporation heat, is taken from the air itself. The result is a drop in surrounding air temperature. In the Mollier diagram, this process is approximately following the constant enthalpy line towards the saturation line. The outcome of this process is increased water content in the air, and reduced temperature. Adding water is more efficient than adding steam when it comes to the RH, as the gradient towards the constant RH- lines is steeper.

In order to prevent accumulation of high moisture concentrations over time it is significantly important to place extract and supply valves at recommendations locations. From a perspective seen by RH it is crucial to remove excess moisture in places the production is high. In a residential building this mainly applies to the kitchen, bathroom (or other wet rooms) and at night time, the bedrooms. If using a mechanical ventilation system, extract valves should be placed in these rooms to prevent the air from escaping through infiltration to other zones with lower moisture levels. Thus, the contaminated air is sealed from other zones due to the under pressure and ventilated out of the building.

2.4 Moisture production

When estimating a moisture production, the natural balance between moisture gains and losses is essential. The total indoor moisture content is a direct consequence of the indoor moisture generation and gains or losses through infiltration and mechanical ventilation. The supply of moisture is the difference in moisture content between supplied and extracted air, whereas the significance of the moisture production is primarily governed by the size of the air supplied and extracted to and from a zone (Johansson et al., 2010). The impact of a local moisture generation on the indoor environment is reduced when the air change rate increases. The air change rate in

2. Theoretical background

modern buildings is primarily controlled by the mechanical ventilation system. In zones where the moisture production is higher than average, the ventilation extract valve usually the possibility for forced ventilation. The forced ventilation temporarily increases the air change of the zone to rapidly ventilate humidity, odor and other substances out of the room.

Equation (11) (Geving and Thue, 2002) is a method for calculating the stationary moisture content of indoor air, based on air changes with outdoor and a moisture generation. With the exclusion of the moisture buffer capacity of the building materials and indoor furniture's and equipment, the stationary water vapor concentration in the indoor air can be calculated by

$$x_e = x_s + \frac{G'}{\rho * n * V} \quad (11)$$

x_e	=	specific humidity inside/ extracted air (kg/kg)
x_s	=	specific humidity outside/ supplied air (kg/kg)
G'	=	indoor moisture production rate (g/h)
n	=	air exchange rate of the building/ zone (h^{-1})
V	=	total internal air volume of the building/ zone (m^3)
ρ	=	average density of the air (kg/m^3)

Equation (11) indicates that the specific humidity of the extracted air is a result of the moisture content of the supplied air, the moisture produced indoor, the ventilation rate and the room geometry. Sometimes the geometry of an indoor environment can be hard to predict, especially the volume. If the airflow rate extracted from the ventilation system is known, and the changes in air density with pressure and temperature from equation (10) is considered, the equation can be rewritten as (12).

$$G' = (\rho_e x_e - \rho_s x_s) * \dot{V} \quad (12)$$

The stationary indoor moisture generation can thus be calculated based on measurements of the extracted air volume through the ventilation system as well as temperature and RH to and from the zone. It is assumed that the airflow to and from the zone are equal. In other words, the moisture production rate for a stationary situation can be calculated based on a total air- change rate and a moisture supply. If the specific humidity in the supplied- is the same as the extracted air, there is no moisture production and $G' = 0$ g/h.

2.4.1 Calculating the moisture production from a transient process

The indoor humidity level is constantly striving to change towards a stationary condition as an equality with the surroundings. Air changes to and from a control volume makes the present moisture dilute itself towards what is supplied, and if moisture is produced the ventilation system extracts the excess moisture to balance the air. However, if moisture is not added at a

constant rate, equation (11) and (12) becomes transient. This process happens when a moisture producing source is initiated. Water vapor is released to the surrounding air, increasing the specific humidity and the RH.

Based on the mathematics, a moisture producing process implies that the G' on the left hand side of equation (12) is different from zero. For this to happen, this means that the difference in specific humidity between the extracted and the supplied air must be different from each other. If the production of moisture happens within the control volume, this mean that there is moisture production as long as the specific humidity in the extracted air is greater than the supplied air. Thus, when $\Delta x = (x_e - x_s) > 0$, a source is producing moisture. To calculate the total generation, the transient response of equation (12) can be assumed as a finite number of equally spaced sub- intervals from a starting point, a (s) when $\Delta x > 0$, and continues until an end point, b (s) where Δx eventually reaches zero again (Hughes-Hallet and McCullum, 2005). The number of intervals between these two points, n can be chosen freely from the number of total points, or on the measurement interval frequency of the measurement devices used. Equation (12) is then summarized as a (lower) Riemann sum on the interval $[a, b]$ with n equally spaced rectangles, to give the total moisture production in grams, G (g).

$$G = \dot{V} \sum_{i=1}^n (x_e \rho_e - x_s \rho_s)_{i-1} * \Delta t \quad (13)$$

$$, \Delta t = (b - a)/n$$

The number of measuring points on the interval $[a, b]$ determines the accuracy of the Riemann sum, with decreasing error with increased sub- intervals. The lower Riemann sum uses the left endpoints of each sub- interval to approximate the area of the n rectangles, and sums them up.

Figure 2.8 is an illustration of the use of the Riemann sum, where $n = 6$ rectangles are made up from a data set of 12 points. The lower Riemann sum is most inaccurate when the inclination between the points are the greatest. For moisture production, this can be the case if a rapid release of moisture occurs, i.e. a shower.

2. Theoretical background

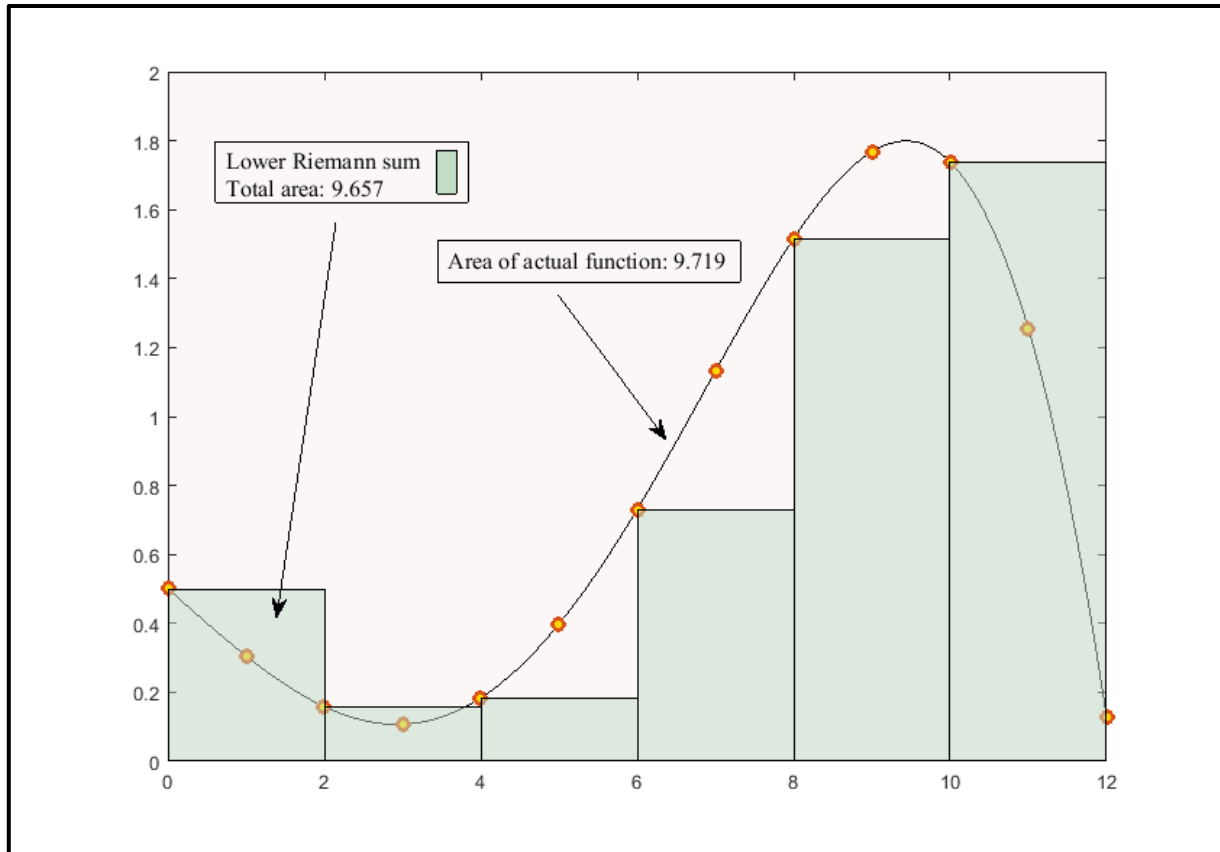


Figure 2.8: Conceptual illustration of a lower Riemann sum with $n = 6$, used to calculate the moisture production in a transient process.

For a greater accuracy, other methods could be applied, such as the composite Simpson's rule. While the Riemann sum uses n rectangles to approximate the area of a set of data points, the Simpson's rule creates parabolas between triplets of points. By summing the area, likewise to the Riemann sum, the area below the graph is approximated. For moisture production the stationary equation (12) becomes equation (14), when utilizing the composite Simpson's rule for a transient process (Mysovskikh, 2011).

$$G = \dot{V} \frac{h}{3} \sum_{j=1}^{n/2} [(x_e \rho_e - x_s \rho_s)_{2j-2} + 4(x_e \rho_e - x_s \rho_s)_{2j-1} + (x_e \rho_e - x_s \rho_s)_{2j}] \quad (14)$$

$$, h = (b - a)/n$$

- a = starting point of the measured interval
- b = end point of the measured interval
- n = the number subintervals of equal length over the range [a, b], $n = \text{even}$

Figure 2.9 shows the use of the composite Simpson's rule. In comparison to Figure 2.8, this figure has the same number of equally spaced sub-intervals, $n = 6$, and the data set made up of 12 points. The Simpson's rule creates parabolas between triplets of points, making the accuracy higher than the Riemann sum.

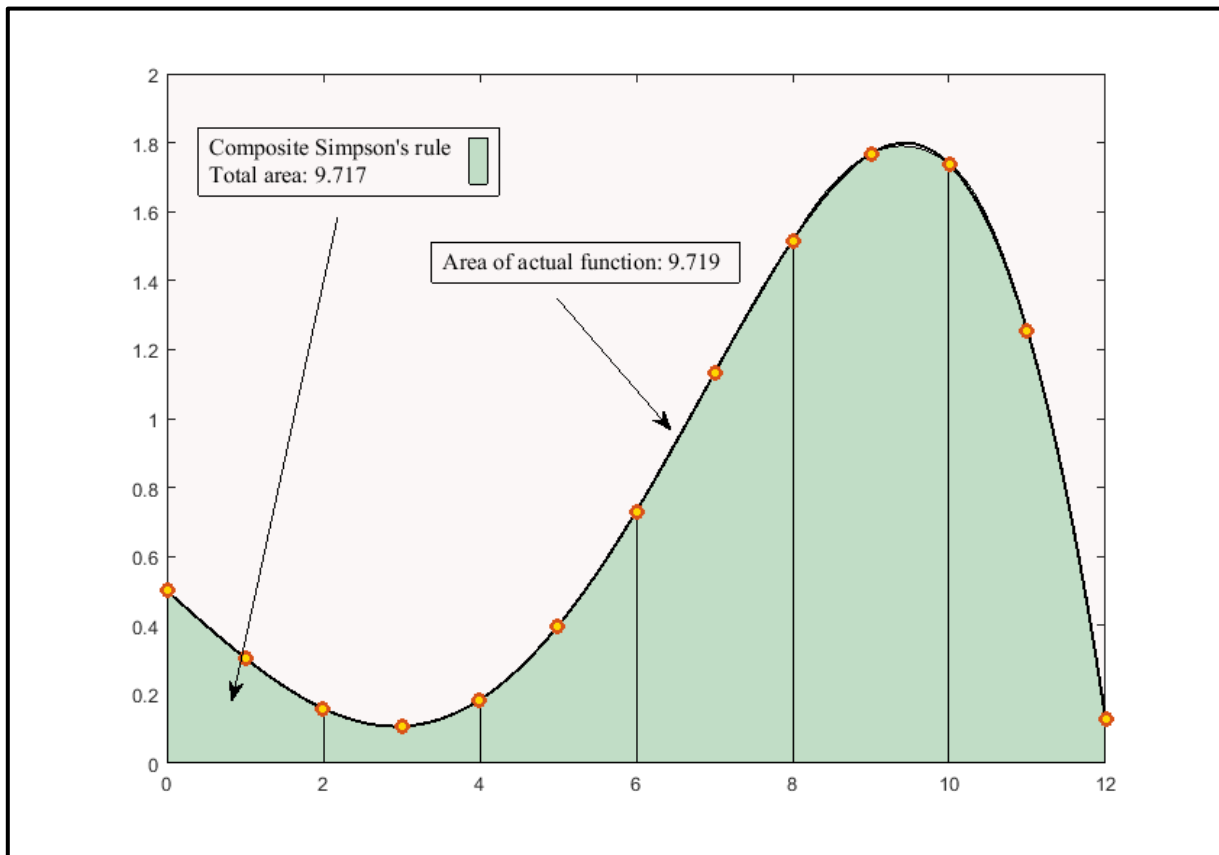


Figure 2.9: Conceptual illustration of composite Simpson's rule with $n = 6$, used to calculate the moisture production in a transient process.

3. Literature Review

This chapter is both a summary and an extension of the literature review from the project work carried in the autumn of 2017, with the same title as this master thesis. The chapter consists of three parts, whereas the first part is about how humid air affects materials and living life. The second part is state of the art data on moisture production rates from indoor sources, and the third part is related to the moisture buffering effect.

3.1 Moisture affections on materials and living life

3.1.1 Thermal environment

Indoor climate is a composite term comprised by the five components thermal-, atmospheric-, acoustic-, actinic- and mechanical environment. Single handedly each of those influences our perception of the indoor climate in different ways, and together with the esthetic- and psychological environment, they are forming the term known as indoor environment. (Ingebrigtsen, 2016a)

One of the terms, the thermal environment, is comprised by those parameters who has an influence on the human heat balance. Heat is lead away from the body by convection with the surrounding air and by radiation to surrounding surfaces. With normal room temperature, each of these stands for about 40 % of the total heat loss, whereas the last 20 % is from evaporation and exhalation. The exact distribution is a result of activity level, air velocity and RH in addition to operative temperature, vertical temperature gradients and mean radiant temperature (Incropera et al., 2013). The RH of indoor air is a parameter that can greatly affect the functional performance of a building, as well as resident health (Jensen et al., 2011). Knowledge of fluctuations and possible influence the variations in RH has on living life and materials is required to avoid potential problems.

3.1.2 Relative humidity

Humans cannot perceive the actual RH of indoor air, as there is no sensory organ to determine the value. According to Ingebrigtsen (2016a) our subjective perception is often misleading compared to accurate measurements. Although humans cannot feel RH, certain phenomena is occurring at different levels, and humans can detect them visually or physically but not from percentage to percentage. It is rather a visual detection on exposed materials or a bodily reaction over time, i.e. seasonal variations in RH, or dampness on surfaces. In modern, high insulated dwellings and offices it is recommended that the indoor RH is kept between 30 % - and 70 % (Ingebrigtsen, 2016a). At certain levels typical problems arises, and some problems arising at

the lower range may not be detectable at all in higher levels. There is not a specific value that is perfect for all purposes, neither for humans or materials.

In a health perspective, the indoor RH should be kept above 30 %. Reinikainen and Jaakkola (2003), Wolkoff and Kjærgaard (2007) and Sato et al. (2003) describes the effects of too low RH on the human body as dryness of skin and throat, sensory irritation of eyes and dryness of the mucous membrane (<10% RH for mucous membrane). When RH is too low asthma and allergy symptoms can worsen, and cold flu viruses may spread more rapidly (Lowen et al., 2007).

If it is Nordic winter like temperatures outside, the risk of condensation increases on structural surfaces. From equation (4) and (5), it can be seen that when there is an increase in RH, the dew point (a RH of 100%) of the air increases. This is due to an increase in the saturation pressure of the vapor. Surfaces of (or within) the construction, like thermal bridges, windows and doors, have the risk of reaching the dew point due to local lower temperatures. If the dew point is reached, condensation of water from the air then settles as droplets on the surface of or is absorbed into the material. If an area is exposed to condensation and moisture over time, and left untreated, the spread of rot, bacterial growth, mould and fungus can be the consequence (Oreszczyn et al., 2006). Arena and Blanford (2010) conducted a research in 60 US homes, and concluded that moisture related problems occurred most often around windows and in the bathroom. Condensation on indoor surfaces facing outdoor also increases the heat transfer through the building envelope, because of the larger specific heat capacity of water compared to a dry wall. Increased heat transfer implies increased energy use for heating and cooling (Yik et al., 2004)

If condensation occurs inside the wall and mould accumulates freely, it can be hard to detect and affect the indoor environment in terms of perceived air quality (Fang et al., 1998). Asthma and allergy sufferers may experience worse or more frequent symptoms from mold or fungus. According to (Kalamees et al., 2006) 30-50 % of increases in respiratory and asthma related problems are linked to building dampness and mold.

3.2 Moisture production

Moisture production or moisture generation is the supplement of water in a gaseous phase from a source to the surrounding air. Depending on the type and size of the supplement of moisture, the process always changes the state of the air as an increase in RH towards the dew point of the present air. The enthalpy, h (kJ/kg) of the humid air either increases or stays the same, depending if direct vapor or liquid water is added. (Moran et al., 2012)

The indoor moisture production from activities varies between the different sources depending on several factors. The total load will not only vary from day to day but also between workdays or weekends and between seasons. Different activities is carried out at different times, based on habits, resident behavior and frequency of moisture producing activities. (Kalamees et al., 2006)

Table 3-1 is an overview, showing the most frequent indoor moisture producing sources and links them to the most probable zone of occurrence. As seen in the table, different rooms has distinct unique sources, while some sources are appearing in more than one zone. These sources cannot be linked to a certain space, but is according to the authors usually found in more than one room.

Table 3-1: Sources of moisture production at different room types of a dwelling (Johansson et al., 2010).

Space	Moisture sources
Living room	<ul style="list-style-type: none"> • Humans • Pets • Aquarium • Plants • Ironing • Floor mopping
Bathroom	<ul style="list-style-type: none"> • Humans • Showering • Bathing • Tumble drier • Clothes drying by hanging • Floor mopping
Bedroom	<ul style="list-style-type: none"> • Humans • Pets • Ironing • Plants • Floor mopping
Kitchen	<ul style="list-style-type: none"> • Humans • Dishwashing machine • Hand dishwashing • Food preparation • Plants • Floor mopping

3.2.1 Moisture production rates

Moisture production from humans is depending on factors such as the state of mind, activity level and metabolism (Johansson et al., 2010). As moisture is produced from both respiration and precipitation, the total production rate is ranging from a calm sleep, to hard work in high temperatures. The most recent work has been conducted by Ilomets et al. (2017), who studied moisture production in bedrooms. The bedroom is a zone that has two distinct differences in moisture release rate throughout a day, in nighttime and in daytime, where it is higher at nighttime. The presence of humans induces a relatively constant moisture production rate in nighttime, while it can be practically zero during daytime. Ilomets et al. (2017) found the average production from a sleeping adult in a master bedroom during nighttime to be 72 ± 50 g/h. The uncertainty comes partly from the found dependency on the outdoor temperature, as the moisture production was measured to increase during winter. However, this could, according to the author, have been a release of moisture through desorption to the air from surrounding surfaces, driven by the low indoor RH when outdoor temperatures crawls below 0 °C. Another author, Johansson et al. (2010) gave an estimate on the moisture production from sleeping as 30 g/h for adults, and 25 % less for a child. In addition the same author gathered

3. Literature Review

metadata on moisture production from humans, from a three other authors. The data can be found in Table 3-2.

In the bathroom, water activities is the dominant source of moisture production. With the use of a tap or a showerhead, the release of moisture can occur at a high rate. The rates seen in this room is usually higher than any other zone in a normal dwelling (Zemitis et al., 2016). The duration of the moisture production usually has an intensive, short duration, before the aftermath slowly releases moisture. This applies for i.e. a shower, where the production is high while the shower is in use, and the aftermath would be the condensed water on surfaces and spilled water on the floor evaporating. Thus, a slow release of moisture occurs after the initial source is turned off. Kalamees et al. (2006) collected and tabulated metadata on moisture production from showering. Whereas the background of the data on the way it presents its units varies, the rates ranges from 220 g/5min – 250 g/5min, or 2460 g/h – 3000 g/h. In comparison Pallin et al. (2011) presents rates up to 400 g/5min, or 4800 g/h.

The use of extract valves in wet rooms draws the excess moisture out of the building efficiently to prevent it from accumulating or escaping to other zones. When a moisture source is active, the RH rises towards the dew point of the air. If the dew point is reached, condensation on the interior surfaces will occur. As described in the previous section, mold and fungus can grow freely if the surfaces are exposed to high humidity levels frequently. However, in wet rooms, the choice of materials must be chosen such that the water vapor permeability, M (g/h*m²*Pa) is low. The choice of materials in wet rooms are regulated such that the rapid release of moisture, and the frequent condensation is not adsorbed, thus chosen to have a low water vapor permeability. (Johansson et al., 2010)

Another intensive source of moisture is washing and drying of clothes. The drying process can happen through a tumble dryer or by hanging the wet clothes on a rack. The total moisture production varies from the amount- and the water content of the cleaned clothes. The frequency of cloth washing is according to Annex27 (1995) between 5 times/ week to every day for a four person household. Zemitis et al. (2016) conducted research on the total release of moisture from washing clothes in a washing machine, and drying them by hanging them up. A number of different scenarios, from the amount and different types of clothes to the centrifugal RPM on the washing machine were tested. The conclusions from the research were that the drying process would account for an average release of 1.22 kg vapor/ day, based on the average number of washes per week (2) for two persons. According to Standard (2002), the total release is 1.5 kg/ day for one person, based on the same assumption as Zemitis et al. (2016). Angell and Olson (1988) concluded that one 3.6 kg load of clothes released 2.2 kg-vapor/ machine – 2.95 kg-vapor/ machine.

Plants can be present in all rooms of a dwelling, and require water from time to time to survive. While most of the water added water is utilized through photosynthesis in the plant, some of it can vaporize from the soil. Zemitis et al. (2016) describes the exact amount of vapor released as a dependency of the size and type of plant studied. In all, the study revealed other authors work, with moisture release rates ranging from 0.84 g/h (Yik et al., 2004) to 20 g/h. In Zemitis et al. (2016) study it was revealed that the release of water vapor calculated from watering and weighing plants, was between 0.07 g/h to 0.12 g/h, or substantially lower than 20 g/h.

Different sources releases different amounts of water vapor to the surrounding air, and both the total amount and rate of release varies greatly. By gathering the presented moisture production rates from different authors work, in addition to values from additional sources and activities, Table 3-2 is generated.

Table 3-2: Moisture production from different indoor sources.

Activity	Main dependencies	Moisture production	Source
Human perspiration and respiration	<ul style="list-style-type: none"> • Activity level • Metabolism • State of mind • Size (age) 	Sleep: 72 ± 50 g/h or 200 g/h/4pers	[1], [2]
		Light activity: 30 – 120 g/h	[3]
		Medium activity: 79 – 200 g/h	[3]
		Hard activity: 102 – 300 g/h	[3]
Showering	<ul style="list-style-type: none"> • Shower length • Water temperature • Flow rate of water • Spillage of water on floor and walls 	Rate: 2640 – 3000 g/h	[4]
		Event: 200 – 400 g/event	[5]
Bathing	<ul style="list-style-type: none"> • Water temperature • Flow rate at filling • Spillage • Bath length 	60 – 160 g/event	[5]
Cooking	<ul style="list-style-type: none"> • Electrical/ gas • Amount • Type • Meal of the day 	Breakfast: 170 – 270 g/event	[4]
		Lunch: 250 – 320 g/event Dinner: 580 – 780 g/event	
Dishwashing	<ul style="list-style-type: none"> • By hand or with washing machine • Amount • Water temperature 	By hand: 100 – 600 g/event	[3], [4]
		Washing machine: 200 – 400 g/event	[4]
Drying clothes	<ul style="list-style-type: none"> • Hanging of clothes or with laundry drier • Amount 	Hanging: 450 – 2300 g/event	[3]
		Hanging: 1660 g/event	[2]
House plants	<ul style="list-style-type: none"> • Watering frequency • Size and type of plant • Number of plants 	Varied: 0.07 – 0.12 g/h	[2]
		Small: 0.12 – 0.24 g/h	[4]
		Med: 0.17 – 0.36 g/h	[4]
		Large: 0.5 g/h	[4]
		Single: 0.02 – 0.36 g/h/plant	[3]
Floor cleaning	<ul style="list-style-type: none"> • Size of floor cleaned • Mop type • Quantity of water left on the floor 	10-100 g/m ²	[3]

[1] = Ilomets et al. (2017), [2] = Yik et al. (2004), [3] = Johansson et al. (2010), [4] = Kalamees et al. (2006), [5] = Pallin et al. (2011)

As a summary of the data presented in this section, it is clear that between the same sources, the moisture production rates varies. Moisture generation is difficult to interpret or analyze, as there is such a great variety of ways to conduct each activity. In addition, different authors are presenting their research in different ways, depending on how the experiments is conducted.

3.3 Moisture buffering

Moisture buffering is the ability of a material to moderate indoor humidity variations through adsorption and desorption of water vapor. By utilizing the properties of hygroscopic materials of the building envelope and furnishing the moisture content of the indoor air could possibly be passively controlled to improve the IAQ. It is believed that moisture buffering could smooth out the variations in moisture level, thus reducing the peaks in RH and achieve a more stable indoor climate in terms of RH (Zhang et al., 2017a). Moisture buffering works in the way that a change in RH makes the hygroscopic materials absorb (or desorb) some of the moisture present in the surrounding air, resulting in a lower impact on the indoor climate. Thus, the change in RH is seemingly lower than it could have been. Depending on whether the moisture content increases or decreases, the pores of a material inhales or exhales the moisture through its internal structure. By utilizing this phenomenon, the need of active, energy consuming measures like dehumidifiers can be avoided, resulting in a more stable moisture content of the indoor air, better IAQ and a lowered energy need. (Maskell et al., 2017)

An indoor moisture production results in an increase in RH. The impact of the production is mainly depending on the size of the room and the air change rate, but can also be influenced by the choice of furnishing and materials. Pallin et al. (2011) conducted a research on how moisture production influences the RH in two different scenarios. One with, and one without moisture buffering from hygroscopic materials. By simulation of 1000 Swedish households, based on gathered information and statistical data on climate, type of dwelling, resident behavior, indoor moisture production rates and technical parameters, the indoor air humidity was estimated. Figure 3.1 shows a sample of the simulation results, where the indoor RH between three days in February is presented. Hourly mean values of calculated indoor RH with and without moisture buffering from hygroscopic materials is drawn, and as the model predicted, the difference in RH of the dwellings are larger for the case of neglecting hygroscopic buffering compared to when it is accounted for. The author compared the simulated cases, with measurements for the extract air of Swedish multi- family dwellings, and the results showed good coherence.

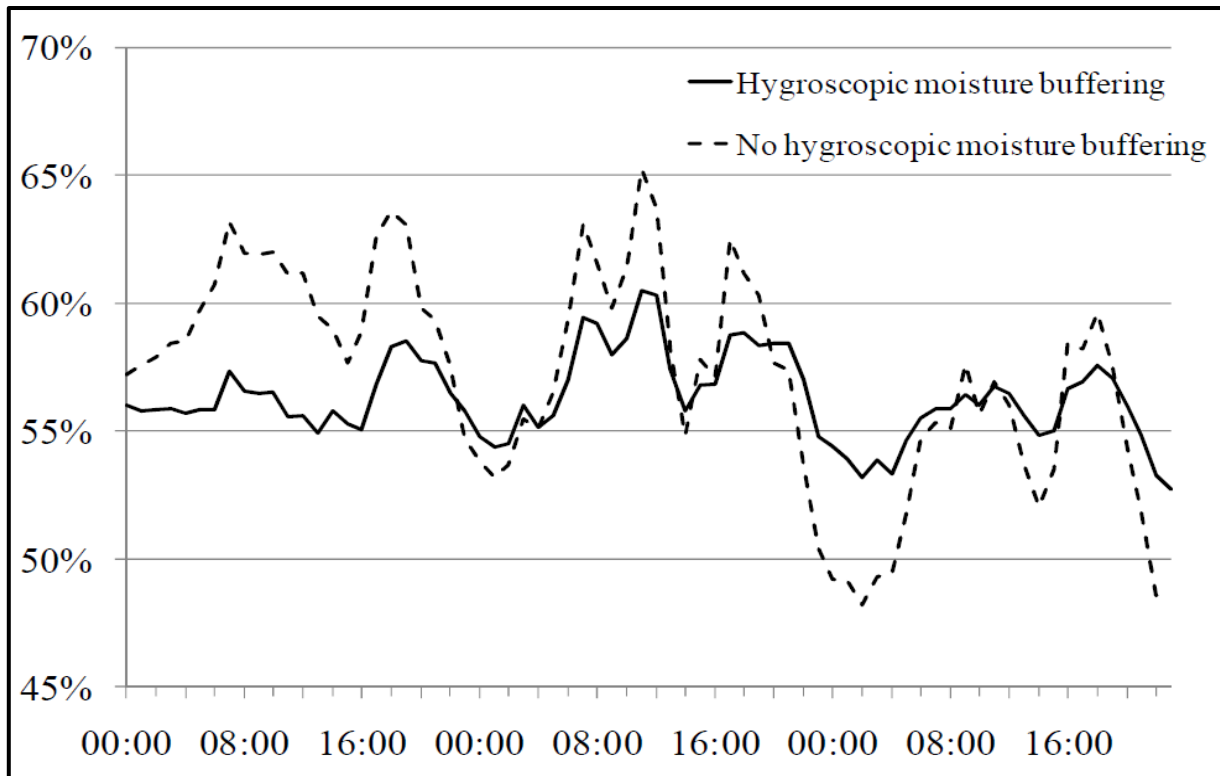


Figure 3.1: The buffering capacity of materials are damping the effects of changes the moisture content of indoor air (Pallin et al., 2011)

The moisture buffering effect can be categorized into three descriptive levels – material level, system level and room level, as illustrated in Figure 3.2. The material level is categorized by the properties of the material, such as density, porosity, water vapor permeability, sorption properties etc. The ideal MBV is found here, where the material properties is used to estimate the moisture capacity. The next level is the system level, where the practical way of estimating MBV is found. This level deals with the influence between material and environment. Furthermore to the last level, known as the room level is characterized by factors such as the total surface area exposed, moisture load, air change rate and the state of supplied air. The effectiveness of moisture buffering is thus a complex function involving material properties and rate of changes in the surrounding air. (Zhang et al., 2011)

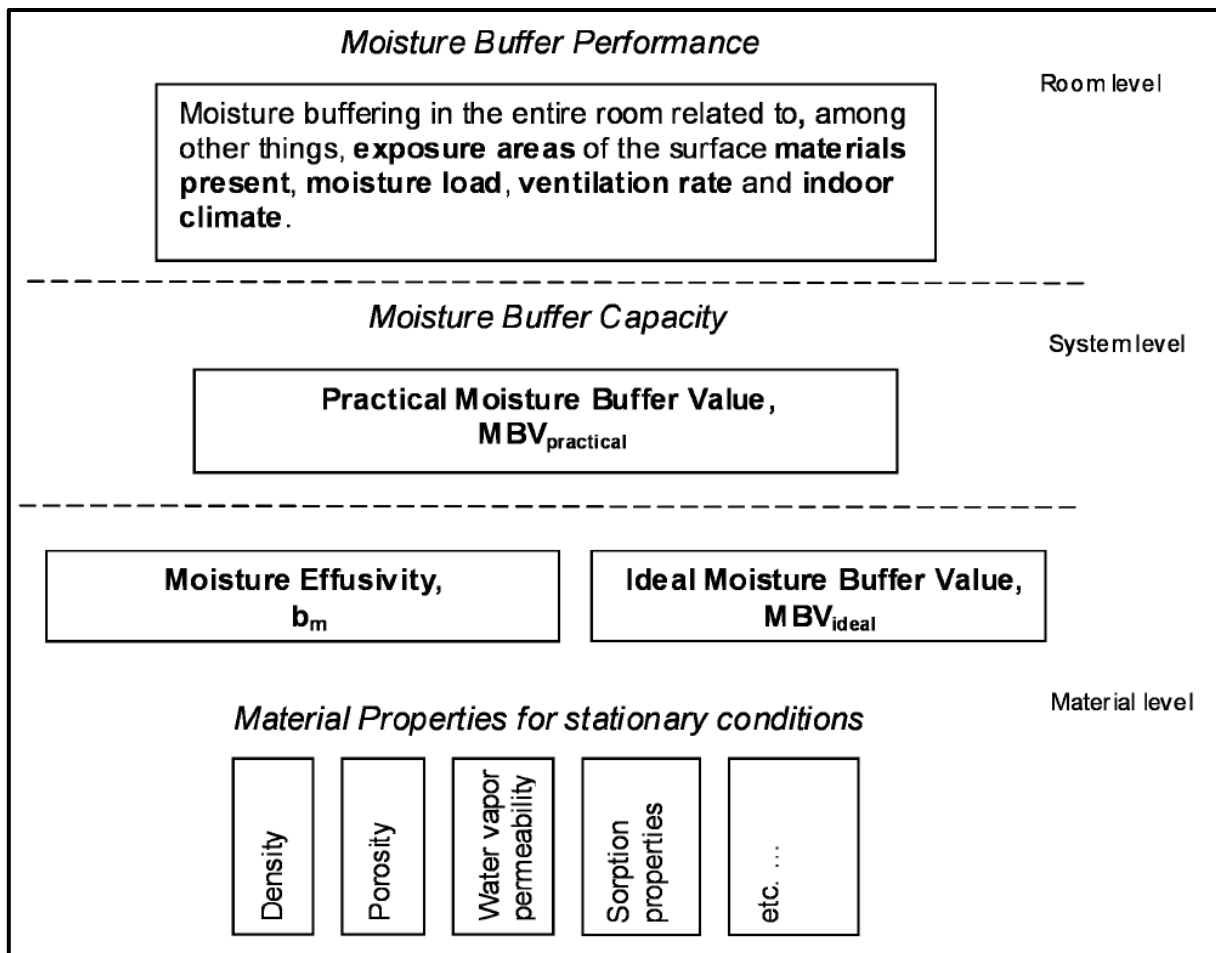


Figure 3.2: The three description levels for the moisture buffering phenomena (Rode et al., 2007).

In the literature review of Rode et al. (2007) the research of other authors work on the characteristics of the moisture buffering in different materials is summarized. The results shows that end grain wood had the best possibility to reduce the RH, due to the rapid diffusion and great moisture capacity of wood. On the other hand, cellular concrete with a covering of gypsum plaster showed the best characteristics within typical commercial construction materials. This is, according to Rode et al. (2007) supported by other authors. Moisture transfer between wood based structures can, according to Rode et al. (2007) reduce the top peak in indoor RH by as much as 35 %, and increase the minimum value with up to 15 %. In addition, it was important to underline that it was necessary to include the effect from indoor furniture's when studying the moisture buffering effect.

3.3.1 Moisture buffer value

A way of categorizing the moisture buffer capability of a material is to use the moisture buffer value (MBV). MBV is an indicator of the adsorption/ desorption of moisture when a material is exposed to diurnal variations in RH. MBV has the unit of $g/ m^2 \cdot RH$. From the unit it can be seen that MBV quantifies the adsorption and desorption of water in grams per square area, per percentage change in RH. There are two ways of finding the MBV, one theoretical and one practical. While the theoretical version estimates the MBV from physics and mathematics, the practical version estimates it, by measurements.

With the practical version of MBV, a test chamber is beneficial to use. A test chamber gives the opportunity to carefully control, and monitor necessary properties under a certain control. In the test chamber a sample of a material, either pure, or a composite with known composition is placed. The air change rate, and the state of the air is monitored, and a change in RH is induced as a square waveform. The material is exposed to cycles of i.e. 8 hours of a RH of 75 % followed by 16 hours of a RH of 33 % (Rode et al., 2007). By tracking the transient response in terms of the material weight between a low- and a high RH cycle, the MBV is estimated. Figure 3.3 is an example of the use of the practical MBV, where the mass of the sample is plotted vs time in addition to showing the square waveform of RH induced. The difference between the lowest and the highest mass of the sample within one cycle is the adsorbed moisture. The MBV is then calculated, based on the difference in RH within the measurement, and the size of the sample. The higher the MBV, the higher the moisture buffering capacity of the material.

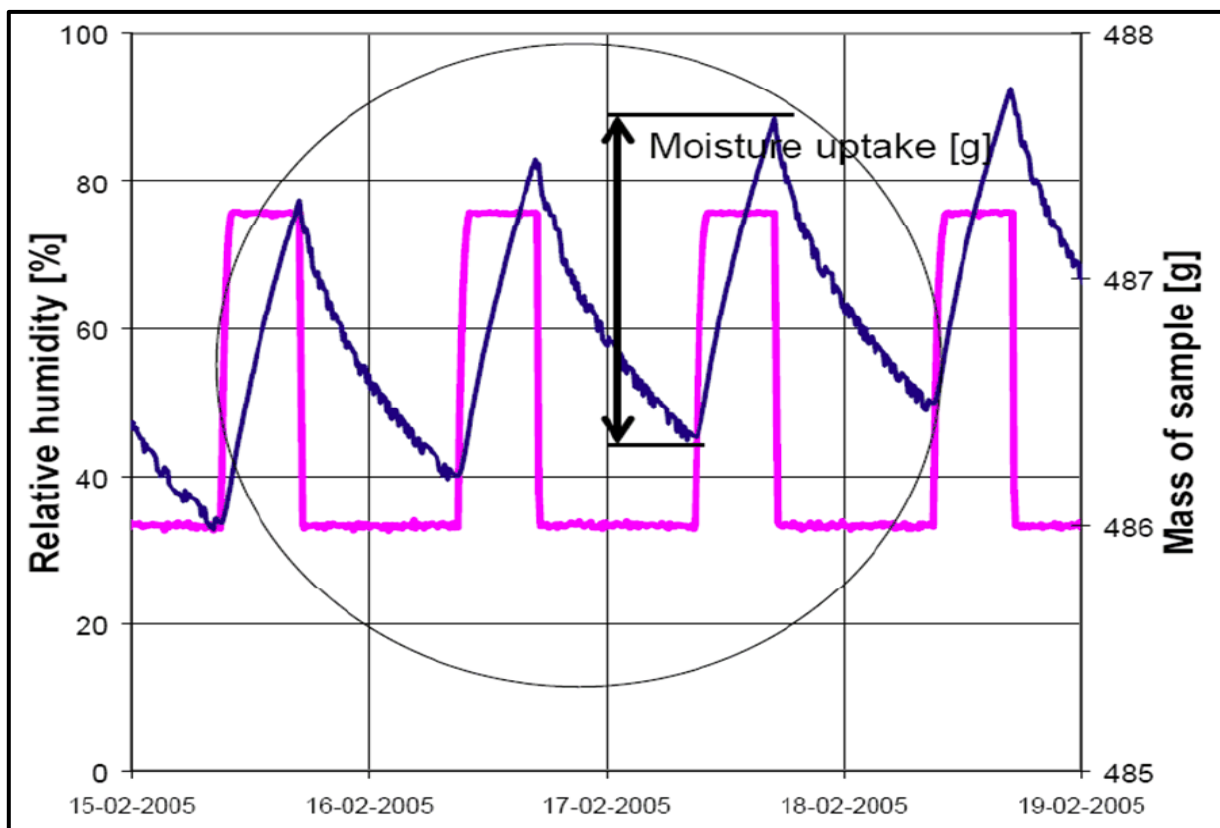


Figure 3.3: Mass change of a material sample, when exposed to waveform changes in RH (Rode et al., 2007).

By measuring a range of applicable materials for an indoor environment, the MBV can be used as a measure on the quality of the moisture buffering. Rode et al. (2007) presented research where three institutions conducted a study to quantify the MBV of a range of materials based on the practical approach. Figure 3.4 shows that the different institutions results are comparable with each other, even though the equipment used was not the same. Materials like untreated spruce and birch boards and cellular concrete performed as best buffers, while materials like brick and concrete were able to buffer under the half of the best buffers.

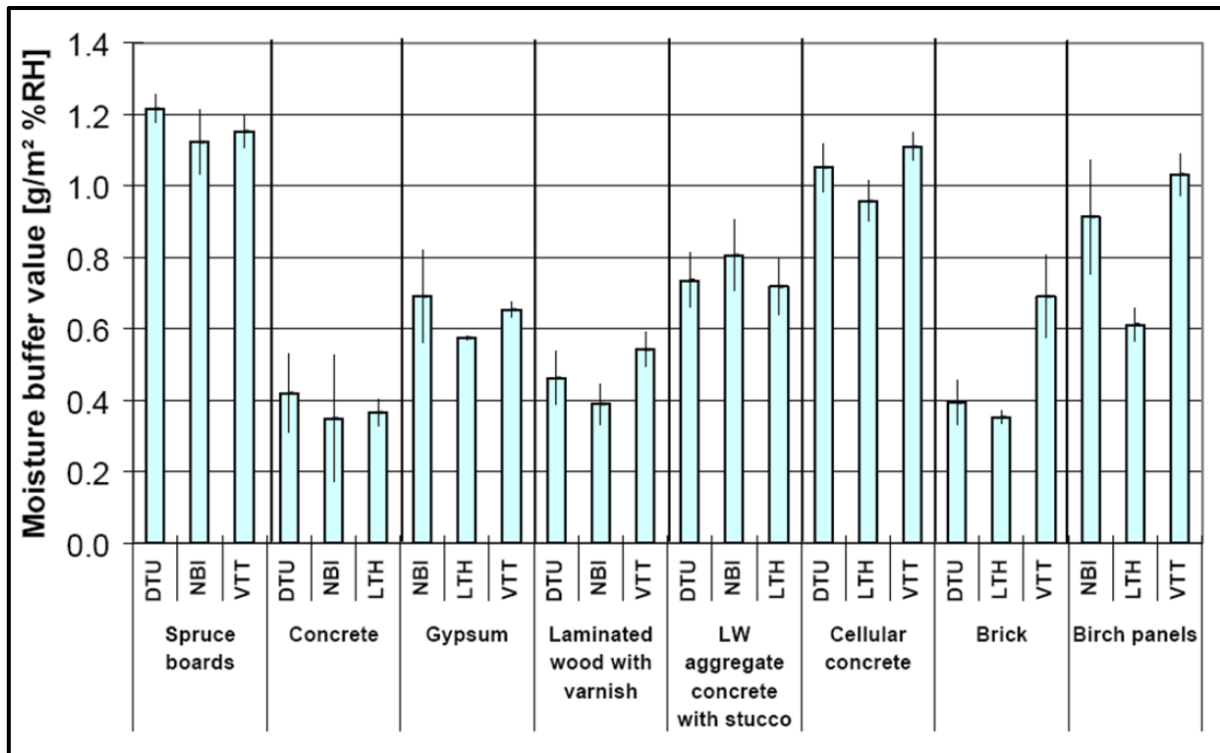


Figure 3.4: Moisture Buffer Values found by different institutions for the different materials (Rode et al., 2007).

A theoretical version of the MBV is based on mathematical expressions and material properties, named MBV_{ideal} , as described in Rode et al. (2007). This expression used heat- and moisture transport analogy, in combination with material properties to calculate the MBV for a given material. The background for the calculation can be thoroughly investigated in Rode et al. (2007), where the physics and mathematics is described. Zhang et al. (2017b), further develops this model, including a correction factor coefficient to deal with a greater range of changes in RH, instead of the previous model, who used a square waveform to track changes in RH.

The speed of which different material absorbs and desorbs moisture varies, and is given by the properties of the materials (Maskell et al., 2017). If moisture buffering is a priority when choosing materials and furnishing, it is necessary to look into the moisture load of the given room. The optimal choice is different depending on if the average RH is high or low. Figure 3.5, obtained from (Maskell et al., 2017), presents three different claddings used as wall materials in dwellings. It can be seen that the rate of moisture sorption is different between the three materials, under the same surrounding air state. Of the three, clay has the superior moisture buffering properties. Thus, Clay absorbs and desorbs moisture from the surrounding air faster than what the other two can.

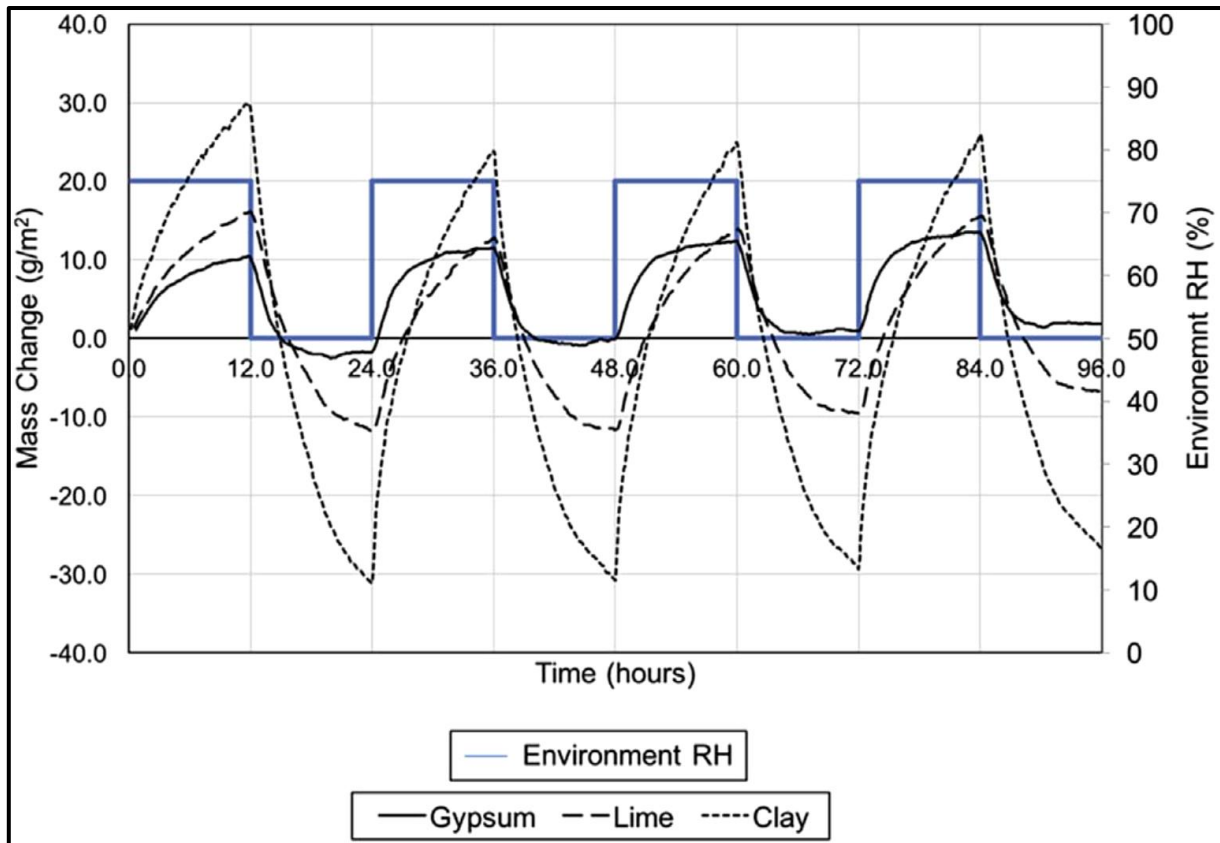


Figure 3.5: Mass change of three types of plasters when exposed to waveform changes in RH. (Maskell et al., 2017)

3.3.2 Material thickness

Different materials have their own unique thermodynamic properties. Within a fluctuation RH-environment, the sorption kinetics of typical surface materials means that moisture can only penetrate to a certain depth during adsorption before desorption begins and water is drawn out of the material. To be able to maximize the benefit from moisture buffering, it is crucial that the material thickness is sufficient to exploit the potential of the process, while at the same time being economically and structurally drivable. In addition, different materials have different properties, thus a different penetration length. Research conducted by Maskell et al. (2017) showed that the moisture sorption capacity was increasing linearly with thickness, and that a point exists where increasing the thickness of the material has no effect on moisture sorption, as illustrated in Figure 3.6. At this point, within a fluctuation RH environment, the moisture cannot penetrate any deeper in the material. In another way, if the thickness is insufficient, the effect will not be fully utilized. Other authors point out that there is a difference between long term and short term buffering effects, and that different surrounding air state, shifts the optimal material thickness slightly. The author does not, according to Maskell et al. (2017) further elaborate this.

3. Literature Review

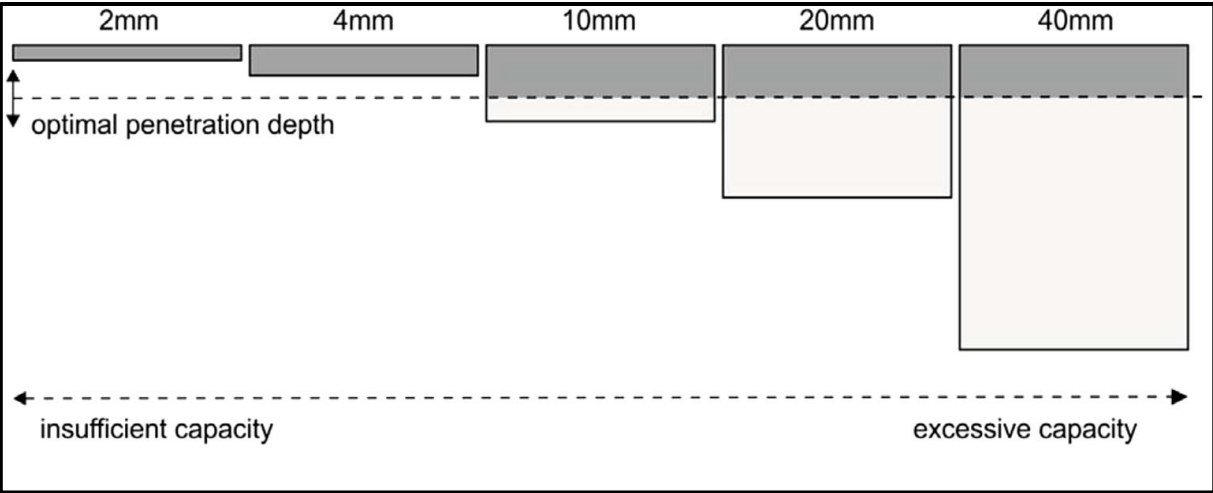


Figure 3.6: Optimal moisture penetration depth for a material, following a period of raised RH. (Maskell et al., 2017)

4. Method

This chapter is a walkthrough of the planning, setup and execution of measurements conducted in Zeb Living lab. First, a review of the test facility is presented, before an explanation of how a logging system was calibrated, set up and ran is given. Afterwards, the systematic execution process of the measurements conducted, in order to estimate the moisture production is explained in detail.

4.1 Introduction

As literature has shown, the total release of moisture from moisture producing sources is limited to amounts determined by each individual process and its boundaries. By monitoring relevant parameters with the use of sensors measuring the state of the air, to and from a carefully defined control volume, the moisture production can be calculated using equation (14). The control volume, sketched in Figure 4.1, shows the quantities than must be measured.

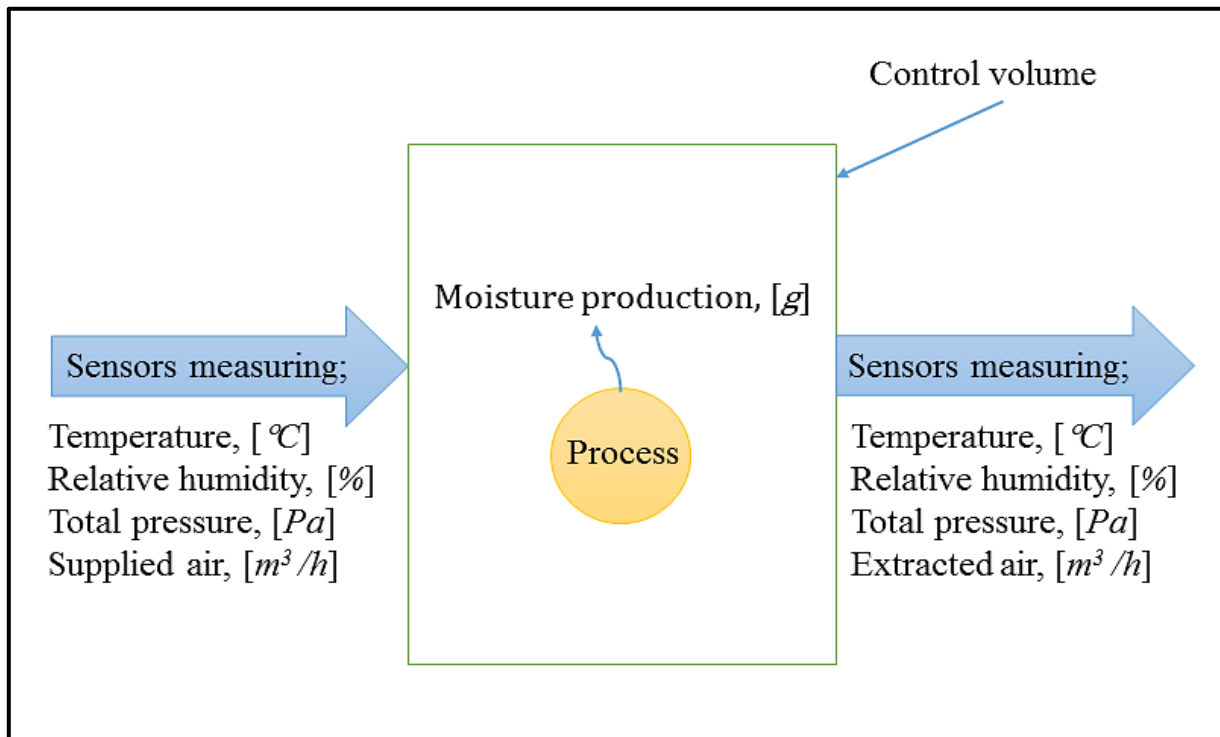


Figure 4.1: Parameters measured to and from a control volume, to calculate the moisture production of a process.

To be able to quantify the moisture production correctly, highly accurate sensors is necessary. The final equation (14) is derived from- and utilizes a number of previous equations, so an error will propagate and grow with extension. The different quantities given in Figure 4.1 are used in several of the equations leading to equation (14), thus, the measuring error must be held as low as possible. To achieve this, sensors should be scientifically calibrated and the mounting and choice of location must be both correct and suitable at the test facility.

The necessary parameters required to determine the moisture production is, by looking at equation (14):

- Volumetric flow rate, \dot{V} , $f(v, d)$
- Specific humidity, x , $f(\text{RH}, T, p_{\text{tot}})$
- Humid air density, ρ , $f(\text{RH}, T, p_{\text{tot}})$
- Time, t , $f(s)$

Moisture production, is by using the described method, a function of relative humidity, RH , temperature, T , total air pressure, p_{tot} , duct air velocity, v , duct diameter, d and time, t .

4.2 Test facility

Zeb Living lab is a research building built as a zero emission building (ZeB), located at the NTNU Gløshaugen campus area. The building was built in 2014 as a single- family home, with state- of- the- art solution for monitoring and controlling energy supply and energy saving. The aim of the building is to investigate how a ZeB can be realized in the harsh Nordic climate. During its lifetime, different types of families has occupied the structure in the name of science, to study the interaction between the user and the building (Francesco et al., 2014). For visualization, a floor plan of Living Lab can be seen in Appendix A.1.

The indoor environment in Zeb living lab is continuously monitored, and logged through the software LabVIEW. Raw voltage and current signals from different types of sensors throughout the building is translated to readable real time measurements on both air velocity, temperature and relative humidity, in addition to several other parameters not used during this master thesis work. The logging frequency can be adjusted to fit the need of the research at the users' choice.

To calculate the moisture production from different indoor sources, a control volume is required. The choice of control volume determines the accuracy, in the form of a boundary for the conducted measurements. A total control of the state of the air that enters and leaves the control volume is at all times necessary not to lose valuable data. Thus, an airtight enclosure with one entrance and one exit is the ideal location. In Living lab, the room that fits these requirements best is the bathroom. The bathroom has one entrance, one small window and a mechanical extract valve for the air to move in and out through. The room, constructed as a wet room, has tiles covering the floor and the walls, and a fiberboard ceiling. The use of tiles and grout makes the walls and the floor as airtight as assumed required for this thesis. Within the pressure level of a normal dwelling, the tiles are preventing air and moisture from escaping through to the inner walls. The interior ceiling of the bathroom is assumed airtight as well. The air can thus only exchange through the window or the door, as well as the ventilation extract valve. In the work, the window is neglected as it is kept closed at all times.

With these assumptions, the only way air can enter the bathroom is through the door opening, and the only way air can leave is through the extract valve. During conducted experiments, the door is kept closed, and an underflow door valve works as a supplier of fresh air to the bathroom.

The bathroom has an internal floor area of measured 5 m². It includes an open shower with glass doors, a toilet, a washing machine and a sink on top of a storage cabinet. About ¼ of the floor area is occupied by the storage cabinet. The ceiling height is measured to be 2.4 m, making the total volume of the room to be 12 m³. For visualization, four images of the bathroom can be seen in Figure 4.2.

Living lab is a modern building, with modern technology built for research. It has installed a balanced mechanical ventilation system to extract the used-, and to supply fresh air to the indoor environment. Along with this, a rotary heat exchanger ensures a significantly lower energy need by reducing the need for preheating of the supply air. As can be seen in Appendix A.2, supply- and extract valves are placed in strategical locations throughout the house, according to recommendations from standards. The supply valves is located in locations that requires fresh air from outside, and extract valves in the kitchen and in the bathroom. Extract valves are located where the production of contaminants have the risk of spreading to other parts of the building and polluting the indoor climate. In the kitchen, fumes and moisture from cooking has the risk of spreading through the building, thus an extract valve is preventing the spread of these to other zones, decreasing the IAQ. In the bathroom, the frequent large excessive load of moisture production makes it necessary to ventilate air out to prevent it from increasing the RH in the rest of the building.



Figure 4.2: Four different views of the test facility at Living lab, Where left image is the entrance to the bathroom, while the other three shows three different angles inside it. The extract valve can be seen in the rightmost image, located above the shower.

4.3 Experimental set- up

To obtain accurate results when conducting experiments, the use of instruments to measure and monitor data was necessary. With the use of three different sensor types, the amount- and state of the supplied and extracted air in the bathroom, as well as the total barometric air pressure was monitored. The sensor type and producer was:

- Temperature and RH: *Vaisala - HMT333/ Vaisala – HMT120*
- Duct air velocity: *S + S Regeltechnik - KLGf-1*
- Barometric pressure: *Delta OHM - HD 52.3D*

4. Method

As moisture production is a process that is happening in relatively small quantities, it is important not to lose valuable data. One way of ensuring that no data is lost, is by having full control of the air that enters and leaves the control volume, the bathroom. As described, an assumption is that there is only one entrance and one exit for the air to travel. Two sensors is thus necessary to measure the state of the air on the boundaries of the control volume. One sensor was thus mounted just outside the bathroom door, at the floor next to the underflow valve. This sensor monitored the RH and the temperature of the air entering the bathroom. It is assumed that the air entering through this crack has uniform temperature and RH, due to the large space in front of the door, the close proximity between the sensor and the door, and the great suction due to under pressure in the bathroom. This was in addition verified by smoke experiments around the door opening. An image of the sensor and the accompanying signal receiver can be seen to the left in Figure 4.3.

Equally to the supply air, the state of the leaving air must be monitored. The sensor registering the state of the air going out of the control volume can be found mounted in the extract duct of the ventilation canal of the bathroom. To reveal this sensor, the interior roof cladding must first be removed. By unscrewing the fiberboard, the sensor is revealed. Images of the location of the sensors can be seen to the right of Figure 4.3. This sensor is thus monitoring the air that leaves the bathroom at ceiling height.

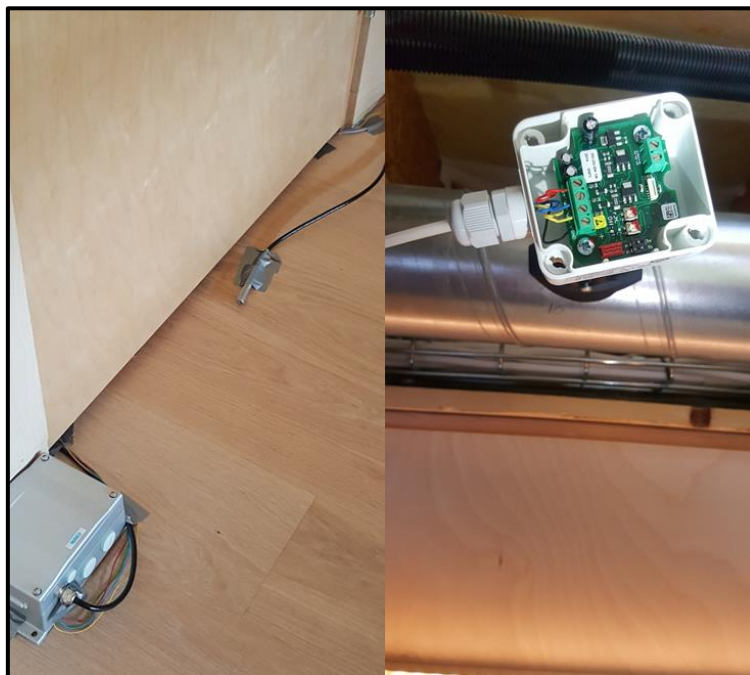


Figure 4.3: The left image shows the placement of the RH/temperature sensor monitoring the state of the supplied air to the bathroom. At the right image, the equivalent sensor registering the state of the extract air from the bathroom can be seen. This sensor is mounted inside the ventilation duct.

In order to use equation (14), to calculate the moisture production of the bathroom, the total amount of air, or the air change rate is required. In Living lab, a sensor measuring air velocity from the bathroom air mounted in the extract duct above the room. This measurement, along with the dimensions of the duct is enough to determine the amount of air entering or leaving the bathroom, under the assumption of tightness, as explained.

The velocity sensor monitoring the air from the bathroom is of type *S+S Regeltechnik: KLG 1*. After spending some time building a rig, and calibrating two of the sensors, it was obvious that the accuracy was lower than expected. The sensor is measuring the velocity by hot-wire anemometry, where the flowing air is cooling a metal wire in the probe. These sensor types has a built in temperature compensation to compensate for the change in air density with temperature. However, on the two sensors tested from Living Lab this function was not working properly. This made the signal representing air velocity increase with increased temperature, thus signaling a higher air velocity with increased air temperature than it actually is. If the sensor were to function as intended, an increase in temperature would activate a built in compensation, reducing the impact of decreased air density. This problem was, during the work, not solved. Thus at a late stage it was decided to instead use a TSI Velocalc instrument from the lab at NTNU to measure the air velocity in the extract duct of Living Lab. The TSI instrument was scientifically calibrated, and utilized to determine the actual air velocity of the duct. To quality ensure the measured velocity, an additional instrument was brought in. This time a volumetric flow meter, a balometer was used to verify the measured data from the TSI instrument. The two numbers complied with each other. The airflow rate in living lab is controlled by the air handling unit in three different stages. During the experiments a flowrate of 50 % was used at all time. Thus, the airflow rate was measured only once, as this was not physically changed. Due to practical reasons, the changes in density was not accounted for, and the airflow rate was assumed constant.

To log the data from the experiments, a data logger of type *HIOKI LR8400-20* was used. This device is a portable data logger that can translate raw current/ voltage signals into real time readable data, and store them as excel files. The logging frequency as well as the timespan of the measurement can be adjusted to fit the need of the current situation. All the sensors used for this research was connected to the data logger, except the barometer which utilized Living Labs own logging system. A setup of the logger with the connected sensors can be seen in Figure 4.4.

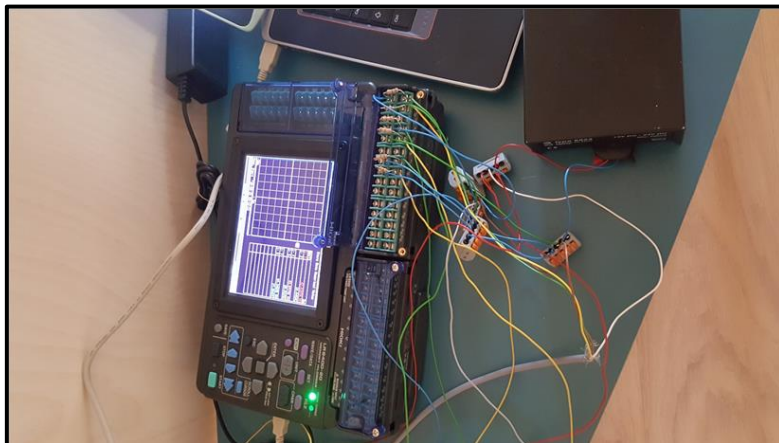


Figure 4.4: All the sensors used to monitor the state of the air was connected to a data logger, as seen to the left of the image. At the right, a DC voltage source for the sensors can be seen.

Living Lab's own logging system was initially going to be used for the data acquisition from the sensors. However, this system has not been working properly during the work, which is the reason for the use of the external logging device.

4.4 Preparations for measurements

4.4.1 Ventilation system

The very last step before finalization of a ventilation system is to balance it. Balancing is (usually) a one- time setting of dampers and valves, to control how the air flows through the different branches of the system. The goal is that each of the air terminals supplies or extracts the projected amount of air through it, to prevent unwanted effects and increased energy demand.

In plants with constant air volume (CAV), balancing is done by manual methods (Ingebrigtsen, 2016b). One common method is the proportional method. Proportional in this setting means that if the total air volume driven from the air- handling unit's fan is changed, the ratio between the different branches' air volume remains constant. The basis of the method is to adjust the different valves and dampers, so that the ratios between them are equal. When the ratios is the same, the system is balanced. An increase or decrease in total air volume leads to a proportional change of air through every valve in every branch. Thus, the ventilation system supplies and extracts a proportional, projected amount of air through each valve independent of ventilation rate. Balancing is an important step in achieving good ventilation efficiency and stable run. The method minimizes the systems total air pressure losses, thus contributing to lower fan speeds and energy saving. Due to the lowered fan speeds, noise is reduced and potential draft problems are reduced (Ingebrigtsen, 2016b).

One of the initial preparations for conducting experiments at Living lab was to balance the ventilation system. This was conducted in the autumn of 2016 by Blandkjenn (2016), however as the valves on the walls are easily accessible, and research had been going on continuously, the system was no longer balanced. This was controlled by the use of a balometer, which confirmed the ventilation system had to be balanced over again. The ventilation system in Living lab is dimensioned as a balanced system. Thus, the supplied and extracted amounts of air are designed as equal. The projected airflow rates can be found in

Table 4-1, which the balancing was conducted according to. For the complete documentation of the actual airflow rates, see Appendix B.

Table 4-1: Nominal airflow rates in ZeB Living lab during normal occupancy.

Supply duct location	Airflow rate [m³/h]	Extract duct location	Airflow rate [m³/h]
Bedroom east	52	Kitchen	-36
Bedroom west	26	Bathroom	-108
Living room south	41		
Living room north	25		
Total supply air	144	Total extract air	-144

The volumetric flow rate of the bathroom extract was measured and calculated to be 105 m³/h. This value is the one used to calculate the moisture production, according to equation (14).

4.4.2 Calibration of sensors

The goal of calibration is to minimize measurement uncertainty by ensuring the accuracy of the equipment. Over time, sensors have the tendency to drift out of accuracy. To be confident the measured values are correct, there is an ongoing need to service and maintain them by calibrating.

When calculating moisture production, accurate results is essential. As the required equations presented involves both temperature, RH, air pressure and air velocity, these measured quantities must be accurate. The sensors located in the ventilation ducts of Living Lab had not been calibrated since 2014, according to Kristian S. Skeie.

The RH- / temperature sensors mounted in the ventilation ducts of Living Lab was originally of type *S+S Regeltechnik: KFTF-I*. The author calibrated nine sensors, before realizing that the response time was not nearly as good enough as the future planned experiments required. The solution was to buy new and better sensors. The choice ended up being of the type *Vaisala HMT120*. These sensors was pre- calibrated at the manufacturer, so it was decided only to verify the calibration of two of the six bought.

4.4.2.1 Relative humidity- and temperature sensors

The calibration of the hygrometers in ZeB Living lab was executed using a calibrator from the company *Vaisala* of the type *Humidity Calibrator HMK15*, as shown in Figure 4.5 in an ongoing calibration process.

The calibration was conducted using a method of saturated salt solutions. Certain pure salts has, when mixed with distilled or de- ionized water, the property that they maintain a constant humidity in a closed container. Different salt solutions maintains a different vapor pressure and thus different RH. The lab at NTNU provided four salts and thus the calibration was conducted using a four- point calibration. The four salts was lithium chloride (LiCl), magnesium chloride (MgCl₂), sodium chloride (NaCl) and potassium sulfide (K₂SO₄). These salts solution exerts a pressure with a RH of respectively 25 %, 33 %, 75 % and 97 % when mixed in distilled water. The RH of these saturated salt solutions are dependent on temperature, so a table relating temperature and RH for the two salts was used. The calibration results of the original sensors mounted in Living Lab can be found in Appendix C.2. It must once again be noted that these sensors were not used during this thesis, as the response time was concluded to be too slow.

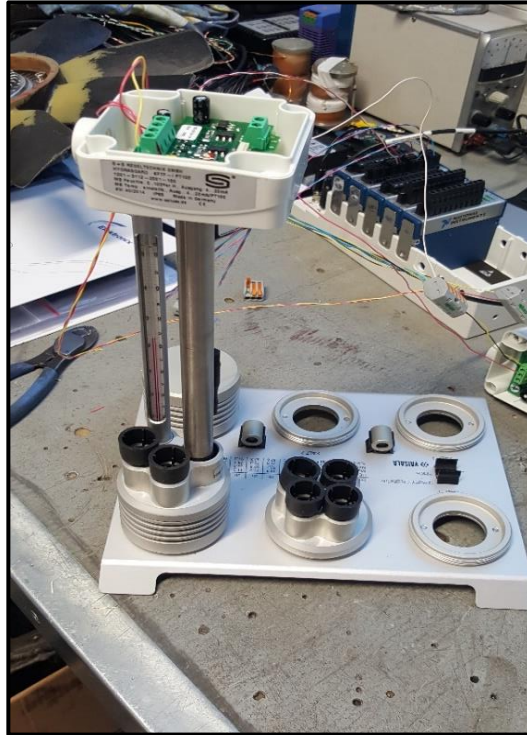


Figure 4.5: In the process of calibrating one of the humidity sensors with Vaisala Humidity Calibrator HMK15.

The final choice of equipment used in the experiments was one sensor of type HMT120 and one of type HMT333. As the calibrator used to calibrate previous sensors was no longer available, the HMT 333 sensor was calibrated towards the factory pre- calibrated HMT 120 sensor installed in the ventilation duct of the bathroom. As illustrated in Figure 4.6, three cables are sticking out of the duct.



Figure 4.6: The calibration of the sensor type HMT333 was conducted towards the installed sensor HMT120 in the ventilation extract duct in the bathroom of Living Lab.

Three separate HMT333 sensors were tested to see which had the highest accuracy towards the calibrated HMT120, as well as the response time. The calibration results can be found in Appendix F. The outcome of the calibration between the two sensor types was an exponential curve fitting, where the measured data from the sensor to be calibrated was multiplied by an exponentiation function. The exponentiation fitting was done by excel, and resulted either in an increase or a decrease of the measured data toward the manufactured pre calibrated sensor. The exponentiation function used can be seen in Table 4-2.

Table 4-2: The numbers of the exponentiation function used to calibrate the sensor type Vaisala HMT333

Quantity	Base	Exponent
RH	1,3918	0,9174
Temperature	1,3796	0,9877

4.4.2.2 Velocity sensors

The calibration of the velocity sensor type *S+S Regeltechnik: KLGf 1*, in ZeB Living lab was executed using a ventilation rig for calibration built by the institute, utilizing the principles of an orifice plate.

4. Method

An orifice plate is a device used for measuring flow rate. The volumetric flow rate of a fluid can be determined based on Bernoulli's principle, which states the relationship between velocity and pressure of a fluid. The orifice plate is a thin circular doughnut shaped disk with a known inner diameter, as seen in Figure 4.7. When a fluid passes through it, the pressure builds up in front of it and as it passes through the disk, the fluid is forced to converge, thus velocity increases and the pressure decreases. By measuring the difference in pressure on both sides of the orifice plate with a manometer, the flow rate is obtained from Bernoulli's principle and equations found in research (Emerson Oroces Management, 2010). In the calibration process an excel spreadsheet, made by Prof. Hans Martin Mathisen was used to calculate the airflow rate. The spreadsheet utilizes the theory based on NS-EN ISO 5167-1 and NS-EN ISO 5167-2.



Figure 4.7: The orifice plate fitted between the two sections, where pressure drop is measured and the airflow rate is accurately calculated.

In Figure 4.8, a picture of the rig can be seen. The direction of the flow of air is from left to right through the duct. To the right in the image a variable flow inline duct fan and a damper is located. Together they give the opportunity to control the airflow rate through the duct in order to calibrate through a velocity range. The damper was necessary since the fan was partly oversized. The mid-section is where the orifice plate is located. Two sections of $\varnothing 100$ ducts is connected, with the orifice plate in between. The exact size of the inner diameter of the orifice plate used is 71mm.

To ensure correct calculations, the velocity profile in the ducts need to be fully developed. All the air must flow in the same direction, and hence it is located several flow straightening vanes in the ducts. According to Johansson and Svensson (1998) the velocity profile is fully developed after 5 diameters of a sudden change in the duct. A change in this setting is either a bend, a T-piece or an inlet. The sensor that were calibrated was thus placed at least 5 diameters after the inlet of the $\varnothing 200$ duct (left duct piece).

When calibrating the velocity sensors, a combination of fan speed and control of the damper were used to regulate the airflow rate to desirable amounts. The pressure drop over the orifice was measured with a manometer and interpreted into the excel spreadsheet. Out of the spreadsheet the airflow rate was calculated from the pressure drop, and by connecting it to the voltage signal of the sensor, a curve connecting voltage and airflow rate was generated. Each of the two sensors were tested at seven different airflow rates, and in three separate runs. The average results from the three runs is the calibration curve, and can be found in Appendix C, along with the spreadsheet and the three runs for each velocity sensor.

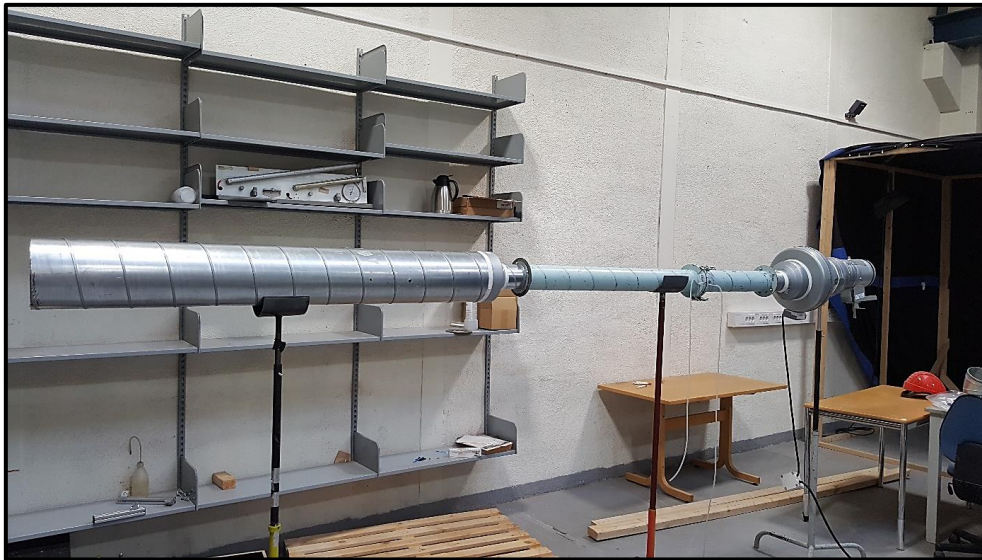


Figure 4.8: The rig built for calibration of velocity sensors.

Much time was spent on the calibration of the velocity sensors. Unfortunately, as explained, the sensors had a malfunction making them unsuitable for use in this thesis due to accuracy related issues.

4.5 From experiment to data

Regarding the type of experiment conducted, the method for measuring in living lab was the same for every trial. The sensor installment was stationary, meaning it was always located in the same place. Once the sensors were calibrated and installed at their respective location, the system was ready to record experiments. Five sensors were monitoring the chosen control volume. One sensor was measuring the RH and temperature in the air supplied to the bathroom, one measuring RH and temperature extracted from the bathroom, and one sensor measuring the total pressure of the air, located on the roof of Living lab. In addition, two additional RH-/temperature sensors were mounted at different heights inside the bathroom.

Figure 4.9 shows the process of how the measured quantities are utilized to calculate the moisture production. The figure is a flow chart representation of equation (14), which again is a part of the equations (9) and (10). The figure shows that three sensors are required to calculate the moisture production. The three sensors measure the five parameters needed to calculate the specific humidity and the humid air density. Together with the airflow rate, measured and calculated beforehand, the moisture production can be calculated.

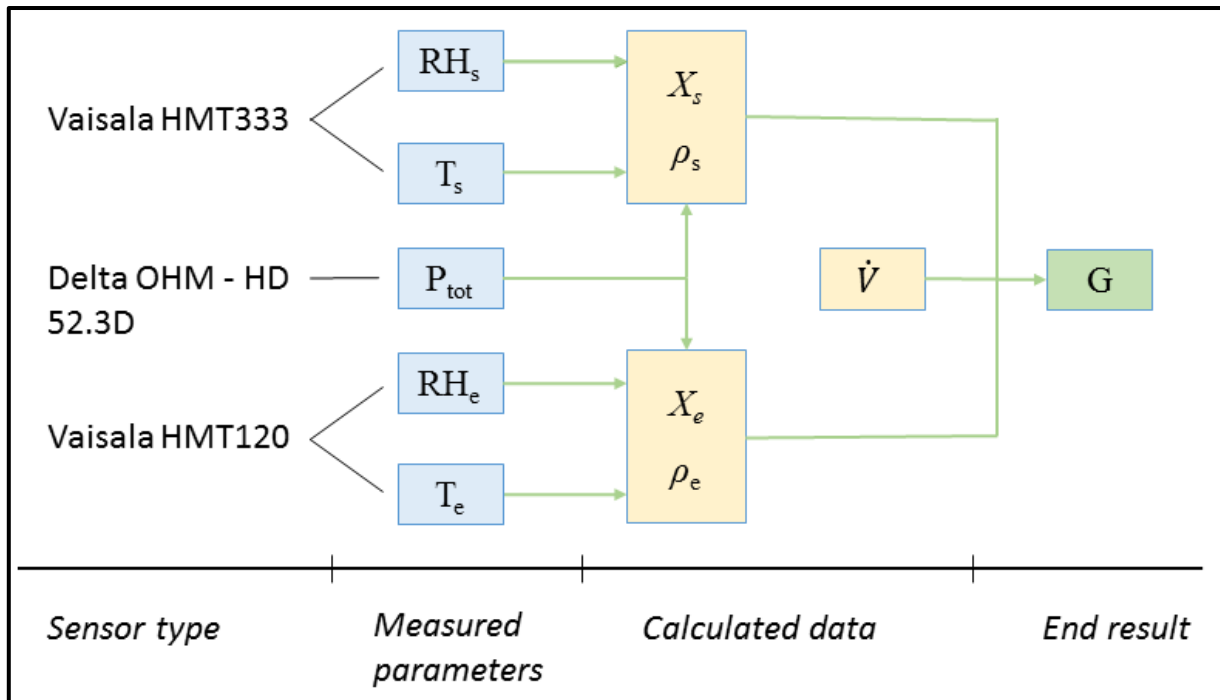


Figure 4.9: Flow process chart on how the excel script calculates the moisture production from a measured data in Living lab. The calculations are based on equation (14), evaluated in the transient regime.

Before starting an induced moisture production, the logging system had to be prepared. A start time (usually current time) and a stop time was chosen based on the type of experiment. The required length of the session was depending on the type of experiment conducted, but for most of the cases, the system was logging for at least 8 hours. 8 hours was considered enough, based on trials and analysis of real cases not presented in this thesis. When the data logger had completed the recording session, the data was automatically stored in the .xlsx file format (excel compatible), and had to manually be extracted from the devices. To translate the raw measured data from an experiment to calculated produced moisture, an excel spreadsheet was made. The spreadsheet was made to do all calculations, regardless of the experiment conducted. After the raw data from the data logger and Living Lab's logging system was acquired through the logging devices, it was inserted into the document. The document then sorted and processed all the data with the basis of Figure 4.9, before presenting the calculated moisture production. In addition, the spreadsheet was implemented to draw graphs representing the transient development of the measured quantities as well as the calculations made.

4.6 Plan for measurements

To verify the moisture production from showering, given in the literature, a series of measurements was conducted. The initial plan was to measure a series of different activities, but at the end only the source with the assumed highest moisture production was tested. The reason for the delays was due to the logging issues in Living Lab, which crashed several times. While at the same time being most practical, showering is the source that releases most moisture, so showering is the focus of this part of the thesis.

A research plan was made with the goal of testing a range of typical real world scenarios on moisture production. By conducting a set of experiment and changing a set of variables one at a time, the moisture production can be estimated within different scenarios. The choice in which parameters was to be changes, was based on the literature from Chapter 3, and assumptions made by the author. The total number of experiments is assumed a representable selection for verification of other authors work. Before the presented data was acquired, a series of test runs was performed. From calibration validity, to impact from different parameters, to different stationary (initial) indoor RH. In addition, time was used to quality ensure the produces excel spreadsheet. All tis to provide reliable results to the reader.

Table 4-3 shows the produces research plan for the showering experiments. The goal with this table is to give an overview which parameters was tested and which was considered excess.

Table 4-3: Research plan for the verification of the moisture produced from showering. “X” implies that the set of parameters was tested, while “- “ was not tested. A total of eight tests were conducted.

	Water temperature 25 °C		Water temperature 35 °C		Water temperature 45 °C	
	Flow rate MAX	Flow rate MED	Flow rate MAX	Flow rate MED	Flow rate MAX	Flor rate MED
	Time 7 min	-	-	-	-	-
Time 5 min	X	-	X	X	X	-
Time 3 min	X	X	X	-	-	-

5. Moisture production model

One of the goals of this thesis is to verify the moisture production rates used in an indoor moisture production model made at NTNU. This chapter presents the model and the main purpose of this, with focus on the parts utilized in the thesis. The model is currently under the ownership of the company Flexit, thus only parts of it can be published and view to the public.

5.1 The model

A moisture production model (MPM) is currently under development at NTNU, accompanied by Flexit. Ph.D. candidate Maria Justo-Alonso is currently working on constructing a model that can accurately predict the changes in indoor RH levels during a day based on user behavior. The ventilation system plays an important role in the transportation of air, and humidity. The model is focused on the use of a balanced mechanical ventilation system, with the use of a regenerative heat exchanger. This type of heat exchanger gives the opportunity to transfer both sensible and latent heat between the supply- and extract air. The outcome of the model is to map the moisture production in residential buildings, to avoid potential problems with frosting or condensation in and around the rotary heat exchanger. The whole model is written in the C-based programming language Matlab.

Without revealing too much of the details, a user of the model will need to have knowledge of building specific parameters such as room type with accompanying floor area and room volume, in addition to ventilation rates in the zones selected. Furthermore, the most important input is the knowledge of when during the day a series of given moisture producing activities is performed. When these values and parameters has been inserted, the model is ran, which then calculates and outputs the transient development in indoor RH in the different zones.

As the literature review has shown, moisture production is dependent on a number of parameters, and there is no answer to how much moisture a particular source releases. An almost infinite number of variables can be connected to each source, and while some are more impacting than others are, the total moisture production varies with each time the activity is performed. In the MPM, the moisture production is assumed constant for each activity. Thus, the given sources is assumed to release a specific amount of moisture to the air when it is performed, at a constant rate. The moisture production rates used in the model has all been gathered from research conducted by Yik et al. (2004). In the paper, moisture generation rates has been collected from other authors work, and presented in a tabular form. The full tabular summary can be found in Appendix D, while a processed version, adapted to the thesis, can be found in Table 5-1.

Table 5-1: Processed moisture production rates used in the moisture production model, originally found in Yik et al. (2004).

Source	Moisture production rate
Humans	55 g/h
Sleeping humans	40 g/h
Cooking (gas)	339 -488 g/h/pers
Cooking (electricity)	150 – 188 g/h/pers
Shower	2250 g/h
Sauna	1280 g/h
Dishwashing machine	137 g/h
Washing machine	75 g/h
Drying of clothes on rack	73 g/h
Drying of clothes in tumble dryer	26 g/h
Plant	33 g/h
Pet	16.5 g/h

* The moisture production from cooking is dependent on whether breakfast, lunch or dinner is cooked.

5.2 Output from the model

The MPM has the ability to output the calculated response in RH, based on the input by the user. The output is a graphical representation, showing the transient development in RH of the different zones of the chosen building. The model utilized weather data as the baseline for supplied air to heat exchanger of the building, and a series of mathematical expressions and coherences from physics to calculate the actual RH.

Figure 5.1 is a representative outline from the output of the MPM. It shows the response in indoor RH of the different zones throughout a day. As can be understood, this specific case is a day where the indoor RH is below the recommended value, in most of the day. The

ventilation rates used in this simulation is equal to the projected amount in Living Lab, as found in

Table 4-1. To view the model in a general way, a series of representative moisture producing sources has been chosen to appear during the day. Below is a list of the source, and the time the activity is conducted, as it is inserted into the model.

- Sleep: 00:00-07:00
- Shower: 07:00-07:04
- Breakfast: 08:00
- Lunch: 12:00
- Dinner: 17:00

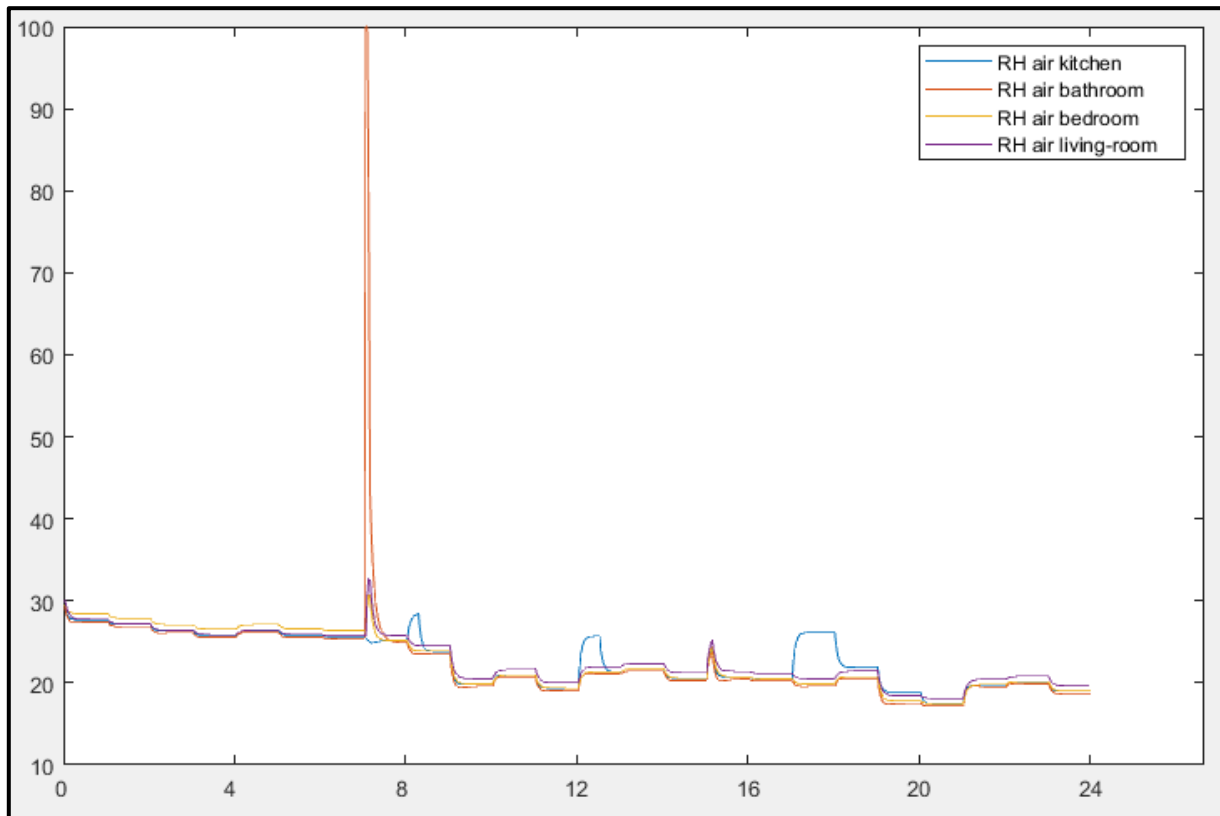


Figure 5.1: Output from the MPM, showing the transient response in RH for four zones of a building, during 24h in the spring of Norway.

The response of a moisture production on the indoor environment is an increase in RH. As can be seen from Figure 5.1, a reaction occurs when a source is initiated, where the coloring represents different zones of the building. Distinct reactions can be seen in the line representing the bathroom, and in the blue line representing the kitchen. Furthermore, it can be seen that the different sources has different impact on the RH. By looking at the x- axis, who represent the hour of the day, distinct changes occurs at certain times. These times are linked to the sources listed above. There is no doubt that showering is the activity that has highest impact on amplitude. During the shower, the RH increases and reaches saturation, but does, almost as fast as it increases, decreases back to initial condition. This is due to the high ventilation rate from the bathroom, where all the air in the bathroom is theoretically exchanged over 5 times per hour. As can be seen from the blue, kitchen line three

5. Moisture production model

The response in RH from an activity can not only be traced in the zone of occurrence, but also in other zones. As can be seen from Figure 5.1, when the shower is initiated at 07:00, an increase in RH occurs in the bathroom, as well an increase in the bedroom and living room, though with a minor time delay. There is no reaction in the kitchen. This effect has to do with the heat exchanger. The bathroom has an extract valve, sucking air out of the room, producing an under pressure. This effect causes the air in the bathroom not to leak to surrounding zones. The increase in humidity in the zones outside the bathroom thus have to enter through the ventilation system. The moisture produced in the bathroom initially travel through the extract duct and out of the building. However, on the way from the bathroom to the exhaust valve, it loses some of its humidity content. This is due to the rotary heat exchanger. The rotary heat exchanger transfers both sensible and latent heat between the supply- and extract air resulting in an increase in RH of the supplied air, and a decrease in the extract air. With the excessive release of moisture from the bathroom during a shower, more humidity is transferred between the airstreams in the heat exchanger. The moisture produced from the showering can thus be traced in the supply air as a temporarily increase in RH. In Figure 5.1 this effect is clearly visible. The RH increases in zones where air is supplied through the ventilation system. Note that the RH in the kitchen is not affected by the shower sequence. This is because there is not located any supply valve in the kitchen, only an extract valve.

The rate of the response in RH of a moisture production is also characteristic for different activities. As can be seen in Figure 5.1, there is a difference in the total affection duration due to a moisture production. This has both to do with the ventilation rate, but also on the duration of the activity in time.

6. Results

This chapter presents the result of the conducted experiments in the bathroom of Living Lab. Common for the presented data is the presence of a table showing the limits and boundary condition of the series of experiments, and the results for the calculated moisture production. In addition, three graphs representing the transient development of the RH, temperature and specific humidity is presented. At the end, the MPM is compared to the real experiments from showering.

6.1 Introduction and results

As the literature review has shown, a shower is releasing moisture equivalent to 200- 400 g/ event. Another author showed that between 2640 – 3000 g/h, or 44 g/min – 50 g/min was produced. To verify these rates a series of experiments has been performed. By varying a set of parameters or boundary conditions, the moisture generation has been calculated, based on calculations from Chapter 2, and method from Chapter 4.

Table 6-1 is a tabular representation of the results from a series of induced moisture productions from showering. The experiments was conducted in the bathroom of Living Lab, with one run each day for 8 days. By waiting 24h between each trial, the state of the air in the bathroom had enough time to completely settle and stabilize so that the order of the conducted experiments did not matter, and that they did not affect each other. Previously a series of trials had been run, but to ensure quality proofed data to the reader, these measurements was only used for acknowledgement of the final results.

The moisture produced from showering is dependent on a number a parameters. From the most evident influencing factors such as the length of the shower and the flow rate, to factors like temperature of the water, spillage on walls and floor, the room temperature, initial state of the air, the volume of the room and ventilation rate. In this thesis, the chosen parameters to vary was chosen based on the trial experiments. The three parameters with highest impact was:

- Water temperature
- Mass flow rate of water
- Length of shower

During experiments, the water temperature was tested on three different stages. These levels represents the temperature ranging from minimum to maximum as the author considered comfortable to shower in. The temperatures was measured with a simple thermometer. The minimum temperature was measured to be approximately 25°C, while the maximum was measure to be circa 45 °C. The temperature in the middle was chosen to be the temperature where the safety switch is located on the armature in the shower. This temperature was

6. Results

measured to be 35 °C. It must be noted that different users has different tolerance for extreme temperatures, however this was the temperatures this particular test person was satisfied with.

The mass flow rate during the experiments was considered on two different stages, denoted medium and max. Medium is approximately 65 % of max flow rate using the armature switch; however, the actual flow rate was not quantified.

The last parameter considered, was the length of the shower. Three, stepwise lengths was chosen and assumed to be representable. A timer was used to determine the accurate showering time during the experiments, and represents the time the shower tap was running. The three steps was ranging from 3 minutes to 5 minutes to 7 minutes.

Table 6-1: Measured moisture production from showering, G [g/event].

	Water temperature 25 °C		Water temperature 35 °C		Water temperature 45 °C	
	Flow rate MAX	Flow rate MED	Flow rate MAX	Flow rate MED	Flow rate MAX	Flow rate MED
	Time 7 min	-	-	-	-	-
Time 5 min	306g	-	481g	381g	656g	-
Time 3 min	244g	198g	303g	-	-	-

The moisture production calculated from the given experiments is as one would expect, increasing with increased parameter load. However, compared to the literature, the production from the experiments are in average higher. By processing the calculated values from Table 6-1 into rates, and isolating the data into parameters, Table 6-2 emerges. It can be seen that for all the parameters, the moisture production is increasing with increased load. The literature suggests that the moisture production is between 44 g/min – 50g/min, which is much lower than the values for this research. In fact, all of the conducted experiments are exceeding the highest rates from the literature. However, another author suggested a total moisture generation of between 200 g/ event – 400 g/ event. This value comprises with a portion of the values from this research, but only with the most conservative variables. For the higher extrema, the production is double of what previous research suggests.

Table 6-2: Analysis of the moisture production rate (per minute showered) categorized after parameter.

Parameter	Variable	Range (g/min)
Time	3 min	66 – 101
	5 min	61 – 131
	7 min	107
Water temperature	25 °C	61 – 81
	35 °C	76 – 101
	45 °C	107 – 131
Mass flow rate	MED	81 – 131
	HIGH	66 – 121

6.2 Transient analysis

Four RH-/ temperature sensors were used for the showering experiments. In addition to the sensor monitoring the state of the air going to and from the bathroom, two additional were used. One was mounted 1.5 m and one 2.0 m above floor level on the inner walls of the bathroom, outside the shower doors. The purpose of these two sensors was to monitor the transient development in RH and temperature at different heights, and to see how the state of the air changed outside of the shower, during and after the experiments. The extract valve is located just above the showerhead, and since the shower creates its own enclosed space during use, due to the glass doors, it was of interest to see whether there would be any difference in the state of the air outside the shower itself.

Figure 6.1 and Figure 6.2 shows the development of the surrounding RH and the temperature during a shower experiment. The two figures is a representative illustration from one of the shower experiments conducted in Living Lab. The boundaries for this particular experiment was a 5 min shower, with 65 % mass flow rate and a water temperature of 35 °C. According to Table 6-1, the moisture production from this experiment was 381 g.

6.2.1 RH

When the data logger started its recording on this experiment, the RH of the extract was 2 % below the supplied. The RH of the supplied air is strongly dependent on the outdoor conditions, which this day was a hot, sunny summer day. There were no indoor activity in Living Lab other than this experiment. The difference of 2 % may be caused by an increase in temperature from the underfloor heating in the bathroom. If looking back at the Mollier diagram from Chapter 2, an increase in temperature results in a shift vertically upwards, which again is a reduction in RH.

When the shower was initiated, it took about ten seconds before the extract air sensor detected a change in RH. As can be seen in Figure 6.1 the RH increases rapidly from the initial 40 % towards saturation, which was reached after one minutes and ten seconds. At saturation, the air can no longer sustain the supplement of more moisture and starts to condensate the excess

6. Results

humidity into liquid water. The condensation effect cannot be seen from the graphs but was notable during the experiments, as the glass doors of the shower started to visually fog down. After the shower had been on for exactly five minutes, it was switched off. The RH of the extract sensor started to decrease after ten seconds. The high ventilation rate and a reduction in moisture production intensity reduces the RH to 71 % in two minutes, before an interesting effect occurs. The RH increases slightly before decreasing once again, but with a much slower rate. This effect is thoroughly discussed in Chapter 7. In total, it took around 2 hours – 2.5 hours for the RH of the extract air to stabilize towards the supplied RH.

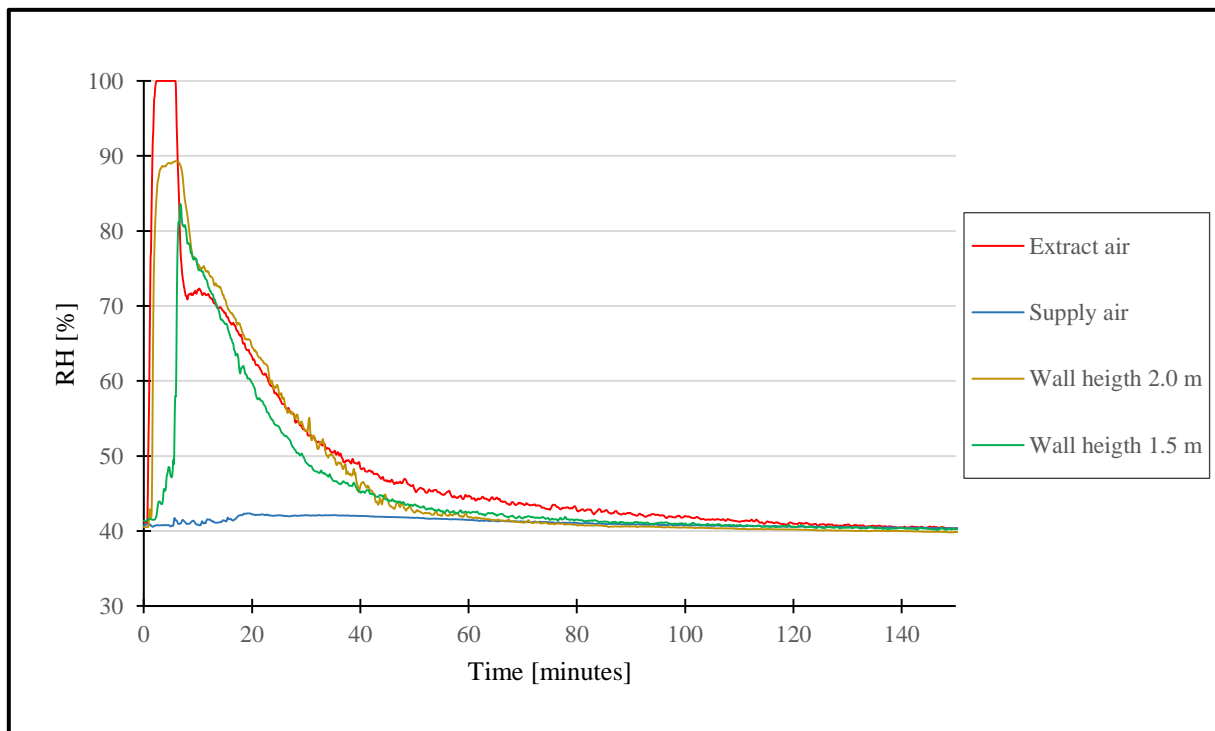


Figure 6.1: The transient development in RH during a 5 min shower experiment, using 4 sensors.

The two sensors mounted at different altitudes outside of the shower walls reacted differently than the extract valve sensor mounted directly above the shower. As can be seen in Figure 6.1 the highest mounted sensor reacted first, but still with a time delay between the extract mounted. The sensor mounted 1.5 m above floor level did not react until after the water was turned off. The reason for the different reaction times is, except for the altitude, that the sensors are located outside of the showering zone. The shower has tall glass doors protecting the bathroom from being spilled with water during a shower. The glass door acts like a shield creating a unique closed atmosphere. As the extract- mounted sensor is located in the valve directly above the shower, this reacts first, due to the buoyancy effect and the convection from the hot air (the temperature of the tap was higher than the surrounding air). Air is primarily ventilated out of the room, however as the glass doors are not ceiling high the warm air eventually crawls down from the ceiling, and reaching the height of the highest mounted wall sensor earlier than the lower one.

Furthermore, it can be seen that the RH of the lowest positioned sensor only increases merely 10 % before the shower is turned off. When the glass doors are opened, cold air is rapidly drawn in to the shower, and mixes with the warmer air. The air spreads in the room, inducing a rapid increase in RH lasting for one minute, before it decreases due to the dilution from the ventilation.

The amplitude of the three sensors affected by the showering has different amplitude. As the sensor mounted in the ventilation canal reaches saturation, the other two only manages to reach approximately 85 % and 90 %, increasing with mounting height.

6.2.2 Temperature

As can be seen in Figure 6.2, the use of the shower increases the air temperature of the ambient air. The temperature of the water is higher than the surrounding air, thus heat energy is transferred from the water to the air. The transition of energy goes from the water and via the material claddings on the floor and walls of the shower. As the materials are heated up by the water, it releases this heat to the surrounding air. Buoyancy and convection forces brings the hot air up towards the ceiling, before it is drawn out through the ventilation. The temperature continued to rise in the full five minutes the shower was in use, before decreasing again. The temperature peaks at an increase of about 3.5 °C after five full minutes, before decreasing towards the supplied temperature. The total duration time for the extract sensor to reach stability is the same as for RH, between 2 hours- 2.5 hours.

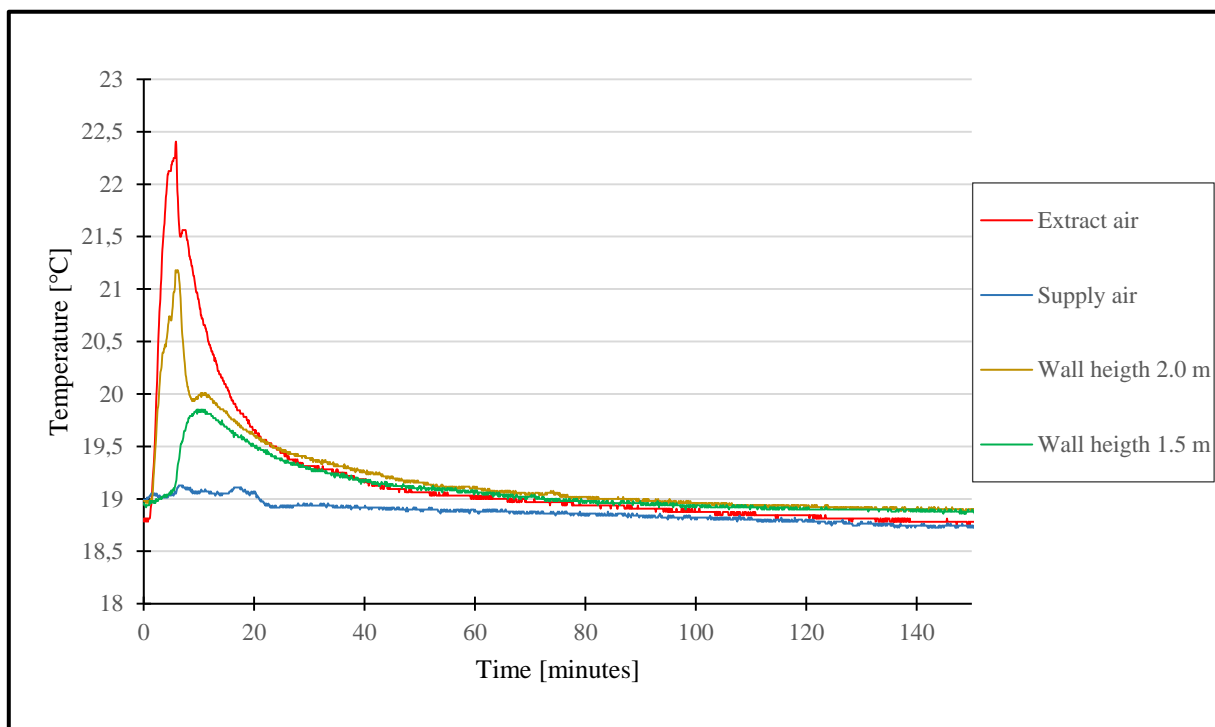


Figure 6.2: The transient development in temperature during a 5 min shower experiment, using 4 sensors.

The response of the two wall- mounted sensor are similar to the reaction in RH. The reaction time is different from the one in the extract, with increased reaction time with lower height. Furthermore, the amplitude is as expected increasing temperature with increasing height, or a positive temperature gradient.

6.2.3 Specific humidity

Figure 6.3 shows the difference in specific humidity between the supply air and the extract air during the experiment. When calculating the total moisture production, this graph is utilized by the excel script to determine how long the production is ongoing. For this particular showering experiment, the humidity level between the supply and extract was equalized after about two hours. This implies that the moisture production from a shower is a continuous process a long time after the water has stopped running. In the figure, the relation is similar to both the RH and temperature, with a rapid increase in difference during the shower, and a rapid decline immediately after the shower is finished. Also in this figure, a notable change happens a couple of minutes after the shower is turned off, where the decline rate reduces.

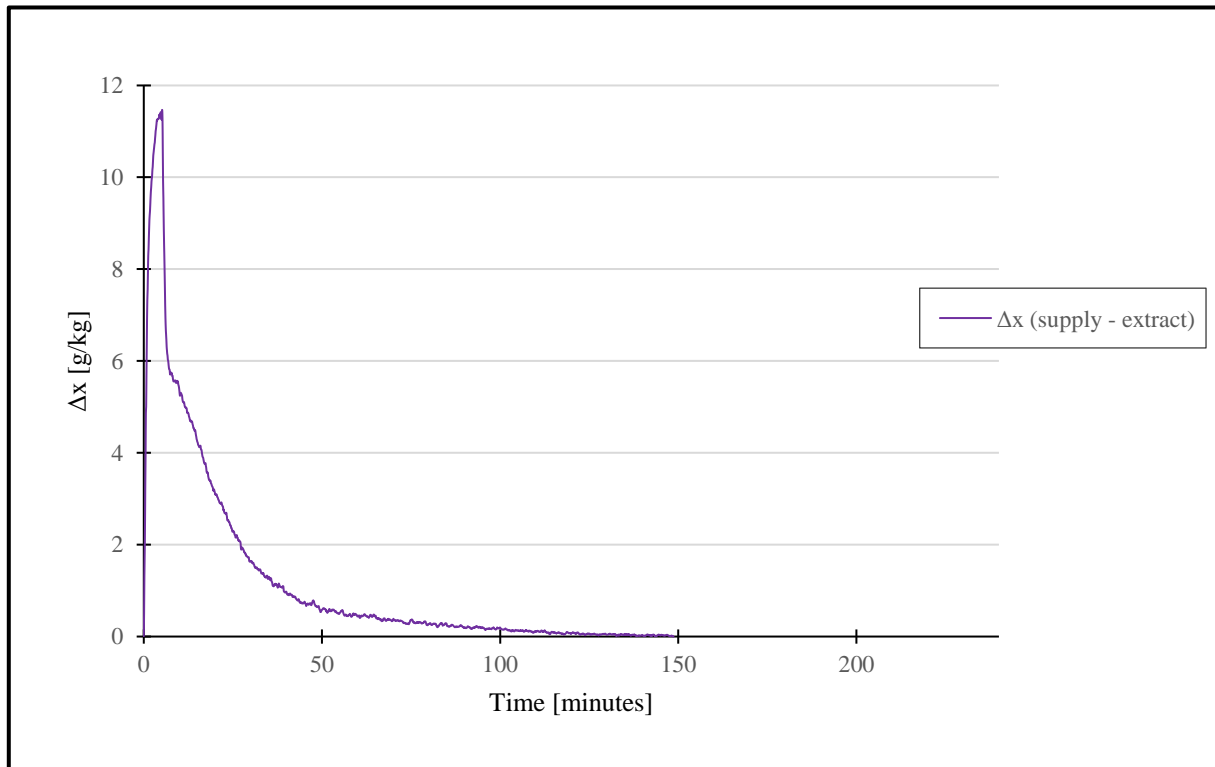


Figure 6.3: The transient difference in specific humidity between extract and supply air during a 5- min shower, with 35 °C water temperature and medium flow rate.

The total time the specific humidity in the extract air is different from supplied air, is hard to define. As can be seen in Figure 6.3, the specific humidity uses a much longer time to stabilize than the time of the showering sequence. The exact moment the specific humidity in the extract is equal to supplied is very much depending on the accuracy of the equipment. The logging system continued to record for several hours after the experiment, but due to lack of accuracy the difference was either passing zero at some point or never reached zero. For the experiment in Figure 6.3, the difference in specific humidity is less than 0.1 g/kg after 107 minutes. After 148 minutes, it reaches 0.02 g/kg, while continuing to fluctuate around 0.02 g/kg \pm 0.01 g/kg for the rest of the recording session. Thus for this particular experiment, the stabilization time was, based on the data set to be 2.5 hours, which implies the total moisture production time.

Moisture production is closely related to the duration of the difference in specific humidity. It is thus interesting to compare the different experiments graphical developments towards each other. Figure 6.4 is comparing this difference for a selection of the experiments. The three

experiments displayed has equal water temperature, but differ in shower length and flow rate. In addition, only the first hour of the transient process is viewed, as the relation between them is uninteresting to compare outside this boundary. There are both similarities and differences between the three graphs.

All three graphs start out with a similar relation, where the increase in specific humidity difference has a positive rate. This similarity continues until the three-minute mark, where suddenly all three graphs differ from each other. The experiment with lowest amplitude is turned off after three minutes, leading to a rapid stop in the increase. The source is removed, and the ventilation makes it dilute and induces a decrease instead.

Between the two experiments with highest amplitude, the only difference in conducted method is the mass flow rate of water. It can be seen that by increasing the mass flow rate, there is no difference the first almost three minutes of the shower. After this, the rate between the two differs, as the experiment with highest mass flow rate continues with an average higher rate for a longer time than the other.

As for the three experiments, the response of a removal of the source is similar. The rate changes from an incline to a decline. With the use of this particular air change rate, it takes two minutes before an effect occurs. What is interesting about this is that though it takes two minutes for each of the sources, the change happens at the same difference in specific humidity. Thus the rate of decline is more rapid the higher the difference. This effect happens at 6 g/kg for these experiments.

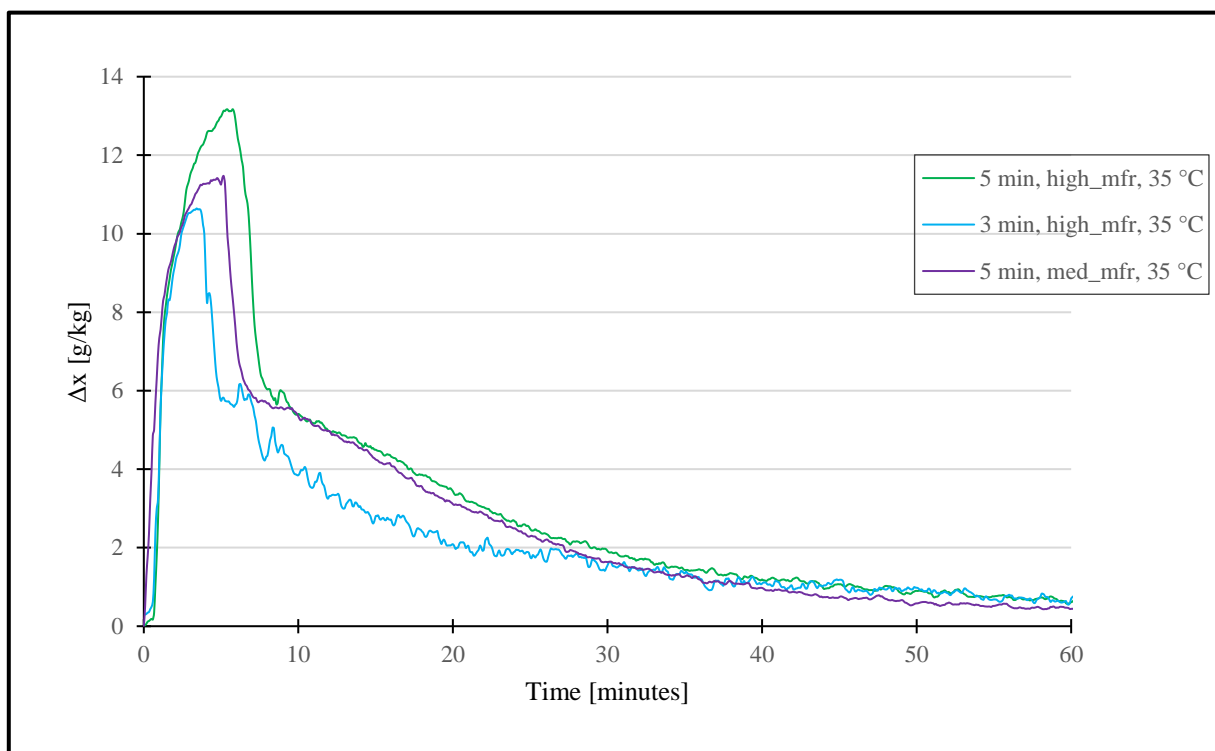


Figure 6.4: Comparison of the transient specific humidity difference between the bathroom inlet and extract, for three different showering experiments.

The most abundant changes between the graphs due to changes in the parameters are the amplitude and the total duration before declination. Both has an increase with longer duration and/ or larger mass flow rate.

6.2.4 Humid air density

The density of the air changes with temperature, air pressure and humidity content, ref. equation (10). As elaborated in Chapter 2, it is important to account for the changes in these variables when calculating the moisture production, to achieve accurate results.

During the experiments, the air density was calculated at every logging point at all the four sensors. The data was utilized as part of equation (14) to calculate the moisture production. The extreme values of the RH was, in the conducted experiments within the range 35 % - 100 % at all time. Within each experiment, the RH was only at saturation for a brief moment considering the length of each experiment, as can be seen from Figure 6.1. Either way it is still important to include the air density changes to obtain accurate results. As for the temperature, the range is between 18 °C and 27 °C for all the conducted research. The barometric air pressure was within 1005 hPa and 1025 hPa. Note from Chapter 2, that the changes in air temperature is the strongest influencing factor for the humid air density.

For the showering experiment previously used for exemplifications, the transient air density has been mapped. Figure 6.5 shows these changes for the four sensors mounted in Living Lab. The greatest change in air density is at the extract sensor. At this sensor the extreme values in both temperature and RH is highest, compared to the other three. The difference in mounting height is evident, as the total impact reduces with height, connected to the buoyancy and convection of air movement. The reasoning regarding the amplitude and the shift in reaction time is similar to previous discussion in this chapter.

The total difference in air density during showering experiments is relatively small. For the particular experiment in Figure 6.5, the total difference is merely 0.02 kg/m³ in the extract sensor. For the supply sensor, the change is practically zero. The air density does not change much for these experiments, however it is still necessary to account for the changes. The temperatures, air pressures and RH encountered in the conducted experiments could have been both higher and lower, thus a greater change in air density, and a greater impact on the accuracy had been present.

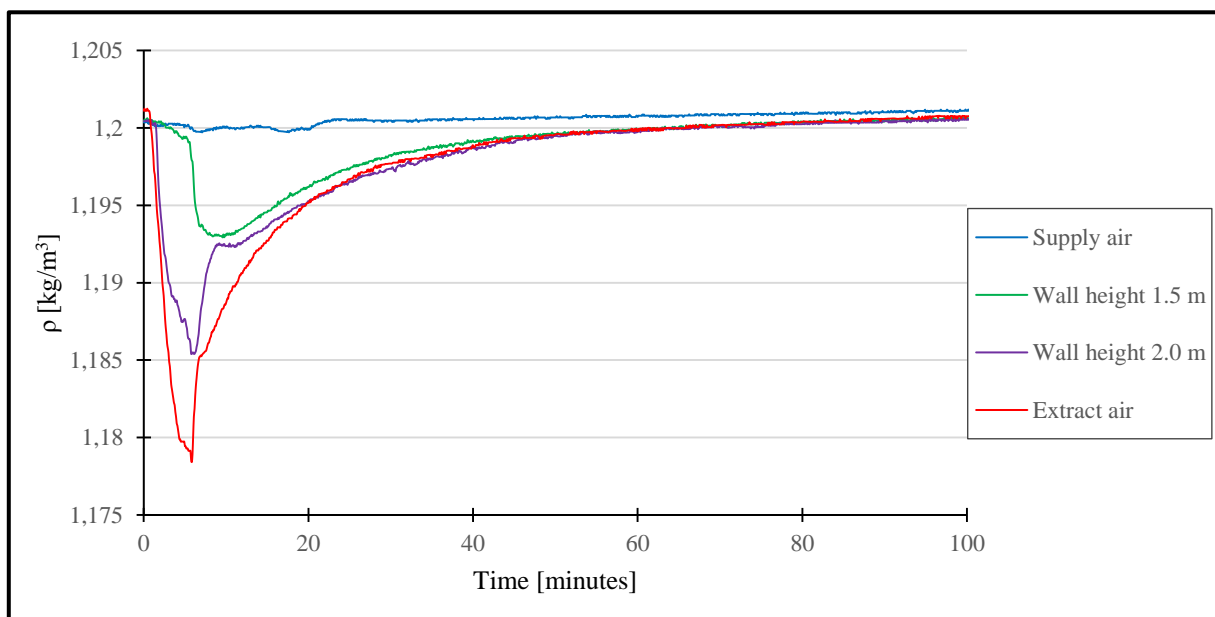


Figure 6.5: The humid air density changes at three different positions during a 5- min shower, with 35 °C water temperature and medium flow rate.

6.3 Moisture production model vs real cases

The moisture production model utilizes a series of mathematical equations to calculate the transient development in RH for predefined zones. The user of the model have to insert physical sizes of the rooms in addition the ventilation rates. The moisture production rates used by the model is constant, and has a predefined or user defined length, depending on source. Based on this the RH of the different zones are calculated.

Different scenarios creates different outcome in RH in the model. Along with the building and technical specifics, the outdoor conditions has influence on the response. In wintertime, the initial RH is lower than in the summer, thus the indoor environment has a lower grade of saturation. The conditions in Living Lab during the experiment period was hot summer days with a stationary indoor RH of around 40 %, when there was no activity in the building. The MPM utilizes real weather data to deal with different conditions.

For showering, the user can choose between two- minute intervals from two- to sixteen- minute shower length, as well as the time of occurrence during the day. Figure 6.6 is a graphical representation of the transient response in RH, during and after four different showering lengths. The building specifics and technical data of Living Lab has been inserted into the model to represent the real case, and the output has been processed into the graphs in Figure 6.6. The RH of the figure is comparable to the extract valve sensor of the real cases, as the model assumes the air is fully mixed. As can be seen from the figure, the four graphs has similar shapes. They all have equal initiation, where the RH increases to saturation the moment the water is turned on. Further, the air stays saturated until the water is turned off, as can be seen is linked to the shower length. The only difference between the graphs is the total time the air is saturated, which is linked to the chosen showering time.

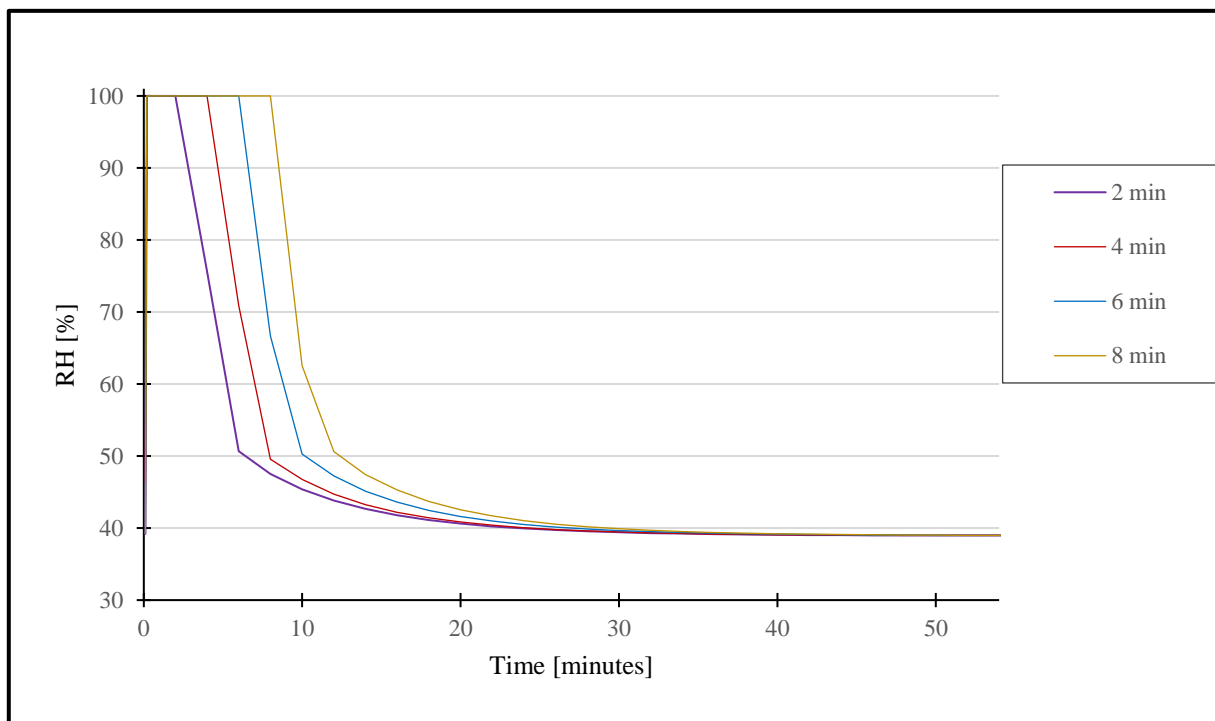


Figure 6.6: The transient response in RH, of four different shower lengths as they appear in the MPM.

6. Results

It is clear that with equal indoor supplied RH at the bathroom, the only difference between the shower lengths are the period the air is saturated. Thus, it does not matter which of the lengths are chosen when conducting the next analysis. It is of interest to see how the development in RH is, when changing the supplied RH to the bathroom, without changing building specifics and the technical values. Figure 6.7 compares four different stepwise changes in initial supplied RH to the bathroom. All four simulations are ran with equal showering length, with supplied RH ranging from 10 % to 40 %. The general result is that the rate of decline after the shower is turned off increases with decreasing initial RH. Furthermore, does the RH reaches its stationary value after longer time the greater the difference in RH amplitude.

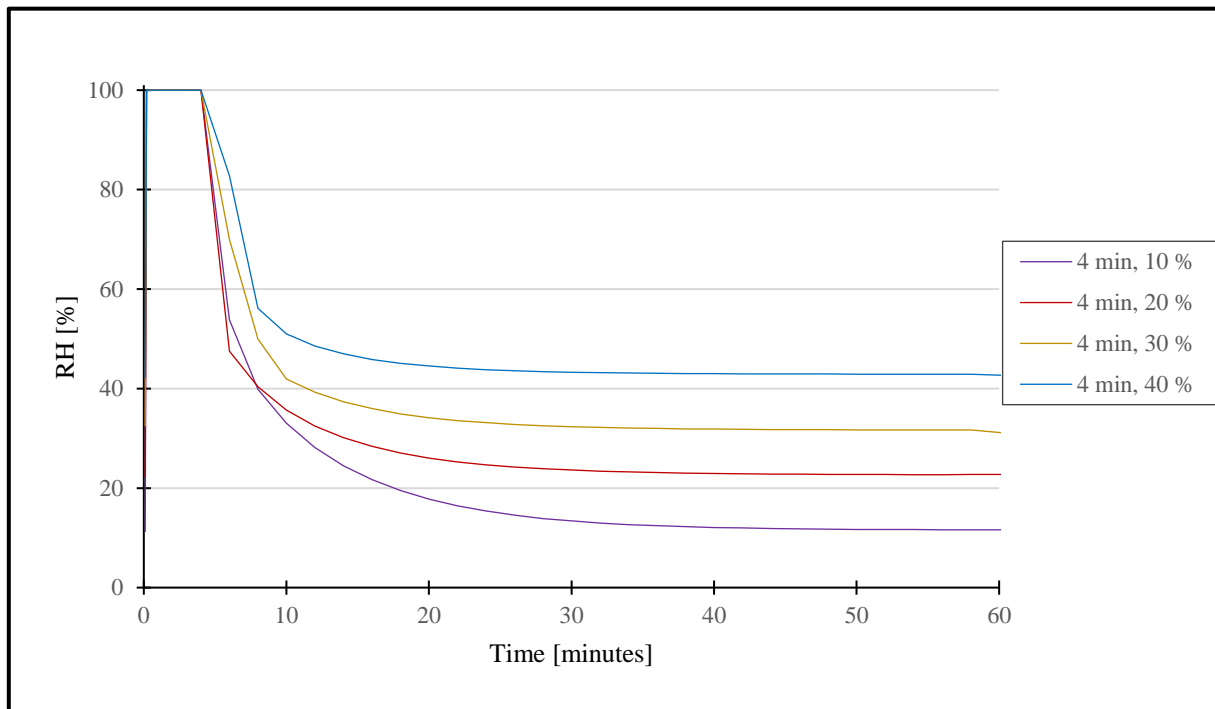


Figure 6.7: Comparison of the transient development in RH, from a four- minute shower with different initial RH.

A part of the goal of this thesis is to verify the MPM. There are several ways of conducting such a comparison. The method chosen is to compare the transient response in RH followed by a shower, between a simulation result from the MPM and a measured response from the experiments in Living Lab. To be able to do this comparison, the data leading to the boundaries has to be equal. Thus, the MPM is written such as the experiments conducted in Living Lab. This is achieved by using the same building specifics in the model as in Living Lab. Furthermore, the ventilation rate has to be equal, and the supplied air to the bathroom must have the same RH.

Figure 6.8 presents the comparison of MPM and a real case. The two cases represents the RH of the bathroom extract, and both situations is a four- minute shower with an initial RH of approximately 40 %, has the same air change rate and the same building specifics. It can be seen from the figure that the two graphs does not comply with each other. At initiation as well as during the four minutes the water is running, the two graphs are as equal as one could expect, but they eventually separates from one another. Two minutes after the water is turned off, the two graphs separates. A sudden change in decline rate occurs for the real case scenario, which slows. The simulated graph continues to decrease at the same rate for another minute before

this one also eventually slows down. It takes about 40 minutes for the simulated result to reach a stationary condition, while it takes the real test about 2.5 hours to reach the same result.

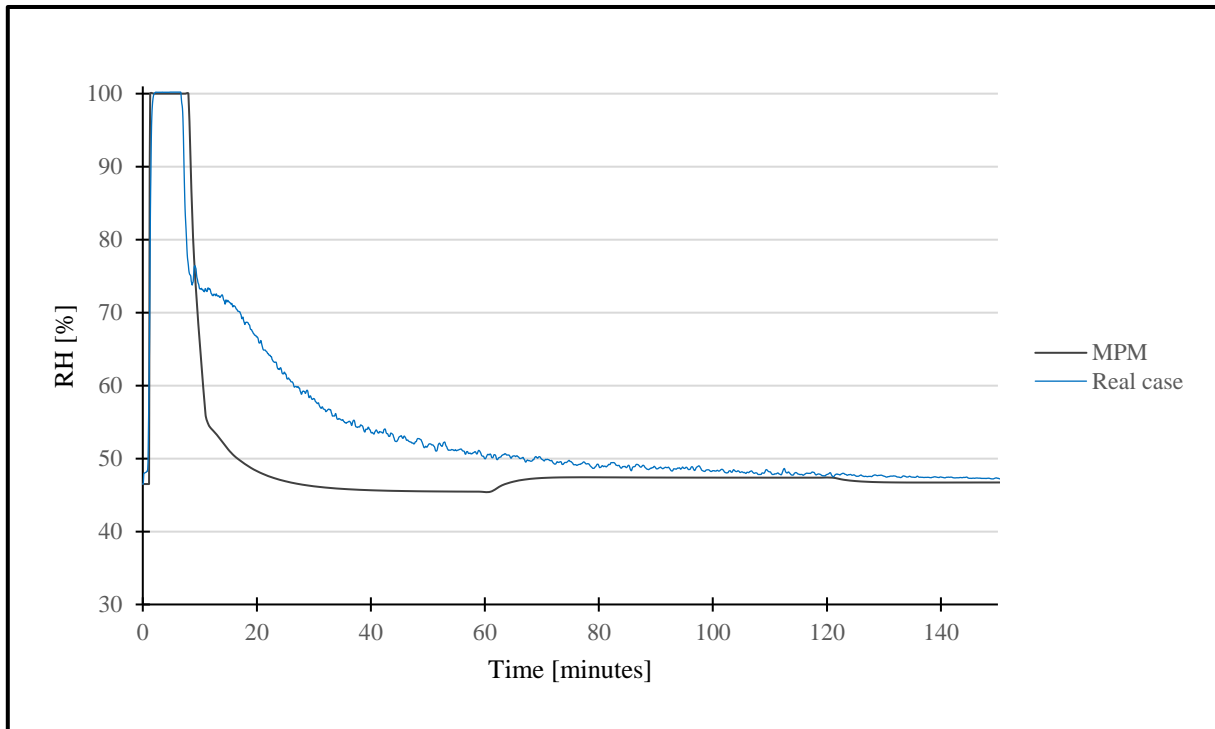


Figure 6.8: A comparison of the transient response in RH during and after a four- minute showering sequence, between a real case experiment conducted in Living Lab, and the MPM.

7. Discussion

This chapter extends the discussion from the previous chapters, where necessary.

7.1 Transient development during and after a showering sequence

The transient development in RH between the experiments and the model were not fully coherent with each other. The relations are almost equal until two minutes after the shower has been turned off. At this point, the decrease rate slows down in the experiments, while the model continues to descend at the same rate. This difference makes the total time for the relative humidity to reach a stationary condition merely 40 minutes for the model, while in reality it takes from 2 hours – 2.5 hours.

The total air volume of the bathroom is constantly exchanged with fresh air, via the underflow door valve and through the extract valve. With the simplification that the air inside the room is uniform and fully mixed, the air is only present for a certain time. This time is dependent on the airflow rate through the ventilation system, \dot{V} [m^3/h] as well as the room volume, V [m^3]. These quantities together constitute the air change rate of the room. Mathematically this is written as:

$$n = \frac{\dot{V}}{V} \quad (15)$$

If looking back at the bathroom of Living Lab, the ventilation rate was measured to be 105 m^3/h , and the volume was calculated as 12 m^3 . By using equation (15), the air change rate of the room is calculated to be $n = 8.75$ 1/h. This means that all the air in the room is exchanged with fresh air 8.75 times per hour. In other words, the air does in average stays in the bathroom for 6:51 minutes.

This reasoning is connected to the conducted experiments by looking into the measured transient response in RH (in theory, both the temperature and specific humidity could be used). Figure 7.1 helps to visualize the following reasoning. After the shower has been turned off, the RH immediately starts to decrease. The decrease occurs with a certain rate. This rate is initially determined by the ventilation rate and the size of the room.

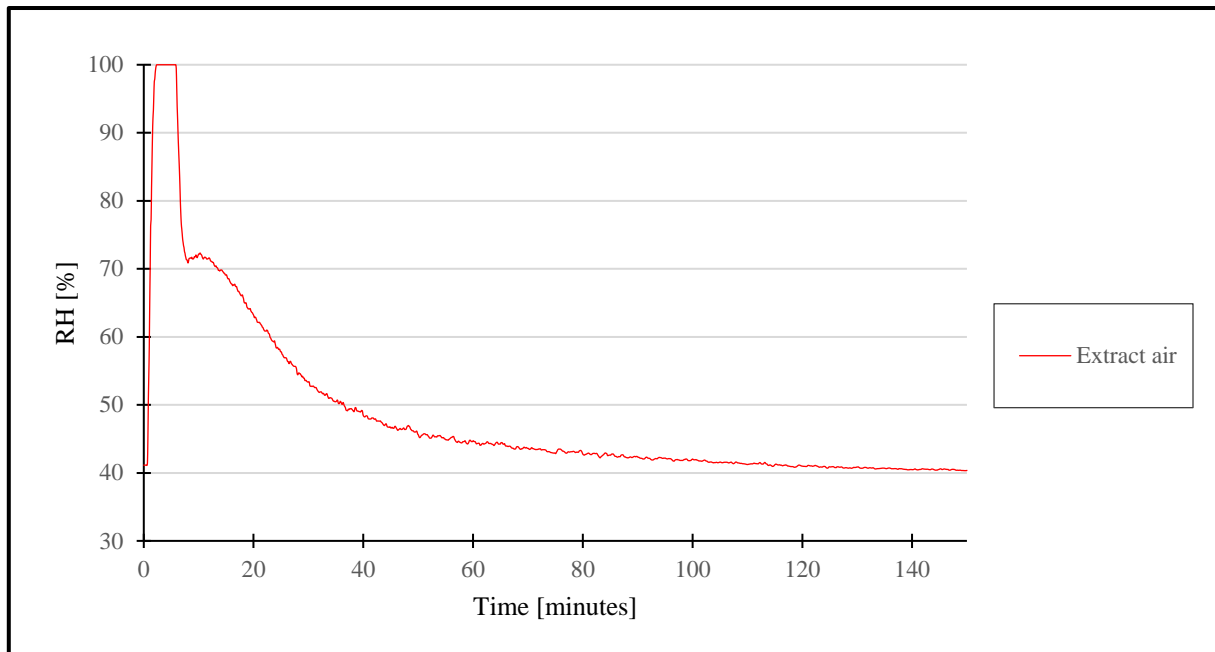


Figure 7.1: The transient relation in RH during and after a shower experiment.

An exponential decay curve is a convenient way to show the actual air change rate of an experiment. By redrawing Figure 7.1, by changing the y- scale to logarithmic and drawing an exponential fitting to the decay curve, the air change rate can actually be read off. The exponential fitting is mathematically written in the following way:

$$C = C_0 e^{-n*t} \quad (16)$$

, where the C can represent the value of the y- axis, RH, C_0 is the initial value, starting (highest) RH of the decay curve, e is Euler's number, n is the air change rate, and t is the time. When drawing an exponential fitting, it is important to shift the y- axis so that the stationary value is zero. In this context, it is the value at the last logging point of the experiment. This implies that the highest RH is around 60 %, due to the stationary RH as t goes towards infinity.

Figure 7.2 shows the logarithmic y-axis, as well as the exponential fitting, made by Excel. It can be seen that the coherence between the fitting and the actual curve fits quite well, but a great exception can be seen at the beginning of the curve. This implies that the rate of decrease is changing, but this can already be seen from Figure 7.1. However, by looking at the calculated air change rate of the figure, this can be seen as having the value 0.03 1/min, or an average time for one air change of 33:20 minutes. This is far greater than the measured value of 6:51 minutes.

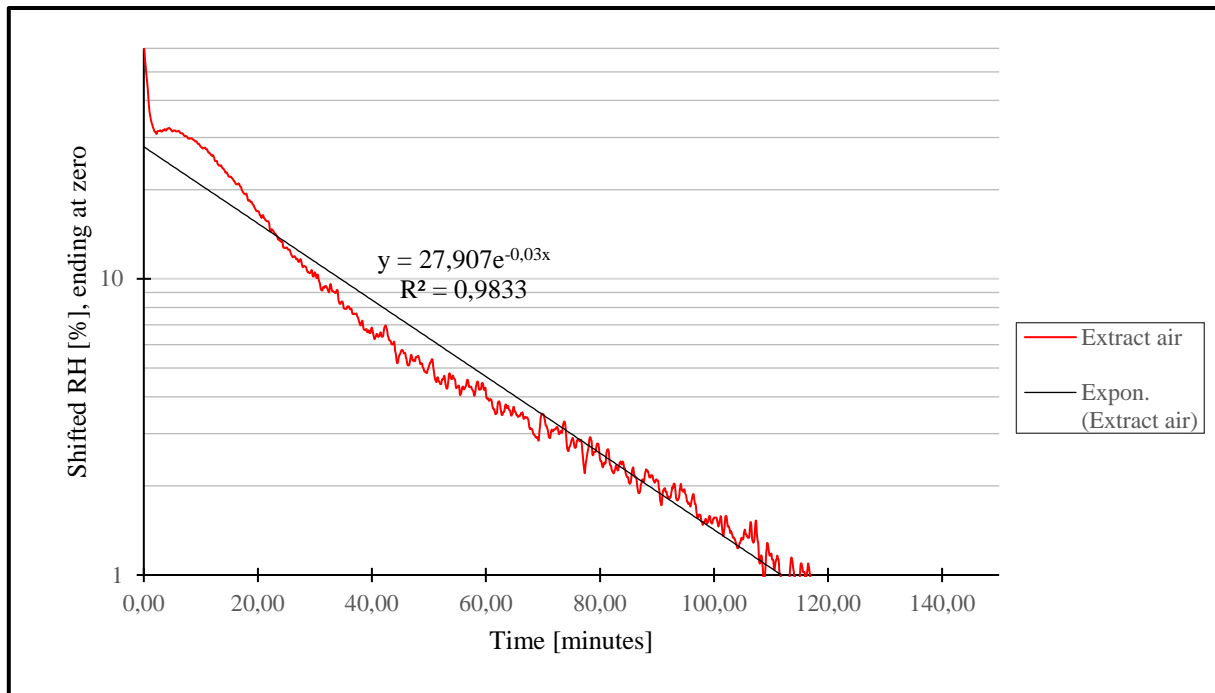


Figure 7.2: Logarithmic presentation of the decay curve in RH from a showering experiment after the water is turned off.

To connect the presented results to the conducted experiments, the air change rate has to be connected to the actual process and the RH. During a shower, moisture is released to the air in the form of water vapor. The RH increases rapidly towards saturation, and stays there as long as the rate of production is higher than the ventilation system can withstand. Once the shower is turned off, the moisture source is removed, and the ventilation takes over the control. During the experiments, the ventilation system exchanged the air in the room 8.75 times per hour, thus diluting the produced humidity at a high rate. However, as can be seen from Figure 7.2, the decrease rate has a distinct change 2 minutes after the source is removed. This change is assumed to be caused by the transition from direct water vapor present in the air during and directly after the shower, to the evaporation of the liquid water present on the floor and walls. The water vapor is rapidly diluted by ventilation, before evaporation of liquid water takes over. Between these two effects, there is assumed to be a transition period, as possibly seen in Figure 7.2.

If the line representing the RH in the extract was to be equal to the exponential fitting, the dilution process had happened with a constant rate. In this setting, depending on how accurate one sees it, there are at least two different rates. To be able to find the actual air change rate from the showering experiments, Figure 7.2 must be split into two parts. It can be seen that a distinct change in rate happens at two minutes (verified from the logging data). By drawing a set of two new graphs, and drawing two new exponential fittings to the decay curves, new air change rates can be found. One for the direct dilution of vapor, which should be close to the measured value, and one air change rate for the evaporation and dilution of liquid water. The two figures can be seen in Figure 7.3 and Figure 7.4.

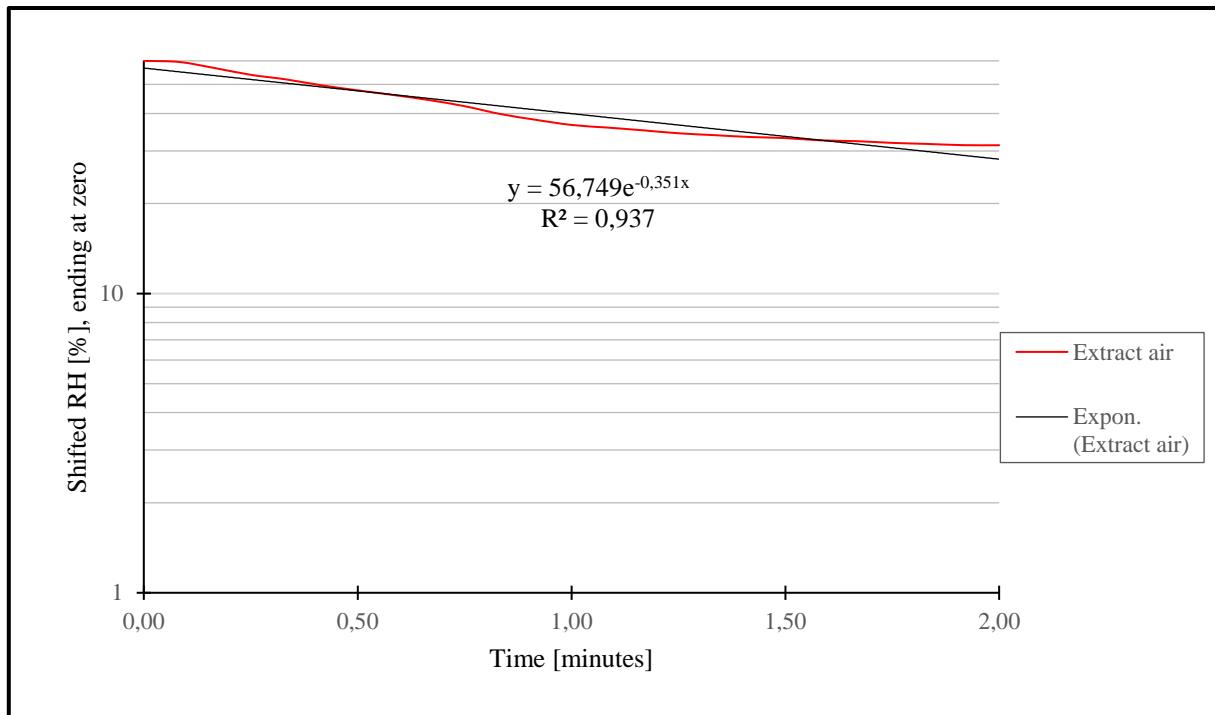


Figure 7.3: Logarithmic presentation of the decay curve in RH from the first two minutes of showering experiment after the water is turned off.

The air change rate from the first two minutes after the shower is turned off, can be seen from Figure 7.3 as being 0.351 1/min, or an average time for one air change of 2:51 minutes. This value is far higher than the measured (6:51 minutes). The reason for this is assumed to be that the extract valve is located directly above the shower, and since the glass doors of the shower creates its own enclosed atmosphere, it is assumed that the air in the bathroom is not fully mixed. A great part of the extracted air is then drawn out directly from the enclosed shower, without even mixing with the rest of the air. This is supported by looking at the sensors mounted at different heights of the bathroom, from Figure 6.1, where it can be seen that in fact not fully mixed.

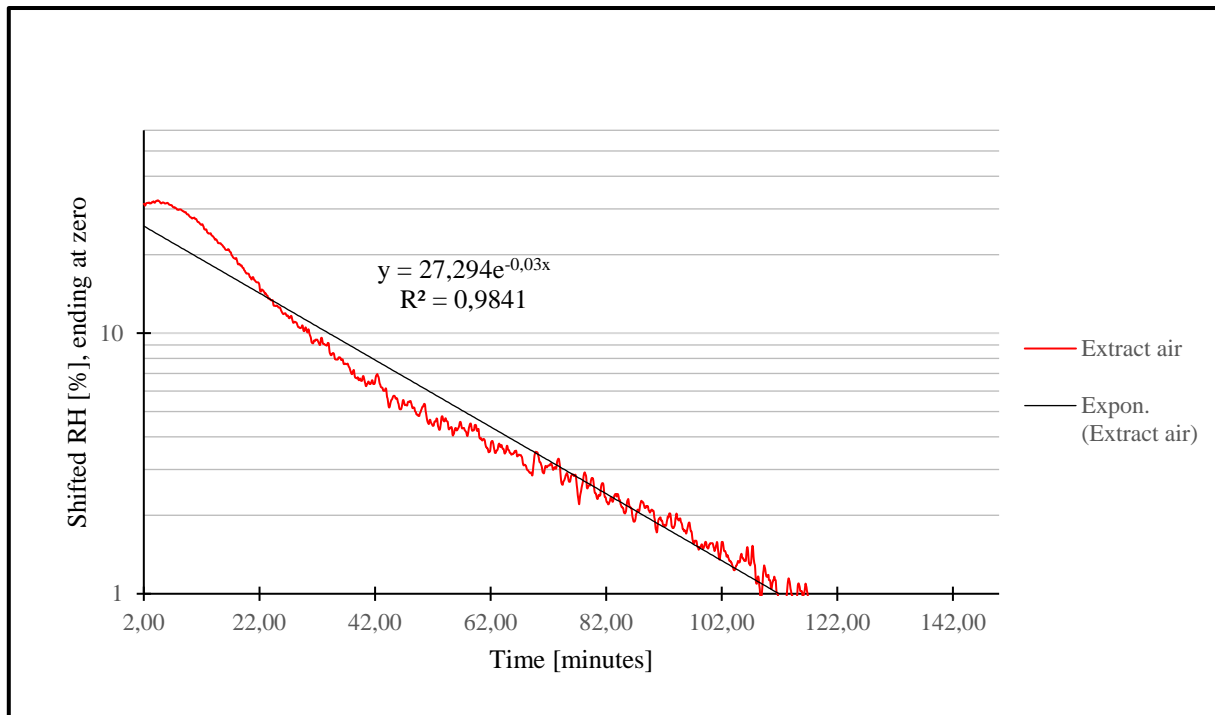


Figure 7.4: Logarithmic presentation of the decay curve in RH after the first two minutes of showering experiment after the water is turned off.

The air change rate *after* the first two minutes after the shower is turned off is, from Figure 7.4, 0.03 1/min, or an average time for one air change of 33:33 minutes. This value is far lower than measured (6:51 minutes). This is assumed to do with the evaporation and dilution of the liquid water left on the interior surfaces of the bathroom. The notable change at the beginning of the graph in Figure 7.4 is believed to be caused by the opening of the shower door, leading cold dry air in towards the shower, and mixing with the saturated.

Compared to the MPM, it was seen from Section 6.3 that the transient development between the real experiments did not cohere after the shower is turned off. The discussion of this had led the believe that the evaporation phase is not considered in the model. It is recommended that it should implement or look into the present implementation of this, since the error between the model and real life is of such great difference. In addition the total time for the RH to reach the stationary condition is far greater in real life compared to the model, which again is believed to be caused by the lack of implementation of the evaporation of the liquids left in the room.

7.2 Moisture production

7.2.1 Humans

The moisture production rates from humans varies greatly between the authors. The data, presented in Section 3, varies from 30 to 300 g/h. The greatest influencing parameter on human moisture production is the level of physical activity level. The lower value of 30 g/h is a rate of generation from a lowest activity level, while the upper limit of 300 g/h is at a highest activity

level. To be able to interpret an as correct value as possible into the MPM, the different activity levels needs to be defined.

The direct release of moisture from humans to the indoor environment is a supply from precipitation and respiration. According to Yik et al. (2004), the determining factor for the rate of moisture production is the state of mind, working load, individual metabolic profile along with surrounding environment. The combination of these four factors shows that to determine the exact generation rate is virtually impossible, as one would have to consider an unlimited amount of situations. In order to reduce the insecurities, a solution could be to gather data from a greater number of different activities and implement these into the model.

The MPM assumes a constant value of generation from awake, non-child humans of 55 g/h. This parameter is probably the most insecure generation factor in the model. The user inserts the number of hours it is indoor during a day, and the total moisture production from this particular activity would be 55 g/h times the number of hours. If considering the extreme values from research data of 30 g/h -300 g/h, the outcome would change significantly. If 8 hours of awake presence in inserted, the moisture release to the surrounding air would range from a total of 240 g – 2 400 g. However, the upper limit would not be probable, as this implies a most high activity during the full 8 hours. The average would be much closer to 55- than 300 g/h.

A solution to this problem could be to implement a number of plausible activities into the MPM. Such an expansion would require an investigation of which activities should be implemented. A selection of activities that has production rates furthest away from 55 g/h could be implemented. It is all about finding the most influencing activities, and interpret these into the model. By doing this, the total moisture production from humans would be estimated in a much more likely way. A suggestion, would be to use a study presented in Johansson et al. (2010). The author has mapped a number of household activities, and assigned them to moisture production rates, in addition to the probability of occurrence. The table can be found in Appendix G. By implementing a selection of the activities into the MPM, the total moisture production would be estimated in a much more probable way than just using a constant value of 55 g/h.

7.2.2 Showering

The moisture production source with the highest impact on RH is showering. During a shower, the RH increases from an initial state and rapidly towards saturation. A series of conducted showering experiments has tried to verify previous authors work on data from showering, and ultimately connect this to the MPM. It is clear that by changing a number of variables greatly affects the moisture production.

While the MPM only takes shower length into consideration, the conducted experiments has looked into three parameters. In addition to shower length, the moisture production was also calculated for varying water temperature and mass flow rate of water. By monitoring the state of the air during and after the showering experiments, it was calculated that a shower releases from 200 g/ shower to 750 g/shower, depending on the combination of the three variables.

As can be seen in Table 5-1, the MPM assumes a constant moisture production rate of 2 250 g/h. This value is the foundation for the transient analysis in the development of RH, as the production is linked to the actual duration of the shower. In the model the user has the possibility to choose between two minute steps of showering, ranging from 2 minutes to 16 minutes. Thus a 2 minute shower releases 75 g of water and a 16 minute shower releases 600 g of water. Per minute, the model assumes a production of 37.5 g/minute. From the conducted experiments this

values are low. Based on shower length, it can be seen from Table 6-1 that the actual release is ranging from 61 g/minute to 107 g/minute, depending on the other two tested variables.

It looks like the rate used in the MPM is underestimated. However, the values are based on research Yik et al. (2004), whose again gathered data from other authors. The rate of 2250 g/h data is presented as an averaged value of the moisture production from a four-member household during one day. This includes two children and two adults. Thus, if an assumption is made that children uses colder water, lower flow rate and in average showers less frequent than adults, the data is closer to valid. The conducted experiments in Living lab did not consider user age. In addition, since the rate is described as a release per day, it is assumed that some sort of frequency of showering behavior is considered. That is, an assumption that the residents are showering less than one time each day. If this is the case, the average generation rate is lower than if generation per hour in general is considered.

The suggestion to the further work on the MPM is to consider interpreting mass flow rate and temperature as a choice within showering. This could lead to far greater accuracy, as the conducted experiments has shown that it has a great effect on total release.

7.3 Moisture buffering

The buffer capacity of materials, furniture's and other hygroscopic materials has an influence on the RH within a short-term period of less than a week (Glass and TenWolde, 2009). The moisture exchange between the indoor air and hygroscopic surfaces occurs when the current relative humidity changes, though a production of moisture from a source or a removal of moisture through ventilation. Thus, when there is a change in indoor RH, hygroscopic materials absorbs or releases moisture. Under steady state conditions, the buffering capacity can be neglected, but including moisture sorption is necessary for accurate modelling on a time scale of hours and days.

A moisture production model developed by Lu (2003) estimated moisture production rate using polynomials to provide a smooth estimation curve, and real time recordings fitting measured values. The model did not considered sorption between indoor materials, and during a 6-month validation period in an unoccupied house, the model anticipated the moisture production rate. The predicted and measured rate differed by less than 10 % in average. It was concluded that this deviation could have been due to sorption.

The MPM does not considers sorption, so the secondary goal of the thesis has been to conduct a literature review on whether moisture buffering can be utilized to reduce the peaks in indoor relative humidity on not. Based on the research it is suggested that the effect should be implemented into the MPM at a later stage. The accuracy of the model is at this stage not high enough that this effect is essential. From the literature it is shown that the capability of a material to reduce the peaks in relative humidity is up to 30 % if used correctly. The author does however doubts that this can happen within a shower, as the moisture is released at such high rate, and ventilated out at almost equal rate. The moisture buffering is thus assumed to be ineffective on damping the effect from showering. However, if moisture buffering is used, the choice of material is essential- both because every material has its unique capability to store moisture, and because the rate of adsorption differs. An optimal penetration depth also exists, whereas if the thickness of the material is increased, it has little or no effect on its moisture buffering capability.

8. Conclusion

This master thesis has investigated the moisture production from indoor activities, and how it influences the indoor relative humidity. The main purpose has been to work towards a verification of a moisture production model, currently under development at NTNU. By both searching through the literature and conducting real case experiments, portions of the model has shown to have margins for improvement.

Moisture in general is the number one cause of building related damages, whereas about 6 % - 8 % is directly related to indoor moisture. With increased demand for building tightness, it is crucial to have a properly sized mechanical ventilation system to ventilate the excess moisture out of the building, preventing it to accumulate. An indoor relative humidity of above 70 % gives favorable conditions for mold and bacterial growth on indoor surfaces, and can worsen asthmatic symptoms. Monitoring and studying the indoor levels of humidity is essential in order to understand and prevent these situations.

A number of processes and activities in an indoor environment generates moisture. Breathing, showering, bathing, cooking, cleaning, and drying of clothes are all generating moisture to the surrounding air. However, the indoor moisture production rates varies greatly between the different sources, as seen from research. The main focus of this thesis has been on moisture production from showering. The moisture production model is developed to study the impact of changes in RH on a rotary heat exchanger, and develop knowledge to prevent frosting and condensation. Thus, it was chosen to study the indoor activity that contributes most to these changes. Showering has the ability to release a significant amount of moisture to the air, within a relatively short amount of time. A calculation method on how the moisture production from a shower could be quantified was presented. By using the bathroom at the test facility Living Lab at NTNU to conduct experiments, a number of sensors were rigged to monitor the state of the air. By varying a set of parameters, a series of showering experiments was conducted, and the moisture production was calculated.

When conducting such delicate experiments as moisture production, instrument accuracy is of great importance. There is no point in using highly accurate calculations, if the measuring devices are completely off. As preparations for the experiments, the author spent a significant time on the calibration of sensors. It was revealed that the sensors monitoring relative humidity/temperature in Living Lab had too slow response time to be utilized fully. The relative humidity during a shower increases to saturation within a few minutes, which the instruments did not fully caught. Six new sensors were thus bought and mounted, by the author. In addition to these sensors, the anemometers in the ventilation ducts of Living lab was malfunctioning, resulting in other methods to measure the airflow rate.

The results from the showering experiments showed that the moisture production from showering varies greatly depending on the boundaries. The length of the shower, the mass flow

8. Conclusion

rate of water and the water temperature fall plays an important role, as the results showed. The moisture production was calculated to range from 200 g/shower to 750 g/shower, depending on the combination of variables. However, there was consistency between the parameters, as the moisture production increased with increased load. Compared to the literature, the production was higher in the real cases. As the literature suggested between 200 g/ shower – 400 g/ shower, most of the results from the experiments was in the upper part of this.

The moisture production model simulates the indoor relative humidity by a series of mathematical equation and input from the user. The model presents data on the transient development in relative humidity. The comparison between the model and the conducted experiments showed a similar behavior until two minutes after the shower has been turned off. At this point the relative humidity decrease rate slows down in real life, while the model continues to descend at the same rate. This difference makes the total time for the relative humidity to reach a stationary condition merely 40 minutes for the model, while in reality it takes from 2 hours – 2.5 hours. This is assumed to have to do with the transition from water vapor present in the air, which is rapidly ventilated out, to the evaporation of liquid water left in the bathroom, which takes a longer time. The model does not take this into consideration, and it is suggested that it should.

The secondary goal of the thesis has been to conduct a literature review on whether moisture buffering can be utilized to reduce the peaks in indoor relative humidity or not. Based on the research it is suggested that the effect should be implemented into the model at a later stage. The accuracy of the model is at this stage not high enough that this effect is essential. From the literature it is shown that the capability of a material to reduce the peaks in relative humidity is up to 30 % if used correctly. The author does however doubt that this can happen within a shower, as the moisture is released at such high rate, and ventilated out at almost equal rate. The moisture buffering is thus assumed to be ineffective on damping the effect from showering. However, if moisture buffering is used, the choice of material is essential- both because every material has its unique capability to store moisture, and because the rate of adsorption differs. An optimal penetration depth also exists, whereas if the thickness of the material is increased, it has little or no effect on its moisture buffering capability.

9. Further work

The validation process of the moisture production model is a time consuming task that has to be performed step by step in the future, in order to achieve a reliable and useful model. This thesis work has merely started to touch the possibilities that surrounds the model, as there are several aspects left to study. It is highly recommended to continue working in the model until similarity between simulated and real life test is achieved, and the model can provide adequately accurate results.

Some recommendations for further work are:

- Implement the suggested improvements regarding showering to the model.
- Conduct showering experiments with a greater range of parameters, such as varying the ventilation rate, different stationary relative humidity and other locations.
- Fix the logging system in Living Lab, as a significant downtime of the system was experienced.
- Continue the testing of other sources in Living lab, as the system is significantly more accurate than what it was.
- Implement a greater set of choices within each source in the model.
- Complete the moisture production model. It still does not run in a stable way.

10. Bibliography

- ADAN, O. C. G. & SAMSON, R. A. 2011. *Fundamentals of mold growth in indoor environments and strategies for healthy living*, Wageningen Academic Publishers.
- ANGELL, W. J. & OLSON, W. W. 1988. Moisture Sources Associated with Potential Damage in Cold Climate Housing CD-F00-3405-1988. *Cold Climate Housing Information Center, Minnesota Extension Service*. MN.
- ANNEX27 1995. Evaluation and demonstration of domestic ventilation system. Sweeden.
- ARENA, L. & BLANFORD, M. 2010. Monitoring of internal moisture loads in residential buildings. *Proceedings of Building Enclosure Science and Technology (BEST2)*. Portland, OR.
- EDVARDBSEN, K. I. & RAMSTAD, T. Ø. 2014. *Håndbok 5: Trehus*, SINTEF akademisk forlag.
- EMERSON OROCES MANAGEMENT 2010. Fundamentals of Orifice Meter Measurement.
- FANG, L., CLAUSEN, G. & FANGER, P. O. 1998. Impact of Temperature and Humidity on the Perception of Indoor Air Quality. *Indoor Air*, 8, 80-90.
- FRANCESCO, G., LUCA, F. & ARILD, G. 2014. The ZEB Living Lab: a multi-purpose experimental facility. *Gent Expert Meeting*. Ghent University – Belgium.
- GEVING, S. & THUE, J. V. 2002. *Håndbok 50 - Fukt i bygninger*, Oslo, Norges byggforskningsinstitutt.
- GLASS, S. V. & TENWOLDE, A. 2009. REVIEW OF MOISTURE BALANCE MODELS FOR RESIDENTIAL INDOOR

- HUMIDITY. *12th Canadian Conference on Building Science and Technology*. Montreal, Quebec.
- HUGHES-HALLET, D. & MCCULLUM, W. G. 2005. *Calculus*, Wiley.
- ILOMETS, S., KALAMEES, T. & VINHA, J. 2017. Indoor hygrothermal loads for the deterministic and stochastic design of the building envelope for dwellings in cold climates. *Journal of Building Physics*, 1-31.
- INCROPERA, F. P., DEWITT, D. P., BERGMAN, T. L. & LAVINE, A. S. 2013. *Principles of Heat and Mass Transfer, Seventh Edition*, John Wiley & Sons, Inc.
- INGEBRIGTSEN, S. 2016a. *Ventilasjonsteknikk 1*, Maura, Skarland Press.
- INGEBRIGTSEN, S. 2016b. *Ventilasjonsteknikk 2*, Maura, Skarland Press.
- JENSEN, K. R., JENSEN, R. L., NØRGAARD, J., JUSTESEN, R., ONSILD, B. & NIELS, C. 2011. Investigation on Moisture and Indoor Environment in Eight Danish Houses. *Proceedings of the 9th Nordic Symposium on Building Physics*, 3, 1127-1134.
- JOHANSSON, P., PALLIN, S. & SHAHRIARI, M. 2010. Risk Assessment Model Applied on Building Physics: Statistical Data Acquisition and Stochastic Modeling of Indoor Moisture Supply in Swedish Multi-family Dwellings *IEA Annex 55 RAP-RETRO*. Copenhagen.
- JOHANSSON, P. & SVENSSON, A. 1998. Metoder för mätning av luftflödet i ventilasjonsinstallasjoner.
- KALAMEES, T., VINHA, J. & KURNITSKI, J. 2006. Indoor Humidity Loads and Moisture Production in Lightweight Timber-frame Detached Houses. *Journal of Building Physics*, 29, 219-246.

-
- LOWEN, A. C., MUBAREKA, S., STEEL, J. & PALESE, P. 2007. Influenza Virus Transmission Is Dependent on Relative Humidity and Temperature. *PLOS Pathogens*, 3, e151.
- LU, X. 2003. Estimation of indoor moisture generation rate from measurement in buildings. *Building and Environment*. 38, 5, 665–675.
- MASKELL, D., THOMSON, A., WALKER, P. & LEMKE, M. 2017. Determination of optimal plaster thickness for moisture buffering of indoor air. *Building and Environment*, 130, 143-150.
- METEOROLOGISK INSTITUTT. 2018. *eKlima* [Online]. Available:
http://sharki.oslo.dnmi.no/portal/page?_pageid=73,39035,73_39057&dad=portal&schema=PORTAL [Accessed January 8 2018].
- MORAN, M. J., SHAPIRO, H. N., BOETTNER, D. D. & BAILEY, M. B. 2012. *Principles of Engineering Thermodynamics, 7th ed.*, John Wiley & Sons, Inc.
- MYSOVSKIKH, I. P. 2011. *Simpson formula* [Online]. Encyclopedia of Mathematics. Available:
http://www.encyclopediaofmath.org/index.php?title=Simpson_formula&oldid=17966 [Accessed 25/7-2018].
- NILSSON, P.-E. (ed.) 2003. *Achieving the Desired Indoor Climate: Energy Efficiency Aspects of System Design*: Lund Studentlitteratur.
- ORESZCZYN, T., RIDLEY, I., HONG, S. H., WILKINSON, P. & GROUP, W. F. S. 2006. Mould and Winter Indoor Relative Humidity in Low Income Households in England. *Indoor and Built Environment*, 15, 125-135.
- OYJ, V. 2013. HUMIDITY CONVERSION FORMULAS: Calculation formulas for humidity.
- PALLIN, S., JOHANSSON, P. & HAGENTOFT, C.-E. 2011. STOCHASTIC MODELING OF MOISTURE SUPPLY IN DWELLINGS BASED ON MOISTURE PRODUCTION AND MOISTURE BUFFERING CAPACITY. *Proceedings of*
-

- Building Simulation 2011: 12th Conference of International Building Performance Simulation Association*. Sydney.
- REINIKAINEN, L. M. & JAAKKOLA, J. J. K. 2003. Significance of humidity and temperature on skin and upper airway symptoms. *Indoor Air*, 13, 344-352.
- RODE, C., PEUHKURI, R., SVENNBERG, K. & OJANEN, T. 2007. Moisture Buffer Value of Building Materials. *Journal of ASTM International*.
- SATO, M., FUKAYO, S. & YANO, E. 2003. Adverse Environmental Health Effects of Ultra-low Relative Humidity Indoor Air. *Journal of Occupational Health*, 45, 133-136.
- SHELQUIST, R. 1998. *An Introduction to Air Density and Density Altitude Calculations* [Online]. Available: https://wahiduddin.net/calc/density_altitude.htm [Accessed].
- STANDARD, B. 2002. BS 5250. *Code of Practice for Control of Condensation in Buildings*.
- WOLKOFF, P. & KJÆRGAARD, S. K. 2007. The dichotomy of relative humidity on indoor air quality. *Environment International*, 33, 850-857.
- YIK, F. W. H., SAT, P. S. K. & NIU, J. L. 2004. Moisture Generation through Chinese Household Activities. *Indoor and Built Environment*, 13, 115-131.
- ZEMITIS, J., BORODINECS, A. & FROLOVA, M. 2016. Measurements of moisture production caused by various sources. *Energy and Buildings*, 127, 884-891.
- ZHANG, H., YOSHINO, H. & HASEGAWA, K. 2011. Assessing the moisture buffering performance of hygroscopic material by using experimental method. *Building and Environment* 48, 48, 27-34.
- ZHANG, M., QIN, M. & CHEN, Z. 2017a. Moisture Buffer Effect and its Impact on Indoor Environment. *10th International Symposium on Heating, Ventilation and Air Conditioning, ISHVAC2017*. Jinan, China: Procedia Engineering.

ZHANG, M., QIN, M., RODE, C. & CHEN, Z. 2017b. Moisture buffering phenomenon and its impact on building energy consumption. *Applied Thermal Engineering*, 124, 337-345.

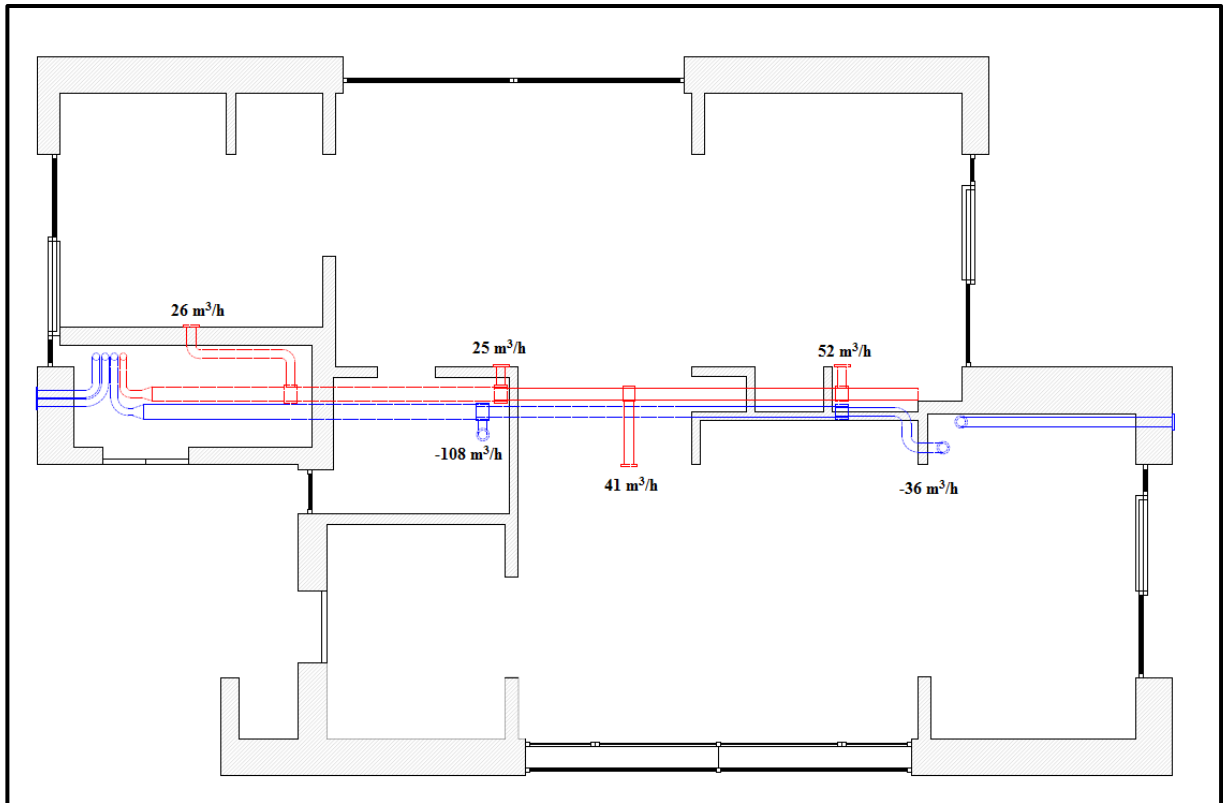


Figure A.2: Projected ventilation rates in Living Lab. A “+” sign implies supply of air, and a “-“ sign implies an extract (PROSJEKTUTVIKLING MIDT-NORGE AS, 2014)

B Balancing chart

The balancing of the ventilation system in ZeB Living lab was conducted on the 20/12-2018. By using a Testo 420 - Air flow capture hood, to measure the flow rates. The measuring range for the device was from 40 – 4000 m³, thus the lower limit was above some of the projected amounts of air through some of the air terminals. By temporarily increasing the overall flow rate of air via the air handling units control panel, this potential problem was avoided. This is due to the proportional air flow rates achieved when balancing. Thus the fan speed was reduced when the balancing was completed, to enable the projected amounts of air flow through each of the air terminals.


 SINTEF SINTEF Byggforsk									
Bygning		<i>ZEB- Living lab</i>							
Anlegg & tilstand		<i>Tilluft – Flexit UNI 3, 90 % luftmengde</i>							
Innregulert av, dato		<i>Anders Saasen Pedersen, 20/12-17</i>							
Tegninger / rev.		<i>Prosjektutvikling Midt- Norge AS</i>							
Etasje & Rom	Gren nr.	Spjeld nr.	K-faktor (l/s)	Prosjektert luftmgde		Innregulering			
				m3/h		Målt	Måle-enhet	Målt/Pr. %	I & R
Bedroom east	A1	T1		52	(52, m3/h)	100	m3/h	192 %	I+R
Living room south	A2	T2		41	(41, m3/h)	75	m3/h	183 %	I+R
Living room north	A3	T3		25	(25, m3/h)	49	m3/h	196 %	I+R
Bedroom west	A4	T4		26	(26, m3/h)	50	m3/h	192 %	I+R

Figure B.1: Balancing chart for supply ducts, before adjusting the fan speed to match projected airflow rate.


 SINTEF SINTEF Byggforsk		Protokoll for innregulering						
Bygning		<i>ZEB- Living lab</i>						
Anlegg & tilstand		<i>Avtrekk – Flexit UNI 3, 90 % luftmengde</i>						
Innregulert av, dato		<i>Anders Saasen Pedersen, 20/12-17</i>						
Tegninger / rev.		<i>Prosjektutvikling Midt- Norge AS</i>						
Etasje & Rom	Gren nr.	Spjeld nr.	K-faktor (l/s)	Prosjektert luftmgde m3/h	Innregulering			
					Målt	Måle-enhet	Målt/Pr. %	I & R
Kitchen extract	B1	T5		36 (36, m3/h)	47 m3/h		131 %	I+R
Bathroom extract	B2	T6		108 (108, m3/h)	110 m3/h		134 %	I+R

Figure B.2: Balancing chart for extract ducts, after adjusting the fan speed to match the projected airflow rate.

C Calibration of sensors

As a preparation for further work, the sensors measuring temperature and relative humidity in the extract ducts in ZeB Living lab was calibrated. See Figure C.1 for the placement of the sensors, where blue ducts represent the extract, and red represent the supply.

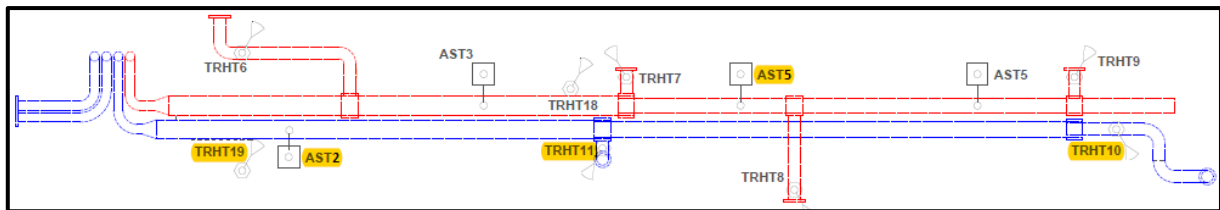


Figure C.1: Location of sensors in the ductwork of ZeB Living Lab. Those calibrated are marked in yellow.

C.1 Velocity

The velocity sensors used to monitor the air velocity in the ventilation ducts in ZeB Living lab is digital sensors of type “S + S Regeltechnik - KLGf-1”. The technical data is extracted from the manufacturer, and can be found through the link: <https://spluss.de/en/products/air-quality-and-flow/airflow-monitor-flow-monitor/1701-3120-1000-000-klgf-1/> (downloaded January 21st 2018).

Technical data:

Voltage supply: 24 V DC

Output: 0 - 10 V

Measuring range: 0.1...30 m/s (adjusted)

Ambient operating temperature: 0...+60 °C at the device and 0...+80 °C medium

	AST2	Air flow rate [m ³ /h] trough orifice calculations	Air velocity [m/s] in ø200 trough orifice calculations	pressure drop [dP] over orifice	Voltage [V] measured with FLUKE 115 voltage meter
Run 1		70,7	0,625442321	29	2,55
		89,6	0,792639774	47	3,3
		109,6	0,969568294	71	4
		125,2	1,107572541	93	4,54
		139,6	1,234961076	115,5	4,94
		158,4	1,401273885	150	5,44
		179,3	1,58616419	193	5,98
Run 2		76,4	0,67586695	34	2,76
		88,6	0,783793347	46	3,26
		111,1	0,982837933	73	4,05
		124,5	1,101380042	92	4,48
		137,8	1,219037509	113	4,85
		157,8	1,39596603	149	5,37
		184,3	1,63039632	204	6,03
Run 3		73,1	0,646673744	31	2,62
		90,5	0,800601557	48	3,32
		109,6	0,969568294	71	3,96
		125,2	1,107572541	93	4,45
		140,7	1,244692144	118	4,89
		164	1,450813871	161	5,49
		177,5	1,570240623	189	5,82

Figure C.2: Results from three runs of calibration of the AST2 velocity sensor.

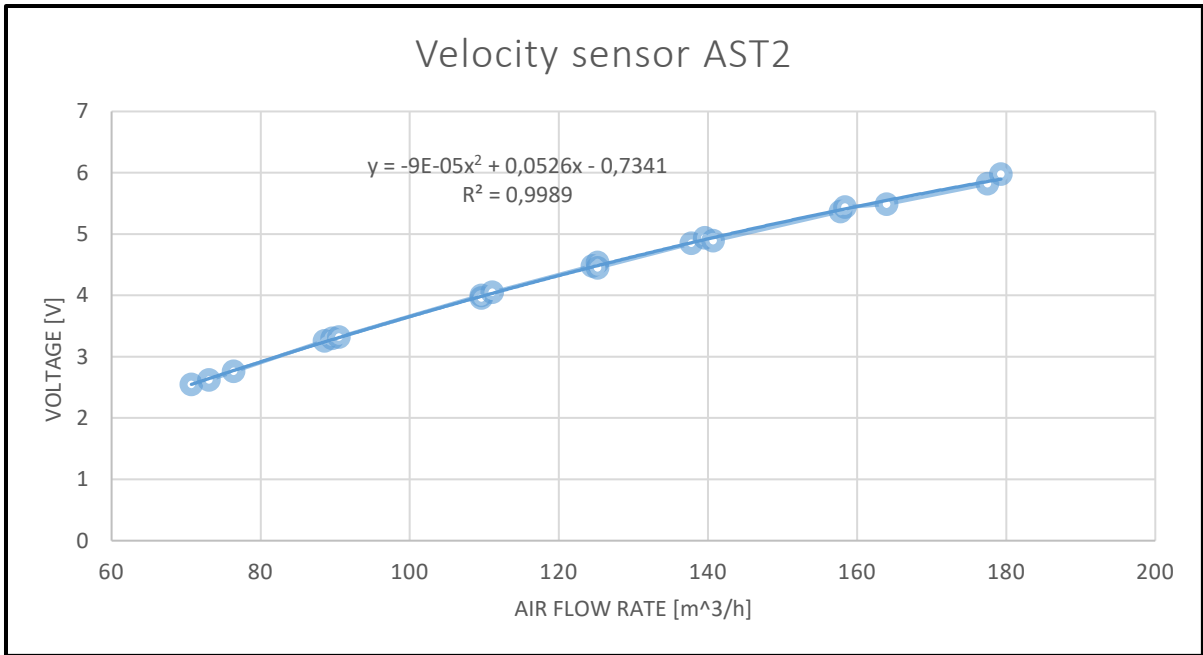


Figure C.3: Calibration data for velocity sensor AST2, based on three separate runs of calibration. A second-degree formula is generated to fit between the three runs.

	AST5	Air flow rate [m ³ /h] trough orifice calculations	Air velocity [m/s] in ø200 trough orifice calculations	pressure drop [dP] over orifice	Voltage [V] measured with FLUKE 115 voltage meter
Run 1		74,2	0,656404812	32	2,7
		83,8	0,741330502	41	3,09
		102,6	0,907643312	62	3,84
		122,5	1,08368719	89	4,54
		141,3	1,25	119	5
		162	1,433121019	157	5,6
		180,2	1,594125973	195	6,02
Run 2		70,7	0,625442321	29	2,5
		80,7	0,713906582	38	2,86
		101,8	0,900566171	61	3,71
		121,1	1,071302194	87	4,38
		135,3	1,196921444	109	4,82
		159,9	1,414543524	153	5,54
		177,7	1,572009908	189,5	5,95
Run 3		71,9	0,636058033	30	2,6
		84,8	0,750176929	42	3,07
		103,4	0,914720453	63	3,78
		122,5	1,08368719	89	4,47
		137,2	1,213729653	112	4,86
		159,9	1,414543524	153	5,51
		180,7	1,598549186	196	6,06

Figure C.4: Results from three runs of calibration of the AST5 velocity sensor.

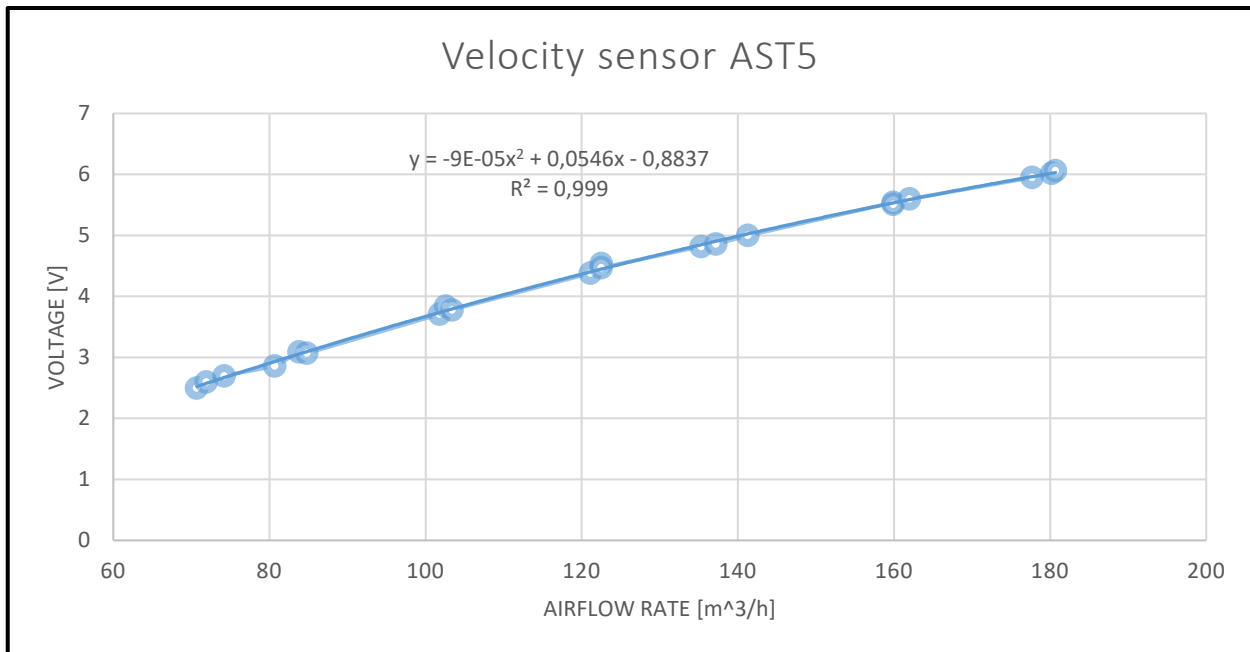


Figure C.5: Calibration data for velocity sensor AST5, based on three separate runs of calibration. A second-degree formula is generated to fit between the three runs.

C.2 Relative humidity

The hygrometers used to monitor temperature and RH in ZeB Living lab is digital sensors of type “S + S Regeltechnik - KFTF-I”. The technical data is extracted from the manufacturer, and can be found through the link: <https://spluss.de/en/products/humidity/duct-humidity-sensor/1201-3112-1000-029-kftf-i/>

Technical data:

Voltage supply: 24 V DC

Measuring range relative humidity 0... 100 % RH

Deviation of humidity: ± 2 % RH. (20...80 % RH); at + 25 °C, otherwise ± 3 % RH

Output RH: 0 – 20 mA (linear)

Measuring range temperature: -35...+80 (adjustable)

Temperature deviation: ± 0.2 K at +25 °C

Output temperature: 4...20 mA (linear)

Ambient temperature: storage -35...+85 °C; Operation - 30...+75 °C, non-precipitating

Long-term stability: ± 1 %/year

C	LiCl	MgCl ₂	NaCl	K ₂ SO ₄
0	*	33.7 ± 0.3	75.5 ± 0.3	98.8 ± 1.1
5	*	33.6 ± 0.3	75.7 ± 0.3	98.5 ± 0.9
10	*	33.5 ± 0.2	75.7 ± 0.2	98.2 ± 0.8
15	*	33.3 ± 0.2	75.6 ± 0.2	97.9 ± 0.6
20	11.3 ± 0.3	33.1 ± 0.2	75.5 ± 0.1	97.6 ± 0.5
25	11.3 ± 0.3	32.8 ± 0.2	75.3 ± 0.1	97.3 ± 0.5
30	11.3 ± 0.2	32.4 ± 0.1	75.1 ± 0.1	97.0 ± 0.4
35	11.3 ± 0.2	32.1 ± 0.1	74.9 ± 0.1	96.7 ± 0.4
40	11.2 ± 0.2	31.6 ± 0.1	74.7 ± 0.1	96.4 ± 0.4
45	11.2 ± 0.2	31.1 ± 0.1	74.5 ± 0.2	96.1 ± 0.4
50	11.1 ± 0.2	30.5 ± 0.1	74.4 ± 0.2	95.8 ± 0.5

Figure C.6: Correlation between temperature and RH when a pure salt/distilled water solution is enclosed in a container (Vaisala, 2018).

TRHT10		Temperature [°C]	Measured current with logger [mA]	RH [%], from table
LiCl		21	7,07	11,3
NaCl		21,2	16,14	75,5
TRHT11		Temperatur [Grader C]	Målt strøm med logger [mA]	Relativ fuktighet [%]
LiCl		21	6,56	11,3
NaCl		20,8	15,2	75,5
TRHT5		Temperatur [Grader C]	Målt strøm med logger [mA]	Relativ fuktighet [%]
LiCl		21,1	5,65	11,3
NaCl		21	15,52	75,5

Figure C.7: Calibration data for three hygrometers, based on average of three separate runs of calibration.

D Moisture production model

Table D-1: Data moisture production rates utilized in the MPM (Yik et al., 2004)

Source of moisture		BS 5250 [15]	CIBSE [16]	Lstiburek [17]	Hanson [18]	Trechsel [19]	Rousseau [20]
People (g · h ⁻¹ per person)	Asleep	40					
	Active	55					
	Light activity					30–120	
	Medium activity					120–200	
	Heavy activity					200–300	
	Perspiration and respiration		40–100	65			
Cooking (g · day ⁻¹ per household)*	Not specified				180		50
	Breakfast (elect/gas)			200/520			
	Lunch (elect/gas)			300/680			
	Dinner (elect/gas)			700/1600			
	3 meals		900–3000		920	1500	957
	Simmer (cover/uncovered)			6/75 (g per 10 min)			
	Boil (covered/uncovered)			270/330 (g per 10 min)			
Whole day (electricity)	2000						
Whole day (gas)	3000			2160		1435	
Dishwashing (g · day ⁻¹)*	Breakfast			30			
	Lunch			25			
	Dinner			100			
	Not specified	400	150–450		450		522
Bathing (g · day ⁻¹)*	Tub			280	200	2400	696
	Shower			1200	920		1216
	Not specified	800	750–1500				
Clothes washing (g · day ⁻¹)*	500	500–1800		1960			
Indoor clothes drying (g · day ⁻¹)*	Unvented	6000		2660–3520 (g per load)	11,970	2200–2920 (g per load)	1740
			5000–14,000				
Floor mopping/washing (g · m ⁻²)	Not specified		100–150	180	150	116	134
Indoor plants (g · day ⁻¹)			800	500	20 g · h ⁻¹	500	391

*For a four-member household.

E Matlab scripts

E.1 Surface plot: Specific humidity

Table E-1: Matlab scrip for producing a surface plot showing the relation between specific humidity, RH and temperature.

```
clear all;
clc;

%Creating meshes to get a smooth plot
[RH,T] = meshgrid(1:2.5:100,-20:1.5:40);

%constants used to calculate the saturation pressure for the humid air
A = 6.116441;
r = 7.591386;
Tn = 240.7263;
Ptot = 1013.25;

%Calculation of the specific humidity as a function of temperature and
relative humidity, with constant atmospheric pressure
X = 1000*(0.621979 .* RH .* A .* 10.^((r .* T)./(T + Tn))./(100 .* Ptot -
RH .* A .* 10.^((r .* T)./(T + Tn)));

%Drawing the surface plot with labeling
surf(RH, T, X);
xlabel('Relative humidity [%]', 'fontsize', 18);
ylabel('Temperature [°C]', 'fontsize', 18);
zlabel('Specific humididty [g/kg]', 'fontsize', 18);
```

E.2 Surface plot: Humid air density

Table E-2: Matlab scrip for producing a surface plot showing the relation between the density of humid air, RH and temperature.

```
hold on;

%Creating enough meshes to get a smooth plot
[Ptot,T] = meshgrid(950:2:1030,-20:1.5:40);

%constants used to calculate the saturation pressure for the humid air
A = 6.116441;
r = 7.591386;
Tn = 240.7263;

RH = 99; % And set to 1% to make the additional surface plot

%Calculation of air density as a function of temperature and total pressure
rho = (Ptot - 0.01 .* RH .* A .* 10.^((r .* T)./(T + Tn)))./(2.870531.*(T
+ 273.15)) + (0.01 .* RH .* A .* 10.^((r .* T)./(T + Tn)))./(4.614964.*(T
+ 273.15));

%Drawing the surface plot with labeling
surf(Ptot, T, rho);
xlabel('Ptot [hPa]', 'fontsize', 18);
ylabel('Temperature [°C]', 'fontsize', 18);
zlabel('rho [kg/m^3]', 'fontsize', 18);
```

F. Calibration via curve fitting

F.1 RH

Three temperature-/RH sensors of type Vaisala HMT333 was placed in the same location as a pre- calibrated sensor of type Vaisala HMT120. A forced change in RH was applied by a moisture production, and the response of the four sensors were drawn, as seen in Figure F.1. By exponential curve fitting in excel, adjustments to the response of the HMT333 sensors was made, resulting in the graphs in Figure F.2.

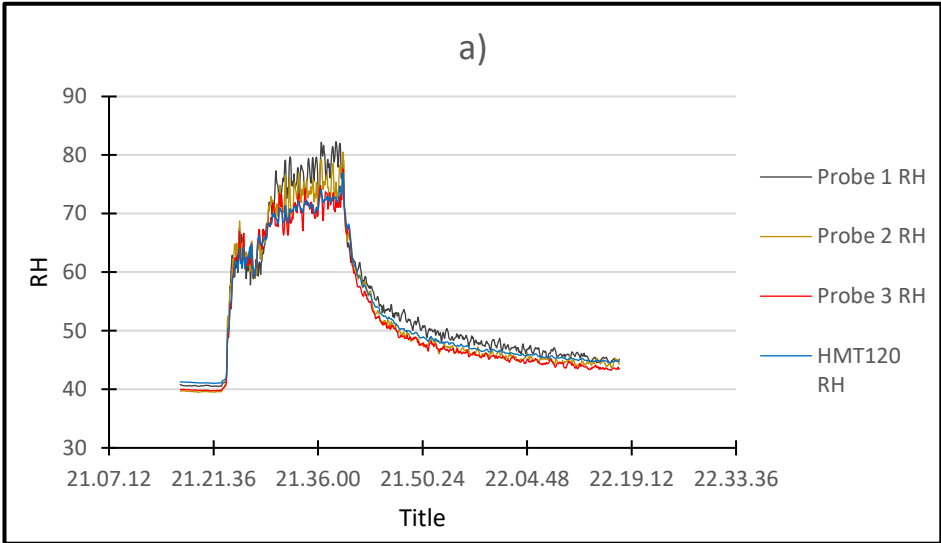


Figure F.1: Calibration of sensor type Vaisala HMT333 vs pre- calibrated sensor type Vaisala HMT120. The graph shows the response in RH, when applying a moisture production, *before* the curve fitting towards the pre- calibrated sensor.

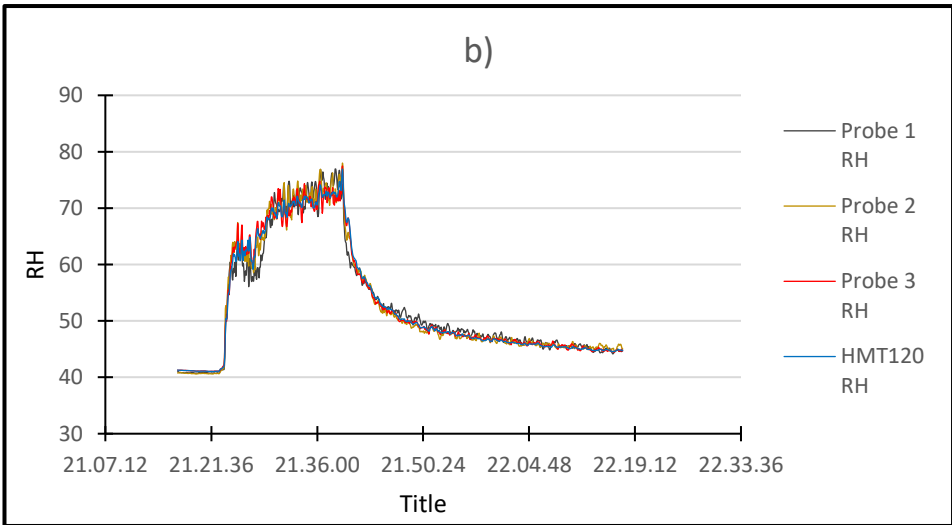


Figure F.2: Calibration of sensor type Vaisala HMT333 vs pre- calibrated sensor type Vaisala HMT120. The graph shows the response in RH, when applying a moisture production, *after* the curve fitting towards the pre- calibrated sensor.

F.2 Temperature

Three temperature-/RH sensors of type Vaisala HMT333 was placed in the same location as a pre- calibrated sensor of type Vaisala HMT120. A forced change in temperature was applied by a moisture production from hot water, and the response of the four sensors were drawn, as seen in Figure F.3. By exponential curve fitting in excel, adjustments to the response of the HMT333 sensors was made, resulting in the graphs in Figure F.4.

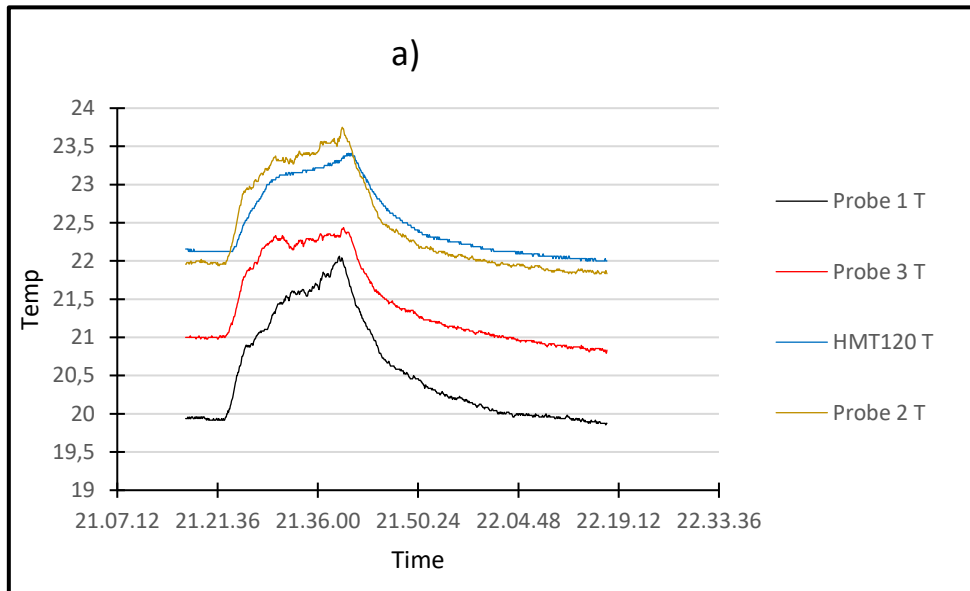


Figure F.3: Calibration of sensor type Vaisala HMT333 vs pre- calibrated sensor type Vaisala HMT120. The graph shows the response in temperature, when applying a moisture production, *before* the curve fitting towards the pre- calibrated sensor.

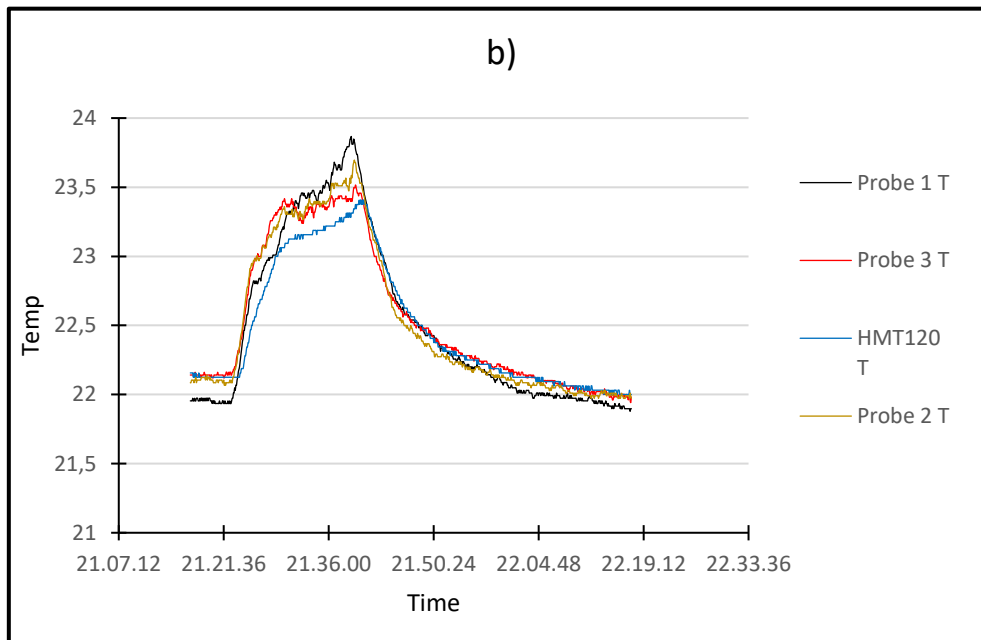


Figure F.4: Calibration of sensor type Vaisala HMT333 vs pre- calibrated sensor type Vaisala HMT120. The graph shows the response in temperature, when applying a moisture production, *after* the curve fitting towards the pre- calibrated sensor.

G.Human activity pattern

User behavior - Time spent at home due to type of physical activity.		Single parent with child/children				Married/Cohabited person with child/children				Prod. rate
		Weekdays		Weekends		Weekdays		Weekends		
Activity		[min]	[%]	[min]	[%]	[min]	[%]	[min]	[%]	[g/h]
[1]	Sleep	404	96.0	508	95.1	420	98.6	510	97.3	30
[2]	Eating	54	92.6	68	94.1	58	96.6	90	95.6	66
[3]	Other personal care	44	88.6	46	89.1	41	95.1	41	92.7	81-100
[4]	Main and second job	162	15.4	0	0.0	144	15.3	79	10.1	66-100
[5]	Homework	0	0.0	0	0.0	0	0.0	0	0.0	66
[6]	Food preparation	33	78.8	49	87.8	36	75.0	59	76.3	81
[7]	Dish washing	22	50.0	27	74.1	22	59.1	32	62.5	81
[8]	Cleaning dwelling	32	46.9	57	75.4	27	44.4	53	58.5	81-118
[9]	Other household upkeep	0	0.0	0	0.0	36	5.6	57	10.5	100-206
[10]	Laundry	32	28.1	43	44.2	26	23.1	36	33.3	100-206
[11]	Ironing	0	0.0	35	11.4	36	8.3	53	9.4	81-118
[12]	Handicraft	0	0.0	0	0.0	0	0.0	53	3.8	66-118
[13]	Caring for pets	0	0.0	18	11.1	19	5.3	22	13.6	66
[14]	Construction and repairs	0	0.0	0	0.0	71	8.5	77	19.5	100-272
[15]	Supervision of child	33	51.5	48	52.1	26	38.5	31	35.5	66-100
[16]	Teaching/reading w. child	32	37.5	42	40.5	34	32.4	39	28.2	51-100
[17]	Other domestic work	22	31.8	26	42.3	29	34.5	40	37.5	81-118
[18]	Visits and feasts	0	0.0	89	10.1	0	0.0	94	11.7	51-66
[19]	Other social life	35	42.9	41	51.2	29	51.7	45	53.3	51-66
[20]	Resting	33	30.3	35	37.1	36	22.2	45	35.6	44-51
[21]	Computer	0	0.0	73	17.8	45	11.1	51	19.6	44-51
[22]	Other hobbies and games	0	0.0	56	8.9	44	6.8	65	12.3	44-66
[23]	Reading books	46	10.9	51	17.6	37	16.2	63	17.5	44
[24]	Other reading	31	35.5	45	40.0	31	41.9	42	42.9	44
[25]	TV and video	87	70.1	139	75.5	90	78.9	140	77.9	44-51
[26]	Radio and music	0	0.0	0	0.0	0	0.0	34	8.8	44-51

Figure G.1: Activity pattern for two types of household families, including moisture production rate. In addition the total time each activity is performed during a day is given, and the percentages represents the probability for the occurrence during a day.(Johansson et al., 2010)